



Identification of a new inhibitor of Schwann cell differentiation

Inaugural-Dissertation

zur Erlangung des Doktorgrades
der Mathematisch-Naturwissenschaftlichen Fakultät
der Heinrich-Heine-Universität Düsseldorf

vorgelegt von

André Heinen
aus Essen

Düsseldorf, November 2008

aus dem Institut für Neurologie
der Heinrich-Heine Universität Düsseldorf

Gedruckt mit der Genehmigung der
Mathematisch-Naturwissenschaftlichen Fakultät der
Heinrich-Heine-Universität Düsseldorf

Referent: PD Dr. Patrick Küry
Koreferent: Prof. Dr. Ulrich Rüther

Tag der mündlichen Prüfung: 13.01.2009

To my family.

1.	SUMMARY / ZUSAMMENFASSUNG	1
1.1	Summary	1
1.2	Zusammenfassung	3
2.	INTRODUCTION	5
2.1	The nervous system – cell types and functions	5
2.2	Myelinating glial cells accelerate the axonal signal propagation	6
2.3	Composition of the myelinated axon	8
2.3.1	Ultrastructure of myelinating Schwann cells	8
2.3.2	The myelin sheath contains specific myelin proteins	10
2.3.3	Structure of the node of Ranvier, the paranode and the juxtaparanode	11
2.3.4	Integrins connect the Schwann cell extracellular matrix with intracellular signalling cascades	12
2.4	Development of the peripheral nervous system and peripheral glial cell differentiation	15
2.4.1	Timescale of Schwann cell development	15
2.4.2	Differentiation of myelinating Schwann cells	16
2.4.3	Marker gene expression during Schwann cell differentiation	17
2.5	The secreted proteins Notch, Lgi4 and Nrg1 as well as the transcription factors Sox10, Krox20 and Oct-6 promote Schwann cell differentiation	18
2.5.1	Sox10	19
2.5.2	Krox20	20
2.5.3	Oct-6	21
2.5.4	Neuregulin (Nrg)	21
2.6	Negative regulators inhibit Schwann cell differentiation	22
2.6.1	c-Jun	23

2.6.2	Notch	24
2.6.3	Sox2	25
2.6.4	Id and basic helix-loop-helix (bHLH) proteins	26
2.6.5	p57kip2 is a target gene of the bHLH protein Mash2	27
2.7	The mammalian cell cycle and its impact on Schwann cell differentiation	27
2.7.1	Cell cycle progression is positively regulated by the coordinated activity of cyclin dependent kinases (CDKs) and inhibited by binding of CDKs to cyclin dependent kinase inhibitors (CKIs)	27
2.7.2	p21cip1 cooperates with PCNA to control the DNA replication	30
2.7.3	p27kip1 controls the proliferation of a variety of cell types	30
2.7.4	p57kip2 contains a domain structure which is distinct from all other CKIs and its function is not redundant	31
2.7.5	The function of cyclin, CDK and CKI expression during Schwann cell differentiation	35
2.7.6	CKI expression alters actin cytoskeletal dynamics by inhibition of the Rho signalling pathway	37
2.8	Aim of this thesis	39
3.	MATERIAL AND METHODS	41
3.1	Material	41
3.1.1	Animals	41
3.1.2	<i>E.coli</i> bacteria strains	41
3.1.3	Reagents and buffers	42
3.1.3.1	Reagents	42
3.1.3.2	Buffers	43
3.1.3.2.1	Buffers, solutions and reagents for cell culture	43
3.1.3.2.2	Buffers and solutions for molecular biology	43
3.1.4	Media	45

3.1.4.1	Media for cell culture	45
3.1.4.2	Media for the cultivation of <i>E.coli</i>	46
3.1.5	Antibiotics	46
3.1.6	Enzymes	46
3.1.7	DNA molecular weight standards	47
3.1.8	Synthetic oligonucleotides	47
3.1.9	Transfection reagents	47
3.1.10	Vectors	47
3.1.11	Kits	48
3.1.12	Technical devices and software	48
3.2	Molecular biological methods	49
3.2.1	Cloning procedures	49
3.2.1.1	Agarose gel electrophoresis	49
3.2.1.2	Digestion of plasmids using restriction endonucleases	49
3.2.1.3	Purification of DNA fragments using QIAquick gel extraction kit	50
3.2.1.4	Dephosphorylation of plasmids	50
3.2.1.5	Annealing of oligonucleotides	50
3.2.1.6	Phosphorylation of annealed oligonucleotides	50
3.2.1.7	Ligation of plasmid and insert	50
3.2.1.8	Transformation of plasmids into <i>E.coli</i>	51
3.2.2	Generation of vector constructs	51
3.2.2.1	pSUPER vector constructs	51
3.2.2.2	rp57kip2-IRES2-EGFP	52
3.2.2.3	pcDNA3.1-HygB-citrine	52
3.2.3	Isolation of nucleic acids	53

3.2.3.1	Isolation of plasmid DNA (plasmid mini preparation)	53
3.2.3.2	Isolation of plasmid DNA (plasmid mini preparation) using the plasmid miniprep kit	53
3.2.3.3	Isolation of plasmid DNA (plasmid maxi preparation)	54
3.2.3.4	Generation of glycerol stocks	54
3.2.3.5	Preparation of RNA	54
3.2.3.5.1	Preparation of total RNA using the RNeasy Mini Kit	54
3.2.3.5.2	Preparation of total RNA using Trizol®-reagent	54
3.2.3.5.3	Preparation of miRNA using the miRVana kit	55
3.2.3.5.4	Photometric nucleic acid concentration determination	55
3.2.4	Reverse transcription	55
3.2.4.1	Reverse transcription of total RNA	55
3.2.4.2	Reverse transcription of micro RNA	56
3.2.5	Amplification of DNA fragments via polymerase chain reaction (PCR)	56
3.2.6	Automatic sequencing using the ABI 310 sequencing device	57
3.2.7	Quantitative real time PCR (qRT-PCR)	58
3.2.8	SDS gel electrophoresis and Western Blot	59
3.2.9	GeneChip array analysis	60
3.2.10	Proteome analysis	61
3.3	Cell culture methods	62
3.3.1	Coating of flasks and culture dishes	62
3.3.1.1	PDL coating of flasks and culture dishes	62
3.3.1.2	Collagen type I coating of culture dishes	62
3.3.2	Culturing of primary Schwann cells	62
3.3.2.1	Preparation of primary rat Schwann cells	62

3.3.2.2	Freezing of primary rat Schwann cells	63
3.3.2.3	Maintenance of rat Schwann cell cultures	63
3.3.3	Culturing of rat dorsal root ganglion (DRG) dissociation cultures	64
3.3.3.1	Preparation of rat DRG dissociation cultures	64
3.3.3.2	Maintenance of rat DRG dissociation cultures	64
3.3.4	Transfection	64
3.3.4.1	Transfection of primary rat Schwann cells with plasmid DNA	64
3.3.4.2	Transfection of rat Schwann cells with siRNAs	65
3.3.4.3	Selection of transfected cells using hygromycin B	66
3.3.4.4	Selection of transfected cells via magnetic sorting	66
3.3.4.5	Selection of transfected cells by fluorescence activated cell sorting (FACS)	66
3.3.5	Immunocytochemistry and immunohistochemistry	67
3.3.6	BrdU incorporation and determination of the proliferation rate	68
3.3.7	Transplantation of transfected rat Schwann cells onto DRG cocultures	69
4.	RESULTS	70
4.1	p57kip2 is dynamically expressed by Schwann cells during postnatal development of the PNS	70
4.2	Expression of p57kip2 and p27kip1 can be suppressed via vector mediated shRNA expression	71
4.3	Suppression of p57kip2 leads to cell cycle exit	73
4.4	Long term suppression of p57kip2 leads to morphological changes	75
4.5	Suppression of p57kip2 leads to myelin gene induction	78
4.6	p57kip2 translocates LIMK-1 from the cytoplasm into Schwann cell nuclei	80
4.7	Suppression of p57kip2 leads to accelerated <i>in vitro</i> myelination	82

4.8	GeneChip array analysis revealed that suppression of p57kip2 leads to a shift of the Schwann cell gene expression pattern	84
4.9	p57kip2 suppression does not induce the interferon response defence reaction	84
4.10	GeneChip array analysis revealed the expression of possible off target genes in p57kip2 suppressed cells	87
4.11	p57kip2 suppression induced shift in gene expression resembles the <i>in vivo</i> gene expression associated with Schwann cell differentiation	89
4.12	GeneChip array analysis revealed changes in cell cycle associated gene expression	94
4.13	2D gel electrophoresis revealed nuclear proteins which are differentially regulated in p57kip2 suppressed Schwann cells	97
5.	DISCUSSION	100
5.1	The role of intrinsic myelination inhibitors	101
5.2	p57kip2 expression and cell cycle control	103
5.3	p57kip2's influence on cell morphology	104
5.4	p57kip2 suppression induces terminal differentiation of Schwann cells	107
5.5	Biomedical relevance of p57kip2 expression	109
5.6	Concluding remarks and open questions	111
6.	REFERENCES	113
7.	ABBREVIATIONS	133
8.	ACKNOWLEDGEMENTS	135

1.1 SUMMARY

Axons are tightly associated with myelinating glial cells, Schwann cells in the peripheral nervous system (PNS) and oligodendrocytes in the central nervous system (CNS). One well described function for these two cell types is the electrical insulation of axons from the environment, which results in the acceleration of electric signal propagation. This is achieved by spirally wrapping of one myelinating glial cell protrusion around an axon, exclusion of cytoplasm, production of myelin proteins and fusion of the membranes, thus displaying the myelinating phenotype.

Schwann cell differentiation depends on axonal signalling. On the other hand, loss of axons, for example following trauma or disease, leads to dedifferentiation, demonstrating that also the maintenance of terminal differentiation depends on axonal signals. Interestingly and in strong contrast to oligodendrocytes, these cells are able to redifferentiate and to myelinate newly sprouting axons, revealing a plastic behaviour and their capacity to promote the regeneration process. However, *in vitro* differentiation of Schwann cells is blocked and the determinants which control Schwann cell differentiation and dedifferentiation *in vivo* and *in vitro* are so far unknown. It is currently believed that intrinsic inhibitors of differentiation exist which have to be differentially regulated both during peripheral nerve development and regeneration.

This thesis identifies a potential candidate for such an intrinsic inhibitor, namely p57kip2. The p57kip2 gene encodes a member of the cyclin dependent kinase inhibitor (CKI) family, which are known to block G1/S phase transition during the mammalian cell cycle. Expression of p57kip2 is dynamically regulated during peripheral nerve development and following crush lesion of nerves. The early downregulation of p57kip2 during the postnatal development suggests a function beyond Schwann cell cycle control. In order to investigate whether downregulation of p57kip2 gene expression has functional consequences on Schwann cell differentiation, p57kip2 gene expression levels were suppressed in cultured Schwann cells by means of vector based RNAi. Surprisingly, suppression of p57kip2 was shown to lead to Schwann cell cycle exit, actin filament stabilization, altered cell morphology and downregulation of promyelinating markers as well as induction of myelin genes and proteins, steps which are characteristic for Schwann cell differentiation. In addition, it was demonstrated that p57kip2 suppression also accelerates *in vitro* myelination of DRG cocultures. Experimental evidence implies

that the observed morphological changes are at least partially mediated by p57kip2/LIMK-1 interactions. Using GeneChip microarray technology it could be shown that these cellular reactions are specific to p57kip2 knockdown, whereas induction of the interferone response could be excluded. Further this approach revealed that the observed cell cycle exit is a consequence of complex changes in cell cycle regulator gene expression and that suppression of p57kip2 leads to a shift in the gene expression program toward the pattern known from Schwann cells in developing nerves.

Since in the absence of axons Schwann cells normally do not display differentiation associated reactions, these results strongly suggest the identification of a mechanism for Schwann cell differentiation and of an important intrinsic negative regulator of myelinating glial cell differentiation. Thus regulation of p57kip2 expression could provide a therapeutic tool to treat demyelinating diseases or to promote myelin restoration after traumatic injury. However, it is currently unsolved which signals control p57kip2 expression *in vivo* and their identification as well as the investigation of p57kip2 *in vivo* functions await future experiments.

1.2 ZUSAMMENFASSUNG

Axone sind eng mit myelinisierenden Gliazellen, Schwannzellen im peripheren Nervensystem (PNS) und Oligodendrozyten im zentralen Nervensystem (ZNS), assoziiert. Hauptfunktion dieser Zelltypen ist die elektrische Isolation von Axonen, die zu einer Beschleunigung der elektrischen Signalweiterleitung führt. Dazu wickelt sich ein Ausläufer einer Gliazelle spiralförmig um ein Axon. Der myelinisierende Phänotyp wird schliesslich durch Verdrängung von Zytoplasma, Synthese von Myelinproteinen und Fusion der Membranen erreicht.

Schwannzelldifferenzierung ist abhängig von axonalen Signalen. Zudem hängt auch die Aufrechterhaltung des terminalen Differenzierungszustandes von diesen Signalen ab. Dies wurde dadurch verdeutlicht, dass axonale Degeneration, wie z.B. nach traumatischen Ereignissen oder im Krankheitsverlauf, zur Dedifferenzierung führt. Interessanterweise und im Gegensatz zu Oligodendrozyten können Schwannzellen in diesem Fall redifferenzieren und neu auswachsende Axone myelinisieren. Durch diese hohe Differenzierungsplastizität kann somit der Regenerationsprozess gefördert werden. Dahingegen ist die *in vitro* Differenzierung von Schwannzellen gehemmt, und die Determinanten, die die Schwannzell-differenzierung *in vivo* und *in vitro* steuern, sind bis heute unbekannt. Gegenwärtig wird vermutet, dass intrinsische Hemmstoffe der Differenzierung existieren, die sowohl während der Entwicklung des peripheren Nervensystems als auch im Regenerationsprozess differentiell exprimiert werden.

In der vorliegenden Dissertation wird mit p57kip2 ein potenzieller Kandidat für diese Art von Differenzierungsinhibitoren identifiziert. Bei p57kip2 handelt es sich um ein Mitglied der Familie von Zyklin-abhängigen Kinaseinhibitoren (CKI), die den Übergang von der G1- in die S-Phase des Zellzyklus blockieren. Die Expression von p57kip2 wird sowohl während der peripheren Nervenentwicklung als auch in Folge von Läsionen peripherer Nerven dynamisch reguliert. Die frühe Herunterregulation von p57kip2 während der peripheren Nervenentwicklung lässt eine Funktion vermuten, die ausserhalb der Zellzyklus-Regulation liegt. Um zu untersuchen, ob die Regulation von p57kip2 funktionelle Konsequenzen bezüglich der Schwannzelldifferenzierung hat, wurde die Expression von p57kip2 mittels Genmodulation (RNA Interferenz) supprimiert. Diese Suppression bewirkte überraschenderweise das Verlassen des Zellzyklus, eine Stabilisierung der Aktinfilamente sowie eine veränderte Zellmorphologie. Zudem wurde eine

Herunterregulation von promyelinisierenden Markergenen bei gleichzeitiger Induktion von Myelinen und Myelinproteinen beobachtet. Die beschriebenen Veränderungen sind charakteristisch für die Differenzierung von Schwannzellen. Zudem konnte gezeigt werden, dass die Suppression von p57kip2 zu einer beschleunigten *in vitro* Differenzierung von dorsalen Wurzelganglien (DRG) Kokulturen führt. Aufgrund experimenteller Belege wird vermutet, dass die beobachteten Morphologieveränderungen zumindest zum Teil durch eine Interaktion von p57kip2 mit LIMK-1 bewirkt wurden. Mit Hilfe von GeneChip Microarray Analysen konnte gezeigt werden, dass diese zellulären Reaktionen spezifisch für die Suppression von p57kip2 sind, während eine mögliche Induktion der Interferon-Antwort ausgeschlossen werden konnte. Ferner konnte mit Hilfe dieser Analysen gezeigt werden, dass das Verlassen des Zellzyklus eine Konsequenz von komplexen Veränderungen der Expression von Zellzyklus-Regulatoren ist und dass aufgrund der Suppression von p57kip2 eine Verlagerung des Genexpressionsmusters in Richtung der Reifung von Schwannzellen während der Nervenentwicklung erreicht wurde.

Da Schwannzellen in Abwesenheit von Axonen normalerweise keine differenzierungsassoziierten Reaktionen zeigen, lassen diese Resultate den Schluss zu, dass mit der Regulation von p57kip2 ein Mechanismus der Schwannzell-differenzierung und ein wichtiges intrinsisches Hemmprotein der myelinisierenden Gliazelldifferenzierung identifiziert wurde. Die Regulation von p57kip2 könnte daher therapeutischen Nutzen bei der Behandlung demyelinisierender Erkrankungen besitzen oder zur Förderung der Regeneration nach Nerven trauma herangezogen werden. Zur Zeit ist nicht bekannt, welche Signale die *in vivo* Expression von p57kip2 regulieren und welche Funktionen p57kip2 *in vivo* ausführt. Diesbezügliche Untersuchungen sind daher Gegenstand zukünftiger Experimente.

2. INTRODUCTION

2.1 The nervous system – cell types and functions

The nervous system fulfils three partially overlapping functions, namely sensory input, processing and motoric output following receptor stimulation. Input of information using receptors as well as motoric output is a function of the peripheral nervous system (PNS), while signal processing is a function of the central nervous system (CNS). Functional subunits of the rather complex CNS are the brain and the spinal cord, whereas the peripheral nervous system is characterized by a rather simple, but efficient structure, including sensory (afferent) and motoric (efferent) subunits.

Two major classes of cells characterize the nervous system. Neurons communicate with each other by propagation of electric signals, whereas glial cells have functions regarding support of axons, stability, immune response and as connective tissue. A major function of specialized glial cells is the acceleration of axonal signals, which is achieved by the generation of a myelin sheath. Hence several glial subtypes exist with divergent functions.

Glial cells are subdivided into microglia and macroglia. Microglia are glial cells of the CNS which form an active immune response. Therefore, these cells migrate through the tissue, brain as well as spinal cord, recognize foreign, infectious agents and remove them. Macroglia are astrocytes, ependymal cells, radial glia and oligodendrocytes (CNS) as well as satellite cells and Schwann cells (PNS). Astrocytes are thought to connect neurons with the blood supply, to provide an appropriate environment for neurons by uptake of residual ions and neurotransmitters and to form the blood brain barrier. Ependymal cells produce the cerebrospinal fluid which serves to protect the brain against mechanical irritations. Oligodendrocytes are the myelinating glial cells of the CNS, which ensheath up to 50 individual axons.

Schwann cells can be subdivided into four classes, namely myelinating Schwann cells, non myelinating Schwann cells, perisynaptic Schwann cells and satellite cells. Perisynaptic Schwann cells are situated at the neuromuscular junction as part of the so called tripartite synapse, which includes the postsynaptic nerve terminal, the postsynaptic muscle membrane and the perisynaptic Schwann cells. Perisynaptic Schwann cells were shown to take up neurotransmitters and ions. Further they regulate the extracellular environment of neurons and monitor synapse activity. Additionally, since perisynaptic Schwann cells have an increased expression

of neurotransmitters and ion channels, a contribution to neurotransmission at the neuromuscular junction was suggested (Robitaille *et al.*, 1998; Auld and Robitaille, 2003a).

Satellite cells were shown to associate with the cell bodies of neurons rather than with their axons. In fact, neuronal cell bodies are covered by a cap consisting of satellite glia, suggesting a specific function for this cell type. Currently it is believed that these cells compensate the lack of the blood brain barrier in dorsal root ganglia and at the neuromuscular junction by generation of a diffusion barrier.

Relatively little is known about non myelinating Schwann cell's role and properties. Non myelinating Schwann cells are associated with a maximum of ten axons to form Remak bundles (Berthold *et al.*, 2005). Most of these unmyelinated fibers are axons of sensory ganglia or sympathetic neurons. Since disruption of the non myelinating Schwann cell/axon interaction leads to a loss of unmyelinated fibers and thus to diminished peripheral pain sensation, non myelinating Schwann cells are thought to possess a role in the maintenance of these axons (Chen *et al.*, 2003).

The best characterized Schwann cells are the myelinating Schwann cells, which function as isolators in order to allow efficient axonal signal propagation. Much of investigation has been done to describe the components and formation of the myelin sheath both during peripheral nerve development and during the redifferentiation process after axotomy. Morphological investigations revealed that myelinating Schwann cells form up to 100 complex spirals of myelin membranes around axons (Webster *et al.*, 1971). In terms of gene expression, the formation of myelinating Schwann cells needs the rearrangement of the genetic program in order to synthesize specialized membrane components and to orchestrate their assembly and the accompanying cytoskeletal changes. These result in cells with distinct areas of either compact myelin, non compact myelin or nodes of Ranvier (Arroyo and Scherer, 2000), hence displaying the myelinating phenotype.

2.2 Myelinating glial cells accelerate the axonal signal propagation

Neuronal communication is based on depolarization of the electric potential of their axons. Action potentials move as waves along the axon and evoke an action potential in the neuron the axon synapses with. Unmyelinated axons generate action potentials along their whole surface. As a consequence of the electric resistance, the propagation velocity depends on the axonal diameter and is proportional to the

diameter. Thin neurons require less expense to propagate action potentials, but high velocities can only be reached in large diameter axons. The high metabolic expense which is necessary to propagate action potentials along large diameter axons precludes the generation of complex structures, such as the brain.

In order to allow energy efficient high propagation velocities, vertebrates, but also some invertebrates (Xu *et al.*, 1999), evolved myelin. Since myelin inhibits the exchange of ions within the internode, the action potentials of myelinated axons are restricted to certain unmyelinated regions called the nodes of Ranvier. Myelinating glial cells support the concentration of voltage gated Na⁺ channels at these nodes (Pedraza *et al.*, 2001). Thus action potentials are forced to jump from one node to the next, a mechanism referred to as saltatory conduction of electric signals. The establishment of unmyelinated nodes and myelinated internodes led to drastically increased propagation velocities. While mammalian unmyelinated axons comprise velocities of less than 1 m/sec, myelinated axons of the same size conduct 10 times faster, and the velocity can reach up to 100 m/sec in large myelinated axons. On the other hand, unmyelinated axons would have to be 100 times thicker in diameter to reach the same velocity.

The myelin sheath is established by the spirally wrapping of specialized myelinating glial cells around axons. Myelinating glial cells are Schwann cells in the peripheral nervous system (PNS) and oligodendrocytes in the central nervous system (CNS). Initially, the myelin sheath was designated to be part of the axon. In 1928, Ramon y Cajal described it as an “adjunct of the axon”. With the invention of the electron microscopy, this postulation could be proven to be false. Geren and Bunge were able to demonstrate that the myelin sheath derives from myelinating glial cells (Geren *et al.*, 1954; Bunge *et al.*, 1962). The myelin sheath has been shown to be a consequence of the spirally wrapping of a glial cell protrusion around an axon. In order to insulate the axon from the environment to provide higher propagation velocities of electric signals, the myelin sheath consists of a unique composition of lipids and proteins. The expression of several of these proteins is restricted to myelin, hence these proteins are called myelin proteins. Another feature of the myelin sheath is the high lipid content. Myelin membranes contain approximately 75 % lipids (Norton and Poduslo, 1973), the highest lipid content among all known bio membranes, again underscoring the special function of this membrane.

2.3 Composition of the myelinated axon

2.3.1 Ultrastructure of myelinating Schwann cells

As introduced, myelinated axons comprise two distinct regions, namely unmyelinated nodes of Ranvier and myelinated internodes. The internodes consist ion their majority of compact myelin whereas minor parts are non-compacted. While compact myelin contains high concentrations of the myelin proteins P0, MBP, PMP-22 (PNS) and PLP, MBP (CNS), these proteins are not found in the non-compact myelin, which contains Connexin 32 (Cx32) and myelin associated glycoprotein (MAG).

Myelin membranes directly contact the axon (Fig. 1; Fig. 2). It is believed that axonal signals are transmitted to the Schwann cells via receptors on the surface of the adaxonal membrane. Further the outermost abaxonal membrane secretes the basal lamina, the extracellular matrix of Schwann cells (Bunge *et al.*, 1980). Interestingly, inhibition of basal lamina formation has been shown to block Schwann cell differentiation (Moya *et al.*, 1980), revealing that the basal lamina is crucial for normal peripheral nerve development. Non compact myelin also includes the paranodal loops of the myelin sheath. At the lateral end of an internode, these paranodal loops are vital for Schwann cell/axon interactions and for the direction of voltage gated Na⁺ channels (Rios *et al.*, 2003).

On electron micrographs, compact myelin appears as alternating dark and light lines which spiral around an axon. During the wrapping process of a Schwann cell or oligodendrocyte protrusion, cytoplasm becomes excluded hence leading to cytoplasm free compacted wraps. This cytoplasmic exclusion allows the fusion of intracellular Schwann cell membranes to generate the major dense lines, which appear dark in electron microscope photographs due to the high lipid content. Compact myelin is crossed by cytoplasmic channels, called Schmidt-Lantermann incisures, which are rich in gap junctions and mitochondria (Fig. 2). It is currently believed that they serve to transport myelin proteins and lipids from the perinuclear cytoplasm to the single wraps of myelin. Another hypothesis is that these incisures connect the outermost and inner membranes of one internode to allow fast communication despite the large number of membranes present. One Schwann cell can generate up to 100 spirals of myelin (Webster, 1971), and the distance between two major dense lines is approximately 15 nm (Fernandez-Moran and Finean, 1957; Kirschner and Hollingshead, 1980; reviewed by Arroyo and Scherer, 2000; Scherer and Arroyo, 2002).

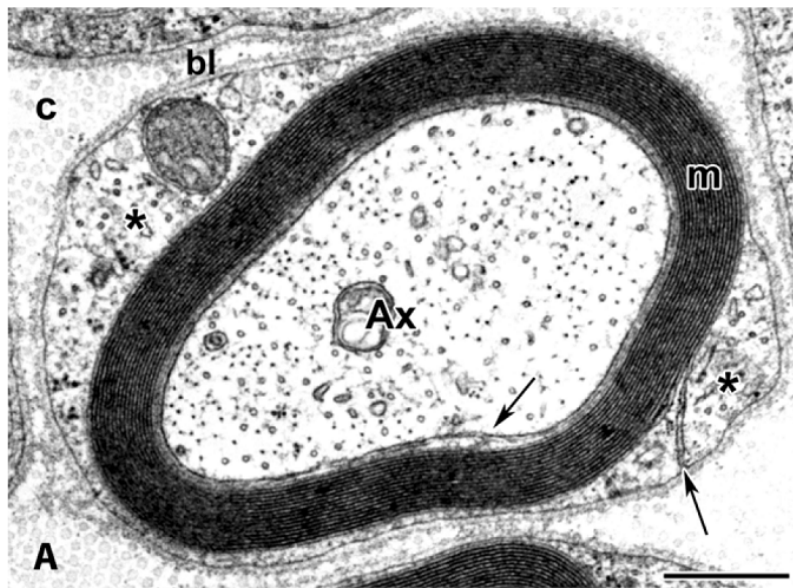


Figure 1. Ultrastructure of a myelinated axon in the PNS. Axons (Ax) are surrounded by spiral wraps of compact myelin sheaths (m). Arrows mark the innermost (adaxonal) and outermost (abaxonal) membranes of the Schwann cell. The outer circumference of the Schwann cell comprises organelle rich cytoplasm (*) and the Schwann cell nucleus. Adjacent fibers are separated by extracellular collagen fibrils (c), and each Schwann cell is surrounded by a basal lamina (bl), displaying the extracellular matrix. Scale bar = 0,5 μm . According to Trapp and Kidd, 2004

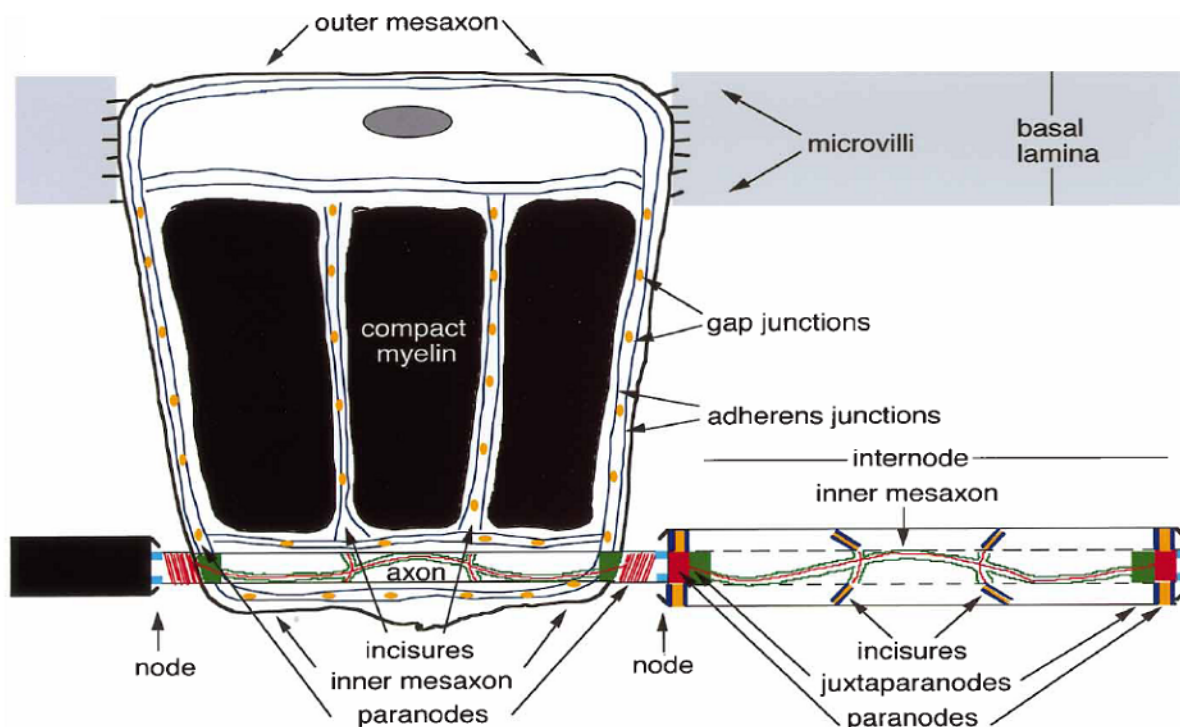


Figure 2. Schematic view of an unwrapped myelinating Schwann cell. Unwrapping of a Schwann cell reveals several functional distinct regions within the cell. The inner mesaxon (adaxonal membrane) is in direct contact and communicates with the axon. Gap junctions (orange) enriched Schmidt-Lanterman incisures connect the cytoplasm rich outer membrane (outer mesaxon) with the inner sheaths thus supporting them with nutrients. The outer mesaxon secretes the basal lamina and connects the Schwann cell with the extracellular matrix. The largest portion of the myelinating Schwann cell consists of compact myelin which includes the myelin specific proteins. Juxtapanodes (green) and paranodes (red) comprise non compact myelin. According to Arroyo and Scherer, 2000.

2.3.2 The myelin sheath contains specific myelin proteins

Myelination of internodes results in the electrical insulation from the environment. Therefore, adhesion has to be considered as a major function of proteins within the myelin sheath. On the other hand, once set up, myelin is relatively non-dynamic and myelin proteins should experience relatively low turnover rates. Slow turnover rates have been shown to be characteristic for myelin proteins (Lajtha *et al.*, 1977; Sabri *et al.*, 1974).

The myelin proteins of the PNS and CNS are distinct (Fig. 3). Myelin proteins of the PNS include myelin protein zero (P0), myelin basic protein (MBP) and peripheral myelin protein-22 (PMP-22; Greenfield *et al.*, 1973), whereas the most abundant proteins of CNS myelin are proteolipid protein (PLP) and MBP. More than 70 % of the total PNS myelin protein consists of P0. The 30 kD protein P0 (Lemke and Axel, 1985) is an integral transmembrane protein which is thought to stabilize the intraperiod lines of compact myelin by interaction of opposing P0 tetramers of two adjacent myelin wraps. In contrast to P0, MBP is localized at the cytoplasmic surface of compact CNS and PNS myelin. MBP proteins act as monomers and include a highly charged family of 15-21 kD proteins (Greenfield *et al.*, 1973; Zeller *et al.*, 1984), which bind to negatively charged lipids. Since the cytoplasmic membranes of MBP deficient mice are not fused, the function of MBP is supposed to be the maintenance of the major dense line. The 22 kD protein PMP-22 is present in PNS compact myelin (Snipes *et al.*, 1992). It is a hydrophilic transmembrane protein the ablation of which leads to severe hypomyelination (Adlkofer *et al.*, 1995), although no apparent effect on the myelin ultrastructure was revealed.

With more than 50 %, the most abundant CNS myelin protein is the 26 kD protein PLP. Interestingly, it has been suggested that PLP exchanged P0 during evolution of the CNS (Waehneltd, 1990; Yoshida and Colman, 1996). Nevertheless, ablation of PLP and replacement through P0 led to mice with a strongly reduced life span due to severe axonal damage, indicating that PLP has neuroprotective abilities as well (Yin *et al.*, 2006).

Of note, it was shown that myelin protein knockout does not necessarily result in loss of myelin membranes. Abundant amounts of multilamellar membranes form in absence of P0 (Giese *et al.*, 1992), PLP (Duncan *et al.*, 1988; Duncan *et al.*, 1989), MBP (Privat *et al.*, 1979) as well as in nerves of mice with a combined knockout of PLP and MBP (Stoffel *et al.*, 1997), indicating that the growth and spiral wrapping of

the glial protrusions does not depend on myelin proteins. Ultrastructural analysis of nerves devoid of PLP or MBP showed that ablation of these proteins leads to a variable space between the membrane wraps, indicating that these proteins are necessary for the normal spacing of CNS myelin membranes (Duncan *et al.*, 1988; Privat *et al.*, 1979) and P0 for the correct spacing of PNS myelin membranes, respectively (Giese *et al.*, 1992).

In addition, it was shown that the total amount of myelin proteins is not necessarily the key factor for establishment and maintenance of myelin sheaths. Since alterations in the myelin composition have been shown to cause hypomyelinating diseases, also the stoichiometry of the myelin proteins appears to be vital for these purposes. For example, alterations in the total amount of PMP-22 has been demonstrated to result either in hereditary neuropathy with liability to pressure palsy (HNPP) due to PMP-22 gene point mutations (loss of function) or in Charcot-Marie-Tooth disease type 1A (CMT-1A) due to PMP-22 gene duplication (gain of function).

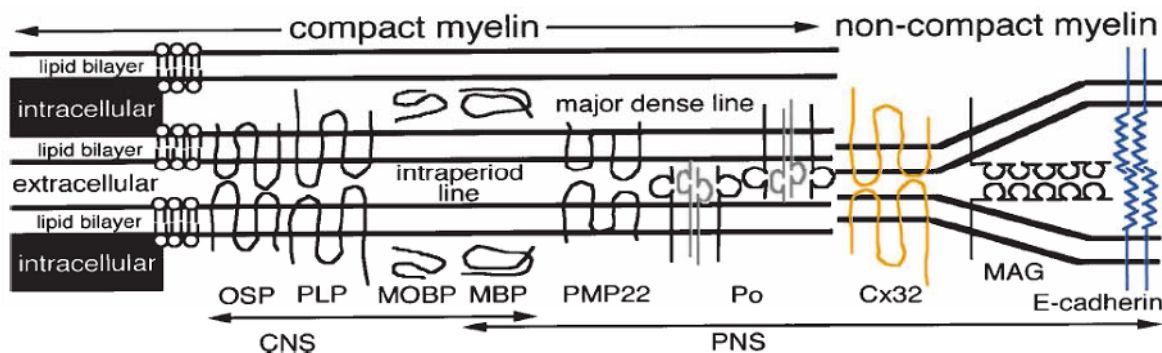


Figure 3. Compact and non compact myelin contains different protein compositions. The PNS compact myelin contains myelin protein zero (P0), peripheral myelin protein 22 (PMP22) and myelin basic protein (MBP). P0 and PMP22 connect the lipid bilayers of two adjacent membranes within the intraperiod line, while MBP is found intracellularly within the major dense line. PNS non compact myelin comprises connexin 32 (Cx32) and myelin-associated glycoprotein (MAG) as well as E-cadherins. The CNS compact myelin also contains MBP, but major myelin proteins are myelin-oligodendrocyte basic protein (MOBP), proteolipid protein (PLP) and oligodendrocyte-specific protein (OSP). According to Arroyo and Scherer, 2000.

2.3.3 Structure of the node of Ranvier, the paranode and the juxtaparanode

Initiation and maintenance of Schwann cell myelination has been shown to depend on axonal signals. On the other hand, Schwann cell signals are also necessary for normal axonal development. For example, the axon diameter and the clustering of voltage gated Na^+ channels at the node of Ranvier are directed by the Schwann cell the axon is associated with (Melendez-Vasquez *et al.*, 2001). The nodes of CNS and

PNS accomplish identical functions, but they differ in their ultrastructure. The nodal axolemma of PNS axons is covered by Schwann cell microvilli, which are enriched in actin filaments (Melendez-Vasquez *et al.*, 2001), while CNS axolemma is surrounded by astrocyte processes (Hildebrand and Waxman, 1984) or possibly also oligodendrocyte precursor cells (Butt *et al.*, 1999).

The node as well as its adjacent structures, the paranode and juxtaparanode, contributes to the saltatory conduction. At the nodal axolemma, Na⁺ channels are concentrated at a density of 1000-1500/μm² (Rosenbluth, 1976). During the development, Schwann cells and oligodendrocytes direct these channels to the nodes (Pedraza *et al.*, 2001). Thus, through clustering of Na⁺ channels, the nodes are directly involved in saltatory conduction. The paranode is the lateral end of the Schwann cell, which is tightly associated with the axolemma by septate like junctions. The axolemma is enriched in the membrane proteins contactin and Caspr, while the paranodal Schwann cell membrane contains neurofascin 155 (NF155), binds to monomeric contactin (Gollan *et al.*, 2003). Since the clustering of ion channels appears normal in contactin null mice while axoglial septate junctions are absent, it seems that the paranode function is to separate Na⁺ from K⁺ channels (Boyle *et al.*, 2001), the latter of which are abundantly expressed in the juxtaparanode (Vabnick *et al.*, 1999). The clustering of K⁺ channels at the juxtaparanodal region suggests that this region plays a role in the rapid repolarization of the membrane potential after depolarization.

2.3.4 Integrins connect the Schwann cell extracellular matrix with intracellular signalling cascades

Schwann cells and axons are surrounded by extracellular matrix components such as collagens, fibronectins and laminins. These components are either Schwann cell or axon derived and organized in the so called basal lamina, which is secreted by immature Schwann cells and is maintained throughout lifetime.

Laminins are a family of proteins which are fused to trimers consisting of one α, β and γ subunits each. Of the 15 isoforms known, only a few appear to possess a specific role during peripheral nerve development. Laminins 2 and 8 are expressed in the basal lamina of peripheral nerves, with high levels of laminin 8 during development and declining levels at maturity, while high levels of laminin 2 are found in mature nerves (Wallquist *et al.*, 2002).

The expression of laminin receptors has also been shown to be differentially regulated during the peripheral nerve development, reflecting different functions for these receptors. Laminin receptors are either dystroglycans or integrins, both of which constitute of one α and one β subunit to form non covalently bound dimers. The combination of α and β specifies the ligand affinity and subsequent intracellular signalling. During development, Schwann cells express the integrins $\alpha1\beta1$, $\alpha6\beta1$ and low levels of $\alpha2\beta1$ and $\alpha3\beta1$. At birth, also the expression of integrin $\alpha6\beta4$ as well as the expression of dystroglycans is initiated. While the expression of dystroglycans is restricted to Schwann cells destined to myelinate (Masaki *et al.*, 2002; Previtali *et al.*, 2003b), the expression of $\alpha1\beta1$ has been shown to specify non myelinating Schwann cells (Stewart *et al.*, 1997).

Interaction of matrix components and their receptors modulate proliferation, survival as well as myelination. It has been proposed that expression of myelin proteins depends on the establishment of a basal lamina. However, this view has been challenged since myelination can also be initiated in absence of a basal lamina as long as laminin is present (Podratz *et al.*, 1998; Podratz *et al.*, 2001), thus reflecting that laminin itself but not the assembly of a functional basal lamina is required for the initiation of myelination. Indeed the need for laminin/integrin signalling regarding Schwann cell differentiation has been shown with conditional knockout mice lacking either laminin or integrin subunits. Depending on the eliminated subunit, these mice show severe radial sorting deficits (Chen and Strickland, 2003; Feltri *et al.*, 2002), polyaxonal myelination (Chen and Strickland, 2003), node of Ranvier defects or abnormal short internodes. These sorting deficits showed that lack of laminin/integrin signalling arrests Schwann cells during the early embryonic development. As the radial sorting process depends on the growth of Schwann cell processes within axonal bundles, these sorting deficits have been suggested to be due to abnormal growth of Schwann cells.

Among the integrins, integrin $\beta1$ is thought to possess a major function regarding signalling to the actin cytoskeleton, as blocking of integrin $\beta1$ by antibodies disrupts the Schwann cell differentiation (Fernandez-Valle *et al.*, 1994b). The intracellular signalling was shown to be mediated either by binding of integrin $\beta1$ to proteins which form a complex composed of focal adhesion kinase (FAK), paxillin, merlin and talin (Chen *et al.*, 2000; Fernandez-Valle *et al.*, 2002) or by binding of integrins to the IPP complex. The IPP complex (Fig. 4) is composed of integrin linked

kinase (ILK), particularly interesting Cys-His-rich protein (PINCH) and p_{ar}vin (reviewed by Legate *et al.*, 2006) and is recruited to focal adhesions by means of paxillin interactions (Nikolopoulos *et al.*, 2001). Interestingly, a recent report revealed developmental abnormalities in brain development of mice with a conditional ablation of ILK, including deficiencies in the glial network and basal lamina formation (Mills *et al.*, 2006). The deficiencies found in these mice resemble those of integrin β 1 conditional knockout mice, underlining the importance of the IPP complex for the integrin signalling cascade. Another report revealed that the five LIM domain containing protein PINCH shuttles between the cytoplasm and nuclei of Schwann cells and that PINCH becomes diffusely localized following nerve injury, suggesting that PINCH has a function as a signalling molecule in these cells (Campana *et al.*, 2003). Moreover, PINCH was also shown to interact with receptor tyrosine kinases (RTKs), thus coupling growth factor signalling with integrin signalling pathways.

Functional connection of the actin cytoskeleton with focal adhesions is necessary for normal Schwann cell differentiation. Notably, it has been shown that depolymerization of actin filaments using cytochalasin D leads to changes in Schwann cell morphology and myelin gene expression in a dose dependent manner (Fernandez-Valle *et al.*, 1997). The authors suggested that filamentous actin is part of a signalling pathway which connects the extracellular matrix to myelin expression, since at lower doses cytochalasin D efficiently blocked their expression independently from morphological changes, which became obvious when higher cytochalasin D doses were applied.

Taking together, the differentiation of Schwann cells depends on laminin/integrin signalling, which in turn is linked to the actin cytoskeleton to permit morphological changes to proceed and myelin genes to become expressed.

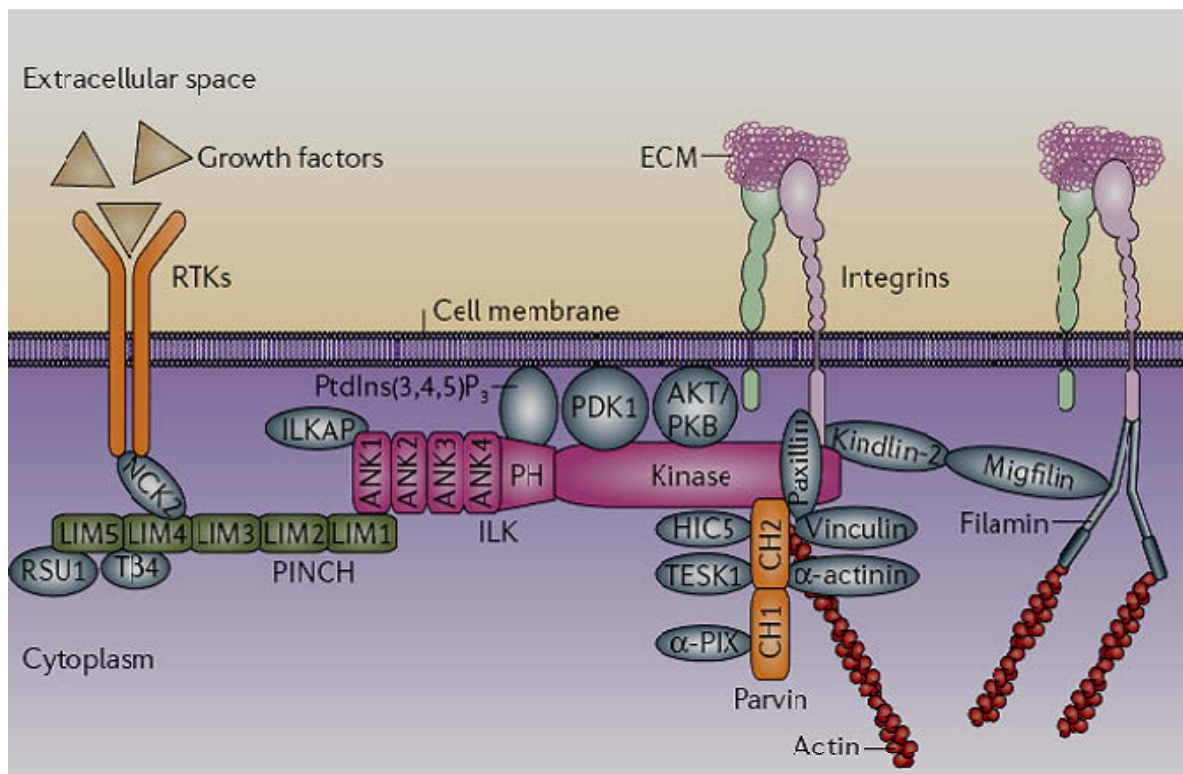


Figure 4. Integrins connect the extracellular matrix with the actin cytoskeleton. The cytoplasmic tail of the β subunit of integrin heterodimers binds to the ILK-PINCH-parvin (IPP) complex at focal adhesion sites. This complex consists of integrin linked kinase (ILK), the LIM domain containing protein particularly interesting Cys-His-rich protein (PINCH) and parvin. Parvins connect the IPP complex with the actin cytoskeleton, either by direct binding or together with paxillin or HIC5. Assembly of the actin cytoskeleton leads to subsequent activation of signalling pathways and thus to changes in gene expression. The IPP complex also interacts with the actin cytoskeleton through binding to migfilin and filamin. PINCH binds to receptor tyrosine kinases (RTKs) through the Src-homology-2-SH3 adaptor NCK2, thus coupling the growth factor signalling with integrin signalling. According to Legate *et al.*, 2006.

2.4 Development of the peripheral nervous system and peripheral glial cell differentiation

2.4.1 Timescale of Schwann cell development

A variety of distinct cell types derives from a precursor population called the neural crest (Le Douarin and Kalcheim, 1999; Knecht and Bronner-Fraser, 2002). The neural crest cells delaminate from the neural tube at the timepoint when the neural tube closes. Some of these cells give rise to skin melanocytes, skeletal elements and smooth muscles and neurons, while others form the precursors of the peripheral glial lineage.

During rat embryonic development, neural crest cells at embryonic day 10/11 (E10/11) detach from the neural tube and migrate through immature connective tissue into the periphery. Schwann cell precursor cells at first arise approximately at E14/E15. These cells become closely associated with axon bundles. At this timepoint, the developing nerve lacks both connective tissue and blood vessels.

Immature Schwann cells arise in rat nerves from about E17/18 until birth (Jessen *et al.*, 1994; Dong, 1995; reviewed by Jessen and Mirsky, 2005). At this stage the nerve is characterized by the so called perineurium, which is composed of connective tissue and surrounds bundles of immature Schwann cells which are tightly associated with axons and develop into nerve fibers. It also consists of endoneurial fibroblasts as well as endoneurial blood vessels. Terminal Schwann cell differentiation, which proceeds during the first postnatal weeks, depends on the axonal diameter the Schwann cell is randomly associated with. In the case of small diameter axons, Schwann cells develop into non myelinating Schwann cells, whereas myelinating Schwann cells arise from Schwann cells which are associated with large diameter axons. Thus paracrine signalling from the axon to the Schwann cell determines the ensheathment fate of axons (Michailov *et al.*, 2004).

2.4.2 Differentiation of myelinating Schwann cells

The differentiation of myelinating Schwann cells involves several distinct steps and lasts during the embryonic development until the first postnatal weeks. During the embryonic development, multipotent neural crest cells give rise to Schwann cell precursors, which migrate along axons and ensheath a couple of axons while developing into immature Schwann cells (an overview is depicted in Fig. 5). During the postnatal development, differentiating cells either stay associated with several axons and become non myelinating Schwann cells, or as a consequence of a segregation process, they sort out one large diameter axon to form a 1:1 relationship with this axon so as to myelinate it and become myelinating Schwann cells. Myelin formation also includes a spiral wrapping process of one Schwann cell protrusion around the segregated axon (reviewed in Arroyo and Scherer, 2000; Poliak and Peles, 2003; Salzer, 2003). Exclusion of cytoplasm is accompanied by expression of myelin proteins, leading to the formation of compact myelin sheaths. Thus the timing of myelination and accompanying morphological changes are strictly regulated.

Schwann cell differentiation from the neural crest involves fully reversible as well as irreversible steps. The generation of Schwann cell precursors and immature Schwann cells stages from neural crest cells are irreversible *in vivo*. Nevertheless, it has been reported that *in vitro* Schwann cell precursors can be induced to generate neurons as well as melanocytes. The differentiation steps towards immature Schwann cells are characterized by extensive proliferation and apoptosis, which

implies that a cell number matching process is taking place. On the other hand, postnatal development is marked by cell cycle exit and protection against apoptosis. Even injuries of the PNS which are accompanied by axonal loss and thus lead to myelin breakdown do not induce broad glial apoptosis. Interestingly, in this case myelinating Schwann cells as well as non myelinating Schwann cells dedifferentiate to develop into immature Schwann cell like cells. Although myelination is the only differentiation step which is clearly linked to cell cycle exit (Stewart *et al.*, 1993), these cells reenter the cell cycle, get into contact with newly sprouting axons and are able to redifferentiate into myelinating Schwann cells, reflecting the highly plastic behaviour of these cells and underlining their function for the regeneration promotion of injured peripheral nerves (Son and Thompson, 1995).

2.4.3 Marker gene expression during Schwann cell differentiation

Single developmental stages during Schwann cell differentiation can be clearly defined using appropriate marker combinations (Jessen and Mirsky, 2005). For example, during embryonic development, only migrating neural crest cells and Schwann cell precursors express both the AP2 α transcription factor and α 4 integrin. Immature Schwann cells do not express these two markers but can be distinguished by the expression of S100 and GFAP, respectively. The postnatal initiation of the myelination program is characterized by the activation of the Krox20 transcription factor and the myelin proteins P0, PMP-22, MBP and PLP, which are not expressed in high concentrations by non myelinating Schwann cells. Additional criteria can be used to identify each stage of the Schwann cell lineage: Both Schwann cell precursors and immature Schwann cells can be distinguished from neural crest cells by their association with axons, while neural crest cells migrate and do not associate with axons. In culture, Schwann cell precursors survive in presence of neuregulin 1 (Nrg1), whereas neural crest cells become apoptotic in absence of extracellular matrix components such as laminin (Woodhoo *et al.*, 2004). In comparison to Schwann cell precursors, immature Schwann cells possess a basal lamina. Moreover, while Schwann cell precursor survival is, as mentioned above, dependent on axonal signals like Nrg1, immature Schwann cells develop an autocrine survival circuit hence becoming independent from axonal signals (Meier *et al.*, 1999). The lack of apoptosis is of particular importance considering the regeneration promoting

role of Schwann cells after peripheral nerve injury or diseases of the peripheral nervous system.

Gliogenesis from the neural crest has been shown to depend on mechanisms similar to those observed during CNS glial development. Experiments revealed that Nrg1 and Notch repress differentiation into neurons thus favouring glial differentiation, while BMP2/4 promote the neuronal development (Shah *et al.*, 1994). Thus the spatial concentration of these proteins determines the fate decision of these multipotent cells. Nevertheless, it could not be demonstrated that Nrg1 and Notch can directly initiate glial development. Since gliogenesis follows neurogenesis during development, it appears that axonal signals are responsible for the glial fate decision and that these signals activate intracellular signalling cascades which lead to the expression of Schwann cell differentiation associated genes.

2.5 The secreted proteins Notch, Lgi4 and Nrg1 as well as the transcription factors Sox10, Krox20 and Oct-6 promote Schwann cell differentiation

Extrinsic as well as intrinsic signals control the differentiation and maturation of Schwann cells. For example, the length of internodes is controlled by the axonal diameter (Friede, 1980), but also Schwann cell intrinsic signalling plays an important role. The claw paw mutation, a 225 bp insertion in the Lgi4 gene, has been shown to lead to mutants with shorter internodes and delayed peripheral myelination (Henry *et al.*, 1991; Koszowski *et al.*, 1998; Bermingham *et al.*, 2006). The dependence on axonal signalling is also displayed by the fact that Schwann cells dedifferentiate *in vivo* upon loss of axons whereas in culture they do not differentiate at all. It appears that, as long as Schwann cells do not receive axonal signals, their differentiation is intrinsically inhibited. Transcription factors which were shown to be important for the progression along the Schwann cell lineage (Fig. 5; Fig. 6) will be described further below.

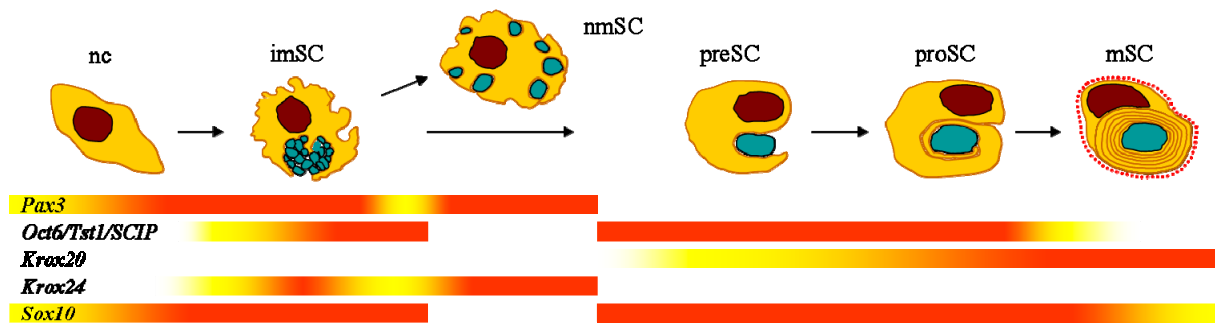


Figure 5. Schwann cell differentiation steps and differential regulation of Schwann cell related genes. Neural crest cells (nc) give rise to immature SCs (imSC) which contact several axons (blue). These cells either stay associated with few axons as non myelinating SCs (nmSC), or they segregate one large diameter axon and differentiate into myelinating SCs (mSC). Therefore, one protrusion of the SC designated to myelinate wraps around the axon in a radial growth and migration process during the premyelinating (preSC) and promyelinating (proSC) SC stage. Cytoplasm is excluded and myelin compacts. During differentiation, SC related genes are differentially expressed. Pax3 and Krox24 are upregulated to determine the nmSC fate, while upregulation of Oct-6 and Sox10 during the pre- and promyelinating stage and their subsequent downregulation as well as upregulation of Krox20 determines the mSC fate. According to Küry *et al.*, 2001.

2.5.1 Sox10

The SRY-related high mobility group transcription factor Sox10 is the only so far known gene the activation of which in neural crest cells is necessary for peripheral glial cells generation (Southard-Smith *et al.*, 1998; Britsch *et al.*, 2001). The importance of Sox10 is underscored by a high degree of sequence conservation among different species. Sox10 is expressed by cells of the Schwann cell lineage (Kuhlbrodt *et al.*, 1998), while it becomes downregulated in developing neurons. The influence of Sox10 concerning differentiation has been demonstrated with Sox10 knockout mice, which contain appropriate numbers of neural crest cells, whereas peripheral glial cells are missing due to increased apoptosis (Southard-Smith *et al.*, 1998; Paratore *et al.*, 2001; Britsch *et al.*, 2001). This implies that Sox10 is not required for early neural crest cell specification and migration, but for the specification of the Schwann cell lineage. Mutations of the Sox10 gene have also been found in humans who display abnormal neural crest development and hypomyelination of peripheral nerves (Pingault *et al.*, 2000; Inoue *et al.*, 2002). Further studies suggest additional involvement of Sox10 also peripheral myelination. Sox10 has the competence to directly regulate the expression of the myelin gene P0 and the glial gap junction component Connexin 32 (Cx32; Peirano *et al.*, 2000; Peirano and Wegner, 2000; Bondurand *et al.*, 2001), and a cooperation with other myelination transcription factors such as Krox20 and Oct-6 has been proposed (Kuhlbrodt *et al.*, 1998; Bondurand *et al.*, 2001).

2.5.2 Krox20

Regarding terminal differentiation of Schwann cells, the zinc finger transcription factor gene Krox20 (early growth response2, Egr2) has been shown to play a vital role. Mutations of the Krox20 gene lead to a block in the myelination onset and interrupt the activation of myelin genes (LeBlanc *et al.*, 2007). As a consequence, Schwann cells are arrested in the promyelinating stage (Topilko *et al.*, 1994). Indeed it could be demonstrated that Krox20 induces myelin genes in culture (Nagarajan *et al.*, 2001). Binding of Krox20 to the first intron of P0 has been shown to activate the P0 expression, and similar binding sites have been revealed in other myelin genes. Hence Krox20 is considered an important regulator of Schwann cell myelination. Interestingly it could be shown that enforced Krox20 expression activates myelin genes also in fibroblasts, implying a master function (Parkinson *et al.*, 2004). After initiation of myelination, Krox20 becomes expressed throughout lifetime. Ablation of the Krox20 gene expression has been shown to result in demyelination of nerves, revealing that also the maintenance of the myelinating stage is due to continued Krox20 expression (Topilko *et al.*, 1994; Decker *et al.*, 2006). Krox20 can bind to the Nab proteins Nab1 and Nab2 and this interaction has been shown to be crucial for myelin gene induction as well as repression of certain target genes, including Id2 and Id4, the expression of which has been shown to decline during PNS development after onset of myelination (Mager *et al.*, 2008; Le *et al.*, 2005). Mutations of Krox20 which either affect the Krox20 gene expression or the interaction of Krox20 with Nab proteins also play a role in human demyelinating diseases, including congenital hypomyelinating disease (Warner *et al.*, 1998; Desmazières *et al.*, 2008). Importantly, Krox20 expression is directly dependent on a combination of Sox10, Oct-6 and Brn2 transcription factor binding to the Krox20 enhancer, and Krox20 and Sox10 were suggested to act synergistically to induce myelin protein zero expression (LeBlanc *et al.*, 2006; Ghislain *et al.*, 2006). Interestingly, beneath the induction of myelin genes, further target genes of Krox20 comprise genes which encode for lipid and cholesterol biosynthesis enzymes, such as HMGCR, SCD and CYP51 (Nagarajan *et al.*, 2001). In addition it also was shown to regulate the SREBP transcription factor gene expression. which acts upstream of more than 20 lipid biosynthesis target genes (LeBlanc *et al.*, 2005). Taking together, Krox20 activation leads to the initiation of myelin gene expression and synergistically induces the expression of lipid

biosynthesis genes. Ablation of Krox20 inhibits the formation of myelin and also myelin maintenance is critically controlled by Krox20.

2.5.3 Oct-6

The Oct-6 (POU3f1, SCIP) transcription factor has been shown to be transiently upregulated before the onset of myelination, peaking at the promyelinating stage (Jaegle *et al.*, 2003). Knockout of Oct-6 leads to a transient delay of myelination (Jaegle *et al.*, 1996), and studies suggest that the related gene Brn2 compensates for this defect, since knockout of both Oct-6 and Brn2 leads to a more severe hypomyelinating phenotype (Jaegle *et al.*, 2003). It has been revealed that Oct-6 binds to a so called Schwann cell enhancer element, designated myelinating Schwann cell element (MSE), which is localized upstream of Krox20 and that this interaction leads to the initiation of Krox20 expression and hence to the subsequent activation of myelin genes (Ghislain *et al.*, 2002). Further reports suggest that Oct-6 can bind to Sox10 in culture (Kuhlbrodt *et al.*, 1998). Moreover, recent studies have shown that both Oct-6 and Brn2 synergistically interact with Sox10 while binding to the MSE and activating Krox20 (Ghislain *et al.*, 2006). Nevertheless, expression of Krox20 has been shown to occur even in Oct6/Brn2 double knockout mutants, suggesting that other members of the POU family of genes may compensate for this defect (Jaegle *et al.*, 2003).

2.5.4 Neuregulin (Nrg)

Designated to be the most important axonal signalling molecule, neuregulin 1 (Nrg1) and the Nrg1 receptors erbB2 and erbB3 play essential roles at several steps of PNS glial development and specification. Similar to Notch, paracrine signalling via Nrg1 inhibits the expression of neurons from the neural crest. Nevertheless, Nrg1 is not indispensable for the generation of Schwann cells, since generation of Schwann cells in cell cultures has been observed even in absence of this signal (Shah *et al.*, 1994). This observation has been challenged by the fact that Schwann cells in Nrg1 knockout mice are missing. To declare this discrepancy, it has been suggested that this lack is due to the survival and migration promoting effect of Nrg1. However, it has been demonstrated that Nrg1 promotes the differentiation of Schwann cell precursors towards immature Schwann cells.

Among several known isoforms for Nrg1, the transmembrane isoform Nrg1 Type III has been shown to be the most important. Nrg1 Type III is retained at the axonal surface and activates Schwann cell erbB receptors as well as PI3-kinase dependent signal transduction (Taveggia *et al.*, 2005). Schwann cell numbers are severely diminished in Nrg1 Type III knockout mice, while knockout of either Nrg1 Type I or Type II does not have an effect on Schwann cell precursor development (Meyer *et al.*, 1997; Garratt *et al.*, 2000a).

In comparison to Schwann cell precursors, immature Schwann cell survival does not depend on Nrg1 signals. Since Nrg1 becomes expressed during the whole lifetime, additional roles during the late development of Schwann cells and for the initiation and maintenance of myelination have been proposed and described. It has been reported that the concentration of axonal Nrg1 determines whether an axon becomes ensheathed to form Remak bundles or segregated and myelinated (Taveggia *et al.*, 2005; Nave and Salzer, 2006). Interestingly, forced expression of Nrg1 Type III in normally unmyelinated sympathetic neurons leads to their myelination, indicating an additional role for Nrg1 for the decision either to myelinate an axon or not (Taveggia *et al.*, 2005). But not only the ensheathment fate of axons is determined by Nrg1, also myelin thickness has been reported to depend on the Nrg1 concentration. Ablation of erbB2 or suppression of Nrg1 both result in myelin membranes with significant diminished numbers of lamellae, while overexpression of Nrg1 leads to hypermyelination of axons, thus underlining the importance of adequate Nrg1 signalling for proper myelination of peripheral nerves (Garratt *et al.*, 2000a; Garratt *et al.*, 2000b; Michailov *et al.*, 2004).

2.6 Negative regulators inhibit Schwann cell differentiation

In comparison to pure primary cultures of oligodendrocyte precursor cells (OPC) which spontaneously differentiate into oligodendrocytes, Schwann cells do not produce myelin in cultures in absence of axons. The terminal differentiation of Schwann cells is blocked and depends on certain axonal signals to overcome this intrinsic inhibition. The expression of these intrinsic inhibitors does not only play a role during the development of Schwann cells. They also have to be differentially expressed to allow de- and subsequent redifferentiation after peripheral injuries or during disease processes, which involve complex cell transformations (Jessen and Mirsky, 2005). Hence myelination is a result of both activation of myelin related genes

and repression of inhibitors of differentiation and has to be seen as a dynamic process (Fig. 6). Consequently, proteins must exist the expression of which is downregulated during the peripheral nerve development and regeneration. Indeed, recent investigations have led to the identification of such inhibitors thus confirming this hypothesis.

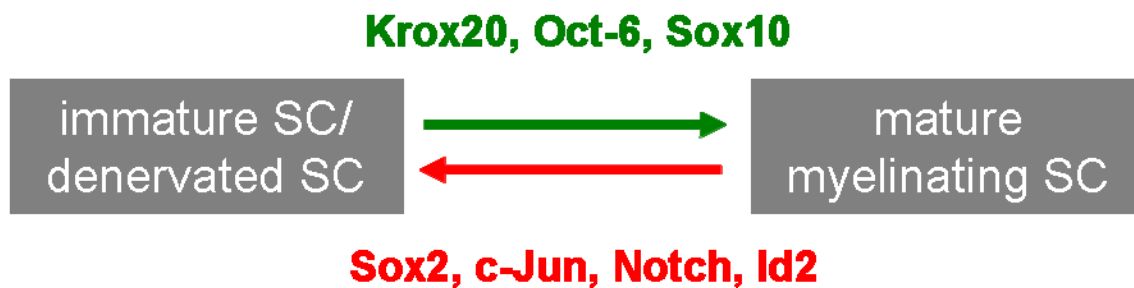


Figure 6. Positive and negative regulators determine the myelination state of Schwann cells. Myelination is a consequence of the adjusted expression of positive and negative Schwann cell (SC) differentiation regulators. Negative regulators are expressed during normal SC differentiation and inhibit myelination. Inhibition of negative regulators results in the expression of positive regulators and subsequent terminal differentiation of SCs. Following peripheral nerve injuries, negative regulators are reexpressed, following demyelination and dedifferentiation of SCs. Adaptation from Jessen and Mirsky, 2008, with modifications.

2.6.1 c-Jun

Demyelination is a prerequisite for a successful regeneration of peripheral nerves after injury. One of the molecules which have been demonstrated to play a role in this regard is the leucine zipper c-Jun. The expression of c-Jun was demonstrated to be downregulated during the peripheral nerve development and strongly induced after axotomy (Parkinson *et al.*, 2008). Consistent with this observation, enforced expression of c-Jun has also been shown to inhibit the myelination of DRG cocultures as well as the expression of myelin genes in presence of Krox20 overexpression or cAMP agonists (Parkinson *et al.*, 2008). Importantly, this study also indicates that the expression of c-Jun and Krox20 appears to be dependent on each other. Expression of c-Jun represses Krox20 expression and vice versa (Parkinson *et al.*, 2004; Parkinson *et al.*, 2008). A central role for c-Jun activation following peripheral nerve injury has been suggested, because lack of c-Jun expression delays the downregulation of myelin genes which is the first step regarding the dedifferentiation of Schwann cells. Hence, Krox20 mediated activation of the myelination program can be reverted by enforced c-Jun expression.

Interestingly, additional roles for c-Jun regarding Schwann cell differentiation have been postulated. It has been shown that c-Jun expression promotes Nrg-1

induced proliferation of Schwann cells and that downregulation of c-Jun uncouples the activation of Nrg-1 receptors from mitogenesis (Parkinson *et al.*, 2004). Further it has been demonstrated that c-Jun promotes the migration of Schwann cells (Yamauchi *et al.*, 2003) and that Krox20 mediated inactivation of c-Jun prevents Schwann cells from TGF- β induced apoptosis (Parkinson *et al.*, 2001). Thus it seems that early functions of c-Jun are the promotion of Schwann cell migration and to control their numbers, while functions of c-Jun in adult nerves comprise the activation of the dedifferentiation process following nerve injury.

2.6.2 Notch

Generally, gliogenesis follows neurogenesis during the embryonic development. Since both neurons and glial cells of the PNS arise from neural crest cells, an open question is how cell type acquisition is achieved. In this regard the expression of Sox10 was shown to be indispensable for the specification of the glial lineage (Southard-Smith *et al.*, 1998; Britsch *et al.*, 2001). In addition, Notch seems to play a vital role for the glial fate decision. Gaiano *et al.* observed a role for Notch1 in the promotion of radial glial cells in the murine forebrain (Gaiano *et al.*, 2000), and enforced *in vivo* expression of Notch has been shown to favour the generation of glial cells in the CNS (Wang and Barres, 2000). The expression of Notch at physiological levels *in vivo* has also been shown to specify the glial fate decision in the CNS as well as in the PNS (Taylor *et al.*, 2007). Ablation of RBPSUH, a downstream target gene of Notch signalling, results in mild defects in neurogenesis, but severe defects regarding gliogenesis. Thus, glial fate decision seems to be dependent on Notch activation. The importance of Notch for the PNS glial fate decision has been demonstrated *in vitro* with neural crest cultures. Activation of Notch in these cultures prevented the generation of neurons and promoted the differentiation into Schwann cell precursors (Morrison *et al.*, 2000). Even if the activation of the Notch signalling pathway was only transient, this fate decision was irreversible, suggesting that Notch signalling does not simply inhibit the neurogenesis. Nevertheless, other reports propose that is unlikely that the function of Notch is to instruct the glial fate (Jessen and Mirsky, 2005; Woodhoo *et al.*, 2007). They suggest a function later in the development, such as the promotion of Schwann cell precursor and of immature Schwann cell generation, control of Schwann cell precursor proliferation and maintenance of their the immature state. They also suggest that Notch acts as an

inhibitor of myelination, since activation of Notch following peripheral nerve injury accelerates the demyelination of Schwann cells. Consistent with this idea is the observation, that Krox20 expression represses Notch to allow the timely onset of myelination in the PNS (Mirsky *et al.*, 2008). On the other hand, it has also been reported that Notch activation prevents the differentiation of OPCs into myelinating oligodendrocytes (Wang *et al.*, 1998; Popko *et al.*, 2003), while ongoing Notch signalling in Schwann cells has been shown to cause the downregulation of Schwann cell differentiation associated markers. It thus appears that transient Notch activation supports glial specification, while it inhibits myelination at later developmental stages.

2.6.3 Sox2

Sox2 is another member of the SRY-related high mobility group transcription factors which plays a crucial role during Schwann cell development. Sox2 is expressed very early during the embryonic development and is thought to maintain and preserve the pluripotency and developmental potential of CNS stem cells (Li *et al.*, 1998). Importantly, it has recently been shown that ectopic expression of Sox2 together with the transcription factors Oct4, c-Myc and Klf4 is sufficient to reprogram both adult murine and human fibroblasts in order to generate pluripotent stem cells (Takahashi *et al.*, 2006; Park *et al.*, 2008). The expression of Sox2 in the neural crest is biphasic. Sox2 is downregulated during neural crest formation and migration of neural crest cells. Either Sox2 expression remains low and supports the generation of neurons, or Sox2 expression increases again resulting in maintenance of glial specification and proliferation. In line with this, constitutive expression of Sox2 has been shown to prevent neuronal differentiation, while suppression of Sox2 leads to cell cycle exit and onset of neuronal differentiation (Graham *et al.*, 2003). Recently, Le *et al.* demonstrated that the Sox2 expression profile is associated with the immature Schwann cell state. Sox2 expression is downregulated immediately before myelination onset, and enforced expression of Sox2 either in Schwann cell cultures or DRG cocultures infected with a Sox2 overexpression plasmid significantly downregulated myelin genes and inhibited myelination (Le *et al.*, 2005). It could also be shown that Sox2 expression is upregulated following crush lesions of peripheral nerves, indicating a function for the dedifferentiation of Schwann cells. The same study revealed that Sox2 expression was abnormally elevated in Schwann cells of mice with a conditional knockout of Krox20, which results in hypomyelination of

peripheral nerves (Le *et al.*, 2005). These results indicate that Sox2 is suppressed, either directly or indirectly, by Krox20. On the other hand, Sox2 overexpression in Schwann cell cultures diminishes the expression of Krox20 and subsequently also of myelin genes. Thus it appears that Krox20 and Sox2 expression, similar to Krox20 and c-Jun expression, inhibit each other. It has been suggested that c-Jun controls Sox2 levels and that some of the inhibitory effects of c-Jun are channelled by Sox2 (Parkinson *et al.*, 2008). Other studies indicate that Sox2 acts downstream of Notch (Wakamatsu *et al.*, 2004). Taken together, Sox2 expression is crucial to specify the glial fate from neural crest cells. During Schwann cell differentiation, Sox2 inhibits the terminal differentiation and maintains the proliferation of immature Schwann cells.

2.6.4 Id and basic helix-loop-helix (bHLH) proteins

Differentiation of numerous tissues is the result of temporarily ordered expression of transcription factors of the basic helix-loop-helix (bHLH) family. This family consists of class I bHLH proteins, designated E proteins, which are expressed ubiquitously and tissue specific class II bHLH proteins. Class I bHLH proteins heterodimerize with class II bHLH proteins, allowing the binding of the basic region the E box sequence on DNA. In contrast to E proteins, the class II bHLH proteins are expressed tissue specifically, thus leading to the activation of a certain subset of target genes in a tissue specific manner and subsequent differentiation.

Generally, the related Id (inhibitors of differentiation) HLH proteins are thought to interfere with tissue differentiation (reviewed by Norton *et al.*, 1998). Binding of Id proteins, which lack the basic region, to bHLH proteins prevents DNA binding and subsequent target gene expression. A correlation between myelin gene induction and Id protein downregulation has been reported, suggesting that Id proteins repress myelin promoter activity (Thatikunta *et al.*, 1999). This is in line with the observation that following axotomy Id1 and Id2 HLH proteins are induced and subsequently downregulated during the redifferentiation of Schwann cells (Stewart *et al.*, 1997). A function for Id2 as an inhibitor of oligodendrocyte differentiation has been demonstrated (Wang *et al.*, 2001), and recently it has been demonstrated that Krox20 in association with Nab proteins not only activates myelin genes, but also suppresses the expression of Id2 and Id4 (Mager *et al.*, 2008). These data imply that Id proteins serve as inhibitors of Schwann cell differentiation.

2.6.5 p57kip2 is a target gene of the bHLH protein Mash2

The existence of so called E-box sequences in the promoter sequences of Schwann cell differentiation related genes and the observation that Id proteins inhibit Schwann cell differentiation suggest that peripheral nerve specific class II bHLH proteins exist and act on Schwann cell differentiation. So far only one class II bHLH protein, namely mammalian achaete scute 2 (Mash2), has been shown to be expressed in Schwann cells. Analysis of crushed sciatic nerves revealed that the expression of Mash2 is regulated both during Schwann cell differentiation and regeneration of peripheral nerves (Küry *et al.*, 2001; Küry *et al.*, 2002). For Mash2 an expression profile similar to that of Krox20 was shown. It is dynamically expressed in Schwann cells during peripheral nerve development and transiently downregulated after nerve crush (Küry *et al.*, 2001; Küry *et al.*, 2002). Transient overexpression of Mash2 in Schwann cells and subsequent array analysis revealed four promising Mash2 target genes. Among these candidates were the promyelinating factors CXCR4 and Krox24, the inflammation and immune response associated gene Mob-1 and the cyclin dependent kinase inhibitor (CKI) p57kip2. p57kip2 was found to be upregulated in Mash2 overexpressing cells and transiently downregulated following peripheral nerve crush (Küry *et al.*, 2002). Although CKIs encode for cell cycle inhibitors, p57kip2 expression was found to be downregulated early during postnatal development, implying that cell cycle inhibition is not the primary function for this gene during peripheral glial development. This led to the decision to focus on p57kip2 and to investigate whether p57kip2 expression is functionally involved in Schwann cell differentiation, implying cell cycle control.

2.7 The mammalian cell cycle and its impact on Schwann cell differentiation

2.7.1 Cell cycle progression is positively regulated by the coordinated activity of cyclin dependent kinases (CDKs) and inhibited by binding of CDKs to cyclin dependent kinase inhibitors (CKIs)

As a member of the cip/kip family of genes, p57kip2 is known to act as a regulator of the mammalian cell cycle by inhibition of cyclin dependent kinases (CDKs). Dividing cells move through four phases of the cell cycle, namely G1- or prereplicative phase, S- or synthesis phase, G2- or premitotic phase and M- or mitotic phase (Fig. 7). One prerequisite for a successful cell cycle is the replication of important cell components, including DNA. Replication of DNA and distribution into two cells are temporarily

separated processes. While replication of DNA occurs in the S-phase, distribution of chromatids arises in the M-phase of the cell cycle. These phases are separated from each other by two G-phases, the G1-phase and the G2-phase. Mitosis cannot start until DNA has been replicated, while DNA replication cannot be initiated as long as the cell performs mitosis. Thus several checkpoint proteins exist the expression of which is alternating during cell cycle progression (Nguyen *et al.*, 2006; Besson *et al.*, 2008). Control of cell proliferation in mammals is complex and depends on extracellular signals within a tissue, mitogens or anti-mitotic agents, which orchestrate either proliferation or proliferation stop. Cells are susceptible for mitogens until they reach the R- or restriction point in the late G1-phase. Upon reaching that point, cells do no longer respond to mitogens and accomplish the cell cycle, until they enter the G1-phase again. As a response to injuries or application of mitogens, even quiescent cells in the G0-phase can be induced to reenter the G1-phase and to accomplish the complete cell cycle.

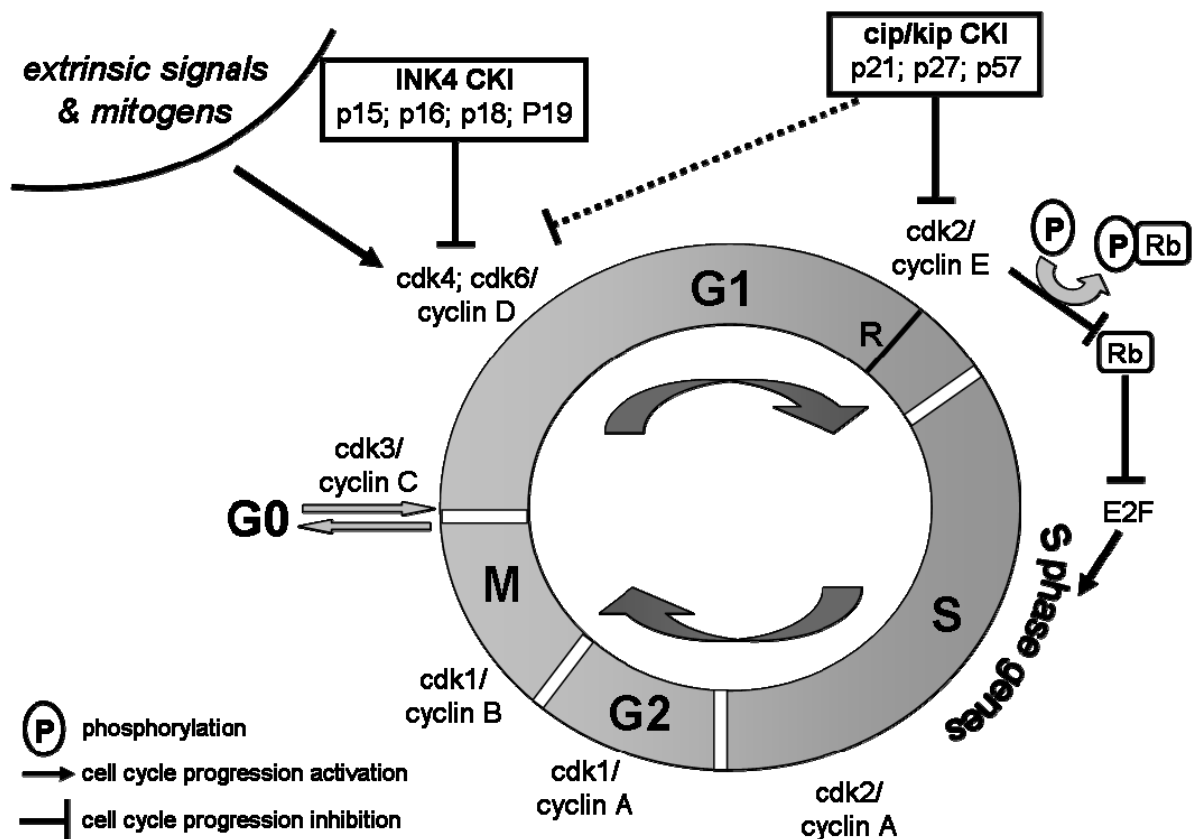


Figure 7. Control of the mammalian cell cycle. In response to extrinsic mitogenic stimuli, mammalian cells progress through the four phases of the cell cycle, namely G1-, S-, G2- and M-phase. Presence of mitogens is necessary until the restriction point (R). The transition from G1 to S-phase needs phosphorylation of the retinoblastoma protein (pRb), hence repression of E2F transcription factors by pRb represents the molecular basis for the R-point. Cyclin dependent kinases (CDKs) are activated by binding to cyclins. As heterodimers, the

cyclin/CDK complexes phosphorylate pRb, thus promoting cell cycle progression. Opposing, cyclin dependent kinase inhibitors (CKIs) bind to cyclin/CDK complexes and inhibit the phosphorylation of pRb, thus acting as inhibitors of the cell cycle. According to Nguyen *et al.*, 2006, with modifications.

To date, the retinoblastoma tumour suppressor protein (pRb) is thought to be the molecular basis for the R-point (Pardee *et al.*, 1989). Phosphorylation and inactivation of pRb is necessary for G₀ exit, entry into G₁ phase and completion of the cell cycle (Sherr *et al.*, 1995). Phosphorylation interrupts binding and hence repression of transcription factors, such as E2F1, by pRb (Sherr *et al.*, 1995; Stevaux and Dyson, 2002). As a consequence, the activation of E2F1 leads to the transcription of several genes required for S-phase entry and subsequent DNA synthesis, including cyclin E. Three classes of cyclin/CDK complexes are known to collaborate in order to phosphorylate pRb (Morgan *et al.*, 1995; Ren and Rollins, 2004). These are cyclin C/CDK3 complexes, which phosphorylate pRb at G₁-phase entry (Ren and Rollins, 2004), cyclin D/CDK4 and cyclin D/CDK6 complexes, which phosphorylate pRb in the early G₁-phase (Sherr *et al.*, 1994a) and cyclin E/CDK2 complexes, which phosphorylate pRb in the late G₁-phase (Ohtsubo *et al.*, 1995). Thus cell cycle progression is tightly regulated by coordinated activities of CDKs.

Not only cell cycle progression, but also inhibition of the cell cycle must be regulated. CDK activity is inhibited as a consequence of CDKs binding of to CKIs. Two families of CKIs are known, namely the INK4 family of genes, characterized by tandemly repeated ankyrin motifs and consisting of p15INK4b, p16INK4a, p18INK4c and p19INK4d, and the cip/kip family of genes, which is characterized by a highly conserved CDK binding domain and consists of p21Cip1, p27kip1 and p57kip2 (Sherr and Roberts, 1999). So far nine different CDKs and ten different cyclins have been found in mammalian cells. Among the cyclins, cyclins D1, -D2 and D3 are the first the expression of which becomes induced after stimulation of cells with mitogens. While INK4 family members only bind to CDK4 and CDK6, Cip/Kip family members are able to bind to complexes consisting of cyclin D, -E, -A and CDK2, 4 and 6.

It seems that different proliferative and anti-proliferative signals lead to the expression of certain subsets of CKIs during proliferation or as response to stress. For example, p21Cip1 mediates G₁ arrest when DNA damage occurs (El-Deiry *et al.*, 1993; Gartel and Tyner, 1999), while p27kip1 expression is high in mitogen starved cells and is rapidly downregulated when cells reenter the cell cycle (Besson *et al.*, 2006; Coats *et al.*, 1996). In line with this finding, the abundance of cyclins and CKIs

is also controlled by proteolytic mechanisms mediated through the ubiquitin proteasome pathway (Wang *et al.*, 1999; Nakayama *et al.*, 2001; Bornstein *et al.*, 2003). Thus different combinations of positive and negative signals control proliferation, including expression of cyclins, CDKs and CKIs as well as their degradation by the ubiquitin proteasome pathway.

2.7.2 p21cip1 cooperates with PCNA to control the DNA replication

The p21cip1 protein has been discovered simultaneously by several groups in 1993 and described as potent inhibitor of CDK activity (Gu *et al.*, 1993; Harper *et al.*, 1993; El-Deiry *et al.*, 1993; Xiong *et al.*, 1993a). Since knockout of p21cip1 does not lead to gross developmental defects or spontaneous malignancies (Deng *et al.*, 1995), it seems that the growth and differentiation control function of p21cip1 is redundant and can thus be fulfilled by other CKIs. Nevertheless, overexpression of p21cip1 has been shown to induce irreversible growth arrest and senescence (Sherr *et al.*, 1999), while inhibition increases cellular proliferation (Gartel *et al.*, 2005). A specific function for p21cip1 is the mediation of p53 induced growth arrest following DNA damage. Independently from p53, p21cip1 has been shown to be upregulated during the terminal differentiation of certain cell types (Parker *et al.*, 1995), and enforced expression of p21cip1 leads to proliferation stop of human brain, lung and colon tumour cells (El-Deiry *et al.*, 1993). Interestingly, the sequence of p21cip1 contains a proliferating cell nuclear antigen (PCNA) binding motif. It has been shown that p21cip1 exists in a quaternary complex consisting of a cyclin, a CDK, PCNA and p21cip1, which allows the direct repression of replication even in absence of CDKs (Li *et al.*, 1994; Shivji *et al.*, 1994; Waga *et al.*, 1994). Recently it has been discovered that p21cip1 also controls the proliferation of stem cell derived neuronal precursor cells in the adult dentate gyrus (Pechnick *et al.*, 2008), revealing that the functions of this protein are not restricted to the embryonic development.

2.7.3 p27kip1 controls the proliferation of a variety of cell types

p27kip1 has been detected as cyclin D1/CDK4 and cyclin E/CDK2 binding protein using yeast protein interaction screens (Polyak *et al.*, 1994a; Polyak *et al.*, 1994b; Toyoshima and Hunter, 1994). The binding of p27kip1 to CDKs has been revealed to occur in a 1:1 stoichiometry (Hengst *et al.*, 1998), and it could be shown that overexpression of p27kip1 interferes with CDK associated cell cycle progression,

leading to G1 arrest of cells. p27kip1 is induced in mitogen starved cells as well as following antiproliferative signals (Reynisdottir *et al.*, 1995). Moreover, it has been demonstrated that cell-cell contact and TGF- β induced cell cycle arrest are mediated by binding of p27kip1 to cyclin E/CDK2 complexes (Polyak *et al.*, 1994a). However, contact inhibition and TGF- β induced cell cycle arrest was also apparent in p27kip1^{-/-} cells (Nakayama *et al.*, 1996), again suggesting that p27kip1 and p21cip1 share many functions. Knockout of p27kip1 leads to an increased body size of mice, attributable to a total cell number increase. Organ hyperplasias, hyperplasia of the intermediate lobe of the pituitary and pituitary tumours as well as female infertility, probably due to impaired development of ovarian follicles, have been observed, reflecting a disturbance of the hypothalamic-pituitary-ovarian axis. The multiplicity of organ abnormalities reveals that p27kip1 acts to regulate a variety of different cell types (Kiyokawa *et al.*, 1996; Nakayama *et al.*, 1996; Fero *et al.*, 1996). Interestingly, some of the p27kip1 knockout mice malformations have also been observed in pRb knockout mice, suggesting that both factors indeed act in the same pathway.

Cristallographic investigations revealed that p27kip1 binds to cyclin A through a groove consisting of conserved cyclin-box residues, while binding to CDK2 leads to insertion into the catalytic cleft, hence mimicking ATP (Russo *et al.*, 1996). The high sequence homology of the CDK binding domain between p27kip1, p21cip1 and p57kip2 suggests that CKIs binding to CDKs is conserved among the cip/kip family of genes.

2.7.4 p57kip2 contains a domain structure which is distinct from all other CKIs and its function is thus not redundant

The 57 kD protein p57kip2 has been isolated by screening of a mouse cDNA expression library (Lee *et al.*, 1995) and using the two hybrid system (Matsuoka *et al.*, 1995). It was identified due to its partial similarity to p27kip1 as a CDK inhibitor belonging to the cip/kip family of genes. Three splice variants of mouse and rat p57kip2 have been reported, differing in the start regions of the open reading frame. p57kip2 includes a domain structure which is unique among the members of the cip/kip family. It consists of four different domains (Fig. 8), namely the N-terminal CDK inhibitory domain which binds to cyclin/CDK complexes, followed by a LIM domain binding proline rich region containing 28% proline, an acidic domain containing 36% glutamic or aspartic acids in tandem repeats and a C-terminal QT

(glutamine and threonine rich) domain which contains the nuclear localization signal and has sequence similarity with p27kip1 but not with p21Cip1. In contrast, the CDK inhibitory domain of p57kip2 has a high sequence similarity with both p21Cip1 and p27kip1, revealing its described function as a CDK inhibitor (Lee *et al.*, 1995; Matsuoka *et al.*, 1995).

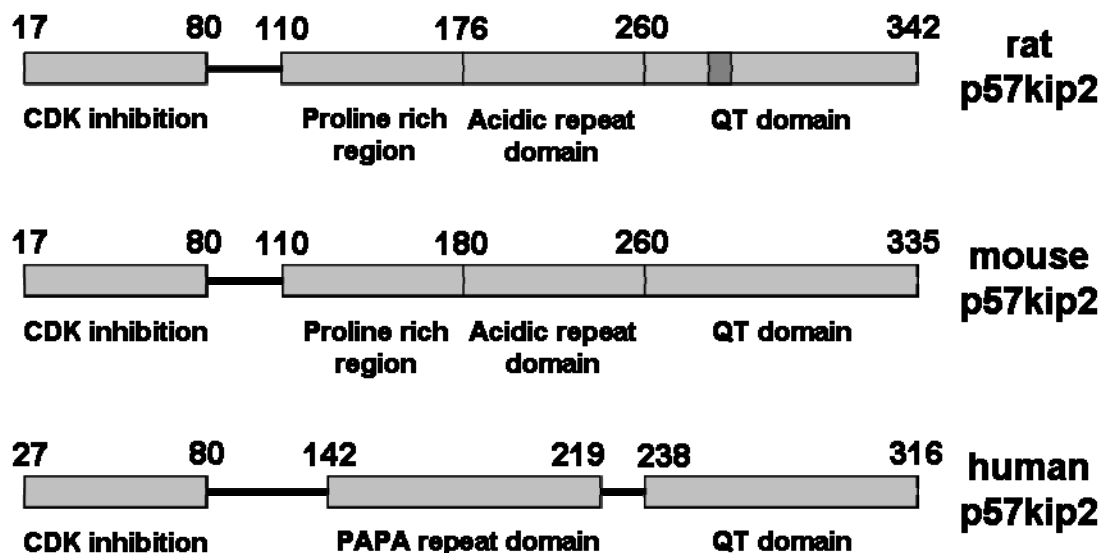


Figure 8. Domain structure of p57kip2 and species comparison. The domain structure of the rat, mouse and human ortholog proteins of p57kip2 is shown. Each protein consists of a highly conserved CDK inhibitory region. Proline rich region, acidic repeat domain and QT domains are also highly conserved between rat and mouse. Instead of the proline rich region and the acidic repeat domain, the mid-portion of the human ortholog consists of a proline-alanine repeat domain (PAPA repeat domain). The dark grey box within the rat QT domain represents the 12 amino acid stretch that results from alternative splicing. Adaptation from Potikha *et al.*, 2005, with modifications.

Mouse and rat p57kip2 sequences share 91% of DNA sequence and 88% of protein sequence similarity. This is in contrast to sequence similarities between rat and human sequences, which share only 81% of DNA sequence and 55% of protein sequence similarities (Potikha *et al.*, 2005; Fig. 8). The main difference between mouse, rat and human sequences lies within the central domain. While the N-terminal and the C-terminal domains are homologous among these species, human p57kip2 lacks the proline rich and the acidic domain, but contains a region with repeats of proline and alanine, called PAPA repeat domain. This PAPA repeat domain is thought to be of additional importance for the ability of p57kip2 to inhibit growth, since deletion of four amino acids within this region interferes with this ability (Tokino *et al.*, 1996). The discrepancy between the central domains of these genes suggests that it might have divergent functions among the species (Matsuoka *et al.*, 1995; Matsuoka *et al.*, 1996).

p57kip2 has been shown to be a potent inhibitor of G1/S phase transition by binding to cyclin E/CDK2, cyclin D2/CDK4, cyclin A/CDK2 and to a lesser extent to cyclin B/Cdc2 (Lee *et al.*, 1995). This protein is predominantly localized in the nucleus. In sharp contrast to p21cip1 and p27kip1, which are expressed ubiquitously, p57kip2 expression is restricted to certain tissues. Human and mouse p57kip2 transcripts were detected in the placenta, skeletal muscle, heart, kidney, pancreas, testis, eye and in the brain (Lee *et al.*, 1995; Matsuoka *et al.* 1995). Since most of the p57kip2 expressing cells are terminally differentiated, a differentiation associated function has been suggested.

The p57kip2 gene is located on mouse chromosome 7F4, rat chromosome 1q42 and human chromosome 11p15.5, regions which have been shown to contain several genes the expression of which is controlled by imprinting. Imprinting is known to be a general mechanism to control embryonic growth (Andrews *et al.*, 2007). Indeed, p57kip2 was shown to be only maternally expressed while the paternal allele is methylated and thus repressed (Hatada and Mukai, 1995; Matsuoka *et al.*, 1996). Mutations of genes within these regions have been reported to cause several tumours, including breast, bladder, lung, ovarian and kidney carcinomas, indicating that p57kip2 could act as a tumour suppressor. Also several kinds of tumours associated with childhood seem to be caused by mutations within these regions, including adrenocortical carcinoma, rhabdomyosarcoma and Wilms' tumour (Reid *et al.*, 1996; Orlow *et al.*, 1996; Hatada *et al.*, 1996). Numerous reports revealed an implication of p57kip2 in Beckwith Wiedemann Syndrome (BWS; Hatada *et al.*, 1996b; Zhang *et al.*, 1997; Lee *et al.*, 1997), which is characterized by several abnormalities, including gigantism, enlarged organs and an increased risk of childhood tumours. These developmental defects can be attributed to the loss of cell cycle control. Nevertheless, mutations of p57kip2 seem to be rare in BWS, while a decreased expression of p57kip2 has been detected in many BWS patients, indicating a dose dependent effect. This dose dependency was also suggested for the involvement of p57kip2 in tumourigenesis of gastric cancers, in which a significantly decreased amount of p57kip2 mRNA has been found (Shin *et al.*, 2000). In line with this, additional copy numbers of p57kip2 lead to embryonic growth retardation, accompanied by 30% loss of weight and embryonic death, while loss of p57kip2 results in 11% heavier embryos (Andrews *et al.*, 2007).

Importantly, among all CKIs, ablation of p57kip2 is the only one which leads to severe developmental aberrations and defects (Yan *et al.*, 1997; Zhang *et al.*, 1997; Takahashi *et al.*, 2000), suggesting a function beyond cell cycle progression and indicating that this ablation cannot be compensated by other CKIs. Genetic ablation of p57kip2 in knockout mice leads to embryonic and perinatal death, and mice suffer from cleft palate, reveal abnormal endochondral ossification accompanied by short limb generation and gastrointestinal abnormalities accompanied by loss of jejunum and ileum as well as body wall muscle dysplasia. The multiplicity of differentiation associated defects indicate a vital role for p57kip2 during embryogenesis. Only 10% of mutant mice survive beyond the weaning period and reveal severe growth retardation, immaturity of the testes and immaturity of the uterus. Interestingly, embryonic fibroblasts prepared from p57kip2 deficient mice show no increase in the proliferation rate, suggesting that in this particular cell type G1 arrest is in part independent from p57kip2 function (Takahashi *et al.*, 2000). p57kip2 expression in many tissues has been revealed to be restricted to embryogenesis, while expression of p27kip1 expression was maintained throughout adulthood, suggesting different functions regarding fate decision and cell cycle control (Nagahama *et al.*, 2001).

Among others, the expression of p57kip2 has been attributed to the cell cycle exit of distinct retinal progenitor cell populations and to the regulation of amacrine interneuron development (Dyer and Cepko, 2000; Gui *et al.*, 2007; Figliola *et al.*, 2008). On the contrary, it has also been proposed that p57kip2 regulates the differentiation of postmitotic midbrain dopamine neurons by binding to the orphan nuclear receptor Nurr1 (Joseph *et al.*, 2003), functions which are not directly related to cell cycle exit. Among the members of the cip/kip family of genes, p57kip2 consists of a structurally distinct proline rich region, which has been shown to bind to the LIM domain protein LIM-kinase 1 (LIMK-1; Yokoo *et al.*, 2003). Interestingly, Yokoo and colleagues have revealed that binding to LIMK-1 leads to the translocation of LIMK-1 from the cytoplasm into the nucleus, hence influencing the local concentration of LIMK-1. The interaction with the LIM domain of LIMK-1 suggests that further yet unknown p57kip2 binding partners exist which can be translocated into the nucleus, thus leading to changes of their subcellular concentrations. Thus non cell cycle associated functions for p57kip2 are thought to be based on interaction with binding partners. The fact that p57kip2 knockout leads to severe developmental aberrations and the finding that not only cell cycle related proteins bind to p57kip2 suggests

important development associated functions for p57kip2, which are probably due to the structurally distinct domains and hence cannot be compensated by other members of the Cip/Kip family of genes.

2.7.5 The function of cyclin, CDK and CKI expression during Schwann cell differentiation

Cell cycle exit is a prerequisite for the terminal differentiation of glial cells. While several reports revealed that CKIs and CDKs have an important function in the control of the oligodendrocyte cell cycle and as an intrinsic timer for the terminal oligodendrocyte differentiation (Casaccia-Bonnel *et al.*, 1997; Tikoo *et al.*, 1997; Dugas *et al.*, 2007), the existence of such an intrinsic timer in Schwann cells could not be shown. In contrast to oligodendrocytes, Schwann cell cycle exit strictly depends on extrinsic, axonal signalling. Of note, since Schwann cells proliferate both during development and as a response to peripheral nerve injuries, differential expression of cell cycle related genes can be expected. Indeed the proliferation of Schwann cells during the development is promoted by axonal Nrg1. Since axons degenerate and thus are missing in early phases after nerve injury, initiation of Schwann cell proliferation after injury seems to depend on different signals.

A specific function for the regulation of Schwann cell proliferation has been shown for the CKIs p16INK4a and p21cip1 (Atanasoski *et al.*, 2006). Expression of p21cip1 in Schwann cells can first be detected at postnatal day seven, a timepoint which is associated with Schwann cell proliferation stop. Interestingly, following peripheral nerve injury, p21cip1 expression is upregulated, suggesting additional functions for p21cip1. The function of p16INK4a regarding Schwann cell proliferation seems to be similar to p21cip1, but with a minor impact, suggesting redundant functions for these two CKIs (Atanasoski *et al.*, 2006). Consistent with its function as a CDK inhibitor, p27kip1 has been shown to be transiently but robustly upregulated in an early postnatal period. Following peripheral nerve injury, p27kip1 expression declines rapidly, indicating that this downregulation is necessary to commit Schwann cells to enter cell cycle and to start proliferation (Tikoo *et al.*, 1998; Shen *et al.*, 2008). A recent study revealed that p27kip1 inhibits the proliferation of Schwann cells and that p27kip1 levels increase following serum starvation but decline following forskolin administration, leading to subsequent proliferation of Schwann cells (Iacovelli *et al.*, 2007). These findings suggest an important proliferation associated function for

p27kip1. So far no data exist for p57kip2 regarding Schwann cell proliferation control, but the presence of p57kip2 in Schwann cells and its differential regulation following peripheral nerve injury has been described and suggests a differentiation associated function (Küry *et al.*, 2002). Interestingly, a function for p57kip2 within the intrinsic timer of terminal oligodendrocyte differentiation has been suggested recently (Dugas *et al.*, 2007).

In line with the finding that CKIs influence the Schwann cell proliferation, also cyclins and CDKs have been found to be involved. The expression of CDK2 increases during Schwann cell proliferation and is downregulated during cell cycle arrest. Interestingly, axonal membrane fractions induce the expression of CDK2, revealing the need for axonal signals to promote proliferation during development. Both CDK2 mRNA and protein expression are undetectable in adult sciatic nerves, suggesting a constant suppression. Nevertheless, the postnatal proliferation rate of mice lacking CDK4 has been found to be dramatically decreased, while embryonic proliferation and myelination of peripheral nerves was unaffected. Notably, ablation of CDK2 and CDK6 had no influence on the postnatal cell proliferation, indicating the need for specific CDKs during pre- and postnatal development, respectively (Atanasoski *et al.*, 2008).

The loss of Schwann cell proliferation in serum starved cultures is accompanied by a decrease of cyclin D1 and cyclin E1 expression. In contrast to this, serum induces high levels of cyclin D1 and cyclin E1 expression and, in presence of forskolin, reduces levels of p27kip1, leading to Schwann cell proliferation (Iacovelli *et al.*, 2007). Cyclin D1 has been shown to be upregulated following peripheral nerve injury. This upregulation is associated with Schwann cell proliferation and translocation of cyclin D1 into the nucleus. In line with this, ablation of cyclin D1 does not lead to development associated proliferation defects in Schwann cells, but interferes with Schwann cell proliferation after injury, indicating that cyclin D1 has a distinct function during the regeneration process after nerve injury. These data indicate that Schwann cell proliferation during development and during the regeneration process are regulated differently (Kim *et al.*, 2000; Atanasoski *et al.*, 2001).

2.7.6 CKI expression alters actin cytoskeletal dynamics by inhibition of the Rho signalling pathway

The Schwann cell wrapping process is based on radial growth and migration of one Schwann cell around an internode of an axon. This together with the expression of myelin genes have been shown to be dependent on the regulation of the actin cytoskeletal dynamics. Disruption of actin filaments by means of cytochalasin D interferes with Schwann cell differentiation in a dose dependent manner (Fernandez-Valle *et al.*, 1997), suggesting that both morphological changes and also the expression of myelin genes depend on the stabilization of actin filaments. Indeed, Schwann cell-axon interaction alone is not sufficient to induce Schwann cell myelination, as adhesion to the basal lamina was also shown to be necessary for myelination initiation (Fernandez-Valle *et al.*, 1993). This is likely due to integrin $\beta 1$, which interacts with laminins present in the basal lamina to initiate a downstream signalling cascade which connects integrin $\beta 1$ with the actin cytoskeleton (see section 2.3.4).

As indicated above, the function of CKIs is not only restricted to cell cycle control. The ability of these proteins to bind to several proteins appears to account for additional functions which are not directly related to cell cycle control (reviewed by Denicourt and Dowdy, 2004; Besson *et al.*, 2008). cip/kip proteins have been shown to be implicated in cell migration and protection against apoptosis (p27kip1, Ophascharoensuk *et al.*, 1998), they act as transcriptional regulators of MyoD and Neurogenin-2 (p57kip2, Reynaud *et al.*, 2000; p27kip1, Nguyen *et al.*, 2007) and promote cell fate determination (p57kip2, Dyer *et al.*, 2000; p57kip2, Joseph *et al.*, 2003; p27Xic1, Ohnuma *et al.*, 1999). Additionally, CKIs have also been implicated in regulation of cytoskeletal dynamics by binding to RhoA, Rho-kinase (ROCK) or LIMK-1 (p27kip1, Besson *et al.*, 2004; p21cip1, Lee and Helfman, 2004; p21cip1, Tanaka *et al.*, 2002; p57kip2, Yokoo *et al.*, 2003).

Proteins of the Rho family regulate multiple signalling pathways. Actin stress fiber formation has been shown to be regulated by the activity of the Rho signalling cascade, comprising RhoA, ROCK, LIMK-1 and cofilin. Also the assembly of focal adhesions and actin-myosin contractility are regulated by this signalling cascade (Etienne-Manneville and Hall, 2002). Actin filament assembly and degeneration is regulated by the activity of the downstream factors LIMK-1 and cofilin, respectively. Unphosphorylated cofilin destabilizes actin filaments, while phosphorylation and

inactivation of cofilin by LIMK-1 promotes the assembly and stability of filamentous actin (Arber *et al.*, 1998). Thus cytoskeletal dynamics, a general feature of cell migration and growth, depends on the temporal and spatial control of Rho signalling cascade members.

Remarkably, all members of the cip/kip family of genes have been shown to be implicated in inhibition of the Rho signalling cascade and hence in cytoskeletal dynamics regulation, although acting at distinct levels (Besson *et al.*, 2004a; Fig. 9). Cytoplasmic p21cip1 was shown to bind ROCK1 (Lee and Helfman, 2004; Tanaka *et al.*, 2002), which inhibits ROCK1 activity and consequently leads to neurite extension of hippocampal neurons and promotes recovery after spinal cord injury (Tanaka *et al.*, 2004).

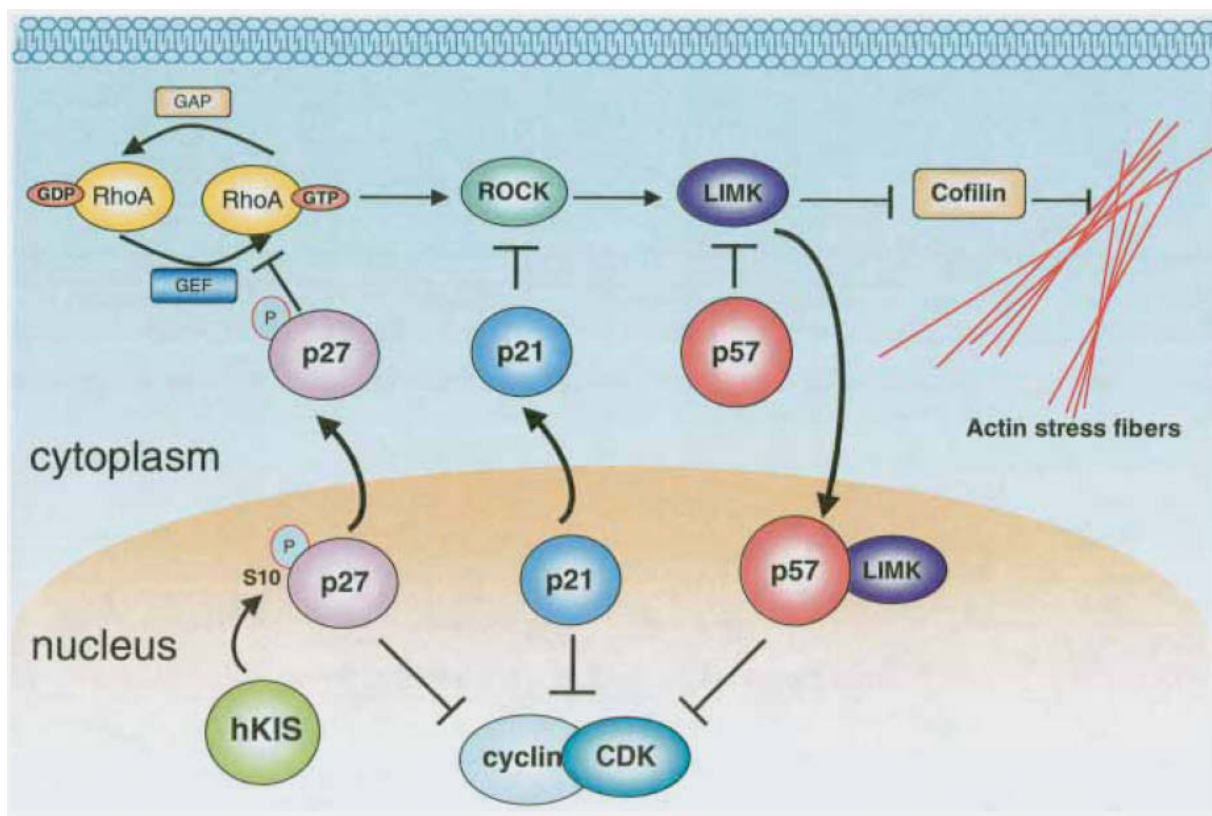


Figure 9. cip/kip proteins converge on the actin cytoskeleton by binding to RhoA, ROCK and LIMK. The members of the cip/kip family of genes are able to regulate the actin cytoskeletal dynamics through inhibition of the Rho-pathway. RhoA switches between an inactive and an active state. Guanine-nucleotide exchange factor (GEF) promoted binding of GTP to RhoA activates RhoA, enabling RhoA to activate Rho kinase (ROCK). Activated ROCK phosphorylates LIMK, which in turn subsequently phosphorylates and thus inactivates cofilin, leading to the formation of long actin filaments. Each of the cip/kip family members can bind to distinct proteins of the Rho-pathway in the cytoplasm. Nuclear export of p27kip1 necessitates the phosphorylation of Ser 10 by hKIS, and binding of p27kip1 to RhoA inhibits the activation of RhoA by GEFs. The RhoA downstream factor ROCK is inhibited by cytoplasmic p21cip1, while p57kip2 binds to LIMK and translocates LIMK from the cytoplasm into the nucleus, thus leading to higher levels of unphosphorylated and thus active cofilin and to favoured degradation of actin filaments. According to Besson *et al.*, 2004.

Expression of p27kip1 has been shown to induce migration of hepatocellular carcinoma cells, migration of neuronal progenitor cells into the subventricular cortex and to enhance the metastatic potential of melanoma cells (Nagahara *et al.*, 1998; Denicourt *et al.*, 2007; Kawauchi *et al.*, 2006; Nguyen *et al.*, 2007). Fibroblasts derived from p27kip1 knockout mice have an impaired motility which can be rescued by ROCK inhibition (Besson *et al.*, 2004). This motility defect could be shown to depend on an increase of RhoA activity which resulted in the accumulation of actin stress fibers. Indeed, it could be shown that p27kip1 interacts with RhoA and prevents RhoA activation by inhibition of guanine-nucleotide exchange factors (GEFs) supported binding of GTP.

The proline rich region of p57kip2 can bind to LIMK-1 (Yokoo *et al.*, 2003). The translocation of LIMK-1 from the cytoplasm into the nucleus leads to a remarkable loss of actin filaments due to a higher cofilin activity. Thus regulation of the p57kip2 expression can serve to determine the stability of actin filaments by shifting the subcellular localization of LIMK-1. In line with the observed function of p57kip2 regarding modifications of the actin cytoskeleton dynamics, also delayed migration of neurons in the cortical plate has been shown in p57kip2 knockout mutants, reflecting that p57kip2 expression is vital for proper neurogenesis.

2.8 Aim of this thesis

The rapid dedifferentiation of Schwann cells following traumatic injuries, their ability to redifferentiate and the lack of *in vitro* differentiation of these cells suggest that intrinsic inhibitors exist, the expression of which has to be downregulated during postnatal peripheral nerve development, dependent on the contact with axons. The molecular determinants for this regulation are poorly understood. Only few inhibitors of Schwann cell differentiation are known up to date, such as Sox2, c-Jun, Notch and Id2. However, loss of function of them is not sufficient to induce *in vitro* Schwann cell differentiation. Thus one major aim in Schwann cell biology is the identification of a main negative regulator of differentiation.

GeneChip array analysis of crush lesioned sciatic nerves revealed promising candidate genes which were dynamically regulated in response to the injury (Küry *et al.*, 2002). The aim of this thesis was to investigate whether one or several of these genes are functionally involved in peripheral glial differentiation.

In order to specifically screen for a function as inhibitor, a gene suppression approach was performed using RNA interference mediating vector constructs. In a first series of experiments, the functionality of these vector constructs was tested. Since these tests revealed that suppression of p57kip2 leads to morphological alterations, ongoing research was focused on this gene. The performance of these experiments aimed at the answering of following question:

“Is downregulation of p57kip2 gene expression a prerequisite for the initiation of the peripheral glial *in vitro* myelination program ?”

3. MATERIAL AND METHODS

3.1 Material

3.1.1 Animals

Sciatic nerves of newborn Wistar rats (P0) were used for the preparation of primary Schwann cell cultures, whereas postnatal Wistar rats of different developmental stages (P0, P1, P4, P6, P10, P14, P28, P90) were used for the preparation of RNA from sciatic nerves. The animals were bred within the animal facility of the Heinrich-Heine-University, Düsseldorf, under pathogen free and defined conditions (temperature 21°C; humidity 50%; 12 h light/dark cycle). Dry and pelleted animal food and water was available ad libitum. All animal handling procedures described were conducted in accordance with the German Animal Protection Law.

3.1.2 *E.coli* bacteria strains

Following *E.coli* strains were used for transformations:

One Shot TOP 10

Invitrogen

F- *mcrA* Δ (*mrr-hsdRMS-mcrBC*) Φ 80*lacZ* Δ M15

Δ *lacX74 deoR recA1 araD139 Δ (*ara-leu*)7697 *galU**

galK rpsL endA1 nupG

SURE2

Stratagene

e14⁻(*mcrA*⁻) Δ (*mcrCB-hsdSMR-mrr*)171 *endA1*

supE44 thi-1 gyrA96 relA1 lac recB recJ sbcC

umuC::Tn5 (Kan^r) *uvrC* [F' *proAB lacI*^q Δ M15 Tn10

(Tet^r) Amy Cam^r]

3.1.3 Reagents and buffers

3.1.3.1 Reagents

Reagent	Supplier
2-mercaptoethanol	Sigma
2-propanol	Merck
adenosine triphosphate (ATP)	Applied Biosystems
agarose	Sigma
aprotinin	Roche
arabinosyl cytosine hydrochloride (Ara-C)	Sigma
ascorbic acid	Merck
bacto agar	Gibco
bovine serum albumin (BSA)	Sigma
bromophenol blue sodium salt	Sigma
diaminobenzidine	Sigma
DAPI	Sigma
deoxynucleotide (dNTPs)	Applied Biosystems
dimethylsulfoxide (DMSO)	Sigma
ethylenediaminetetraacetic acid (EDTA)	Sigma
ethanol abs.	Merck
Fluoromount G	Southern Biotech
forskolin	Sigma
glacial acetic acid	Merck
glycerol	Merck
glycogen	Roche
leupeptin	Roche
hydrochloric acid (HCl)	Merck
LiChrosolv H ₂ O	Merck
magnesium acetate (Mg-acetate) tetrahydrate	Sigma
pefabloc	Roche
pepstatin	Roche
potassium hydroxide (KOH)	Sigma
sodium hydroxide (NaOH)	Merck
sodium chloride (NaCl)	Merck
sodium deoxycholate	Sigma
sodium dodecyl sulphate (SDS)	Merck
trishydroxymethylaminomethan (Tris)	Merck
Trizol®-Reagent	Gibco
trypton	Difco
xylencyanol FF	Sigma
yeast extract	Difco

3.1.3.2 Buffers

3.1.3.2.1 Buffers, solutions and reagents for cell culture

Buffer	Supplier/Composition
Dulbecco's phosphate buffered saline (PBS)	PAA laboratories
PBE	PBS (PAA laboratories) 2 mM EDTA 0.5 % BSA
trypsin (0.05% trypsin + 0.02% EDTA in PBS)	Gibco
poly-D-lysine (PDL), 10 mg/ml	Gibco
collagen type I	BD Biosciences
L-glutamine, 200mM	Gibco
penicillin/streptomycin, 5000 U (pen/strep)	Gibco
forskolin	Sigma
bovine pituitary extract (BPE)	PAA laboratories
baby rabbit complement	Cedarlane
cell dissociation solution, non enzymatic	Sigma
mouse-anti-Thy1.1 monoclonal IgM antibodies	Serotec

3.1.3.2.2 Buffers and solutions for molecular biology

Buffer	Supplier/Composition
TAE buffer, 50x stock solution	121 g Tris 28.55 ml glacial acetic acid 50 ml 0.5 M EDTA, pH8.0 ddH ₂ O ad 500ml
DNA blue marker	0.1% bromophenol blue 0.1% xylencyanol FF 50% glycerol In 1x TAE buffer
DAB working solution	DAB (4 mg/ml) dissolved 1:20 in PBS
H ₂ O ₂ working solution	1% H ₂ O ₂ in A.dest
DAB staining solution	H ₂ O ₂ working solution 1:250 dissolved in DAB working solution
Oligonucleotide annealing buffer	100 mM potassium acetate 30 mM HEPES-KOH, pH 7.4 2 mM Mg-acetate
RIPA buffer	25 mM Tris-HCl, pH 7.6 150 mM NaCl 1% NP-40 0.1% sodium deoxycholate
Lower gel buffer for SDS gels (pH 8.8)	1.5 M Tris 0.4% SDS pH adjusted to 8.8 using HCl ddH ₂ O ad 100 ml

Buffer	Supplier/Composition
Upper gel buffer for SDS gels (pH 6.7)	0.5 M Tris 0.4% SDS pH adjusted to 6.7 using HCl ddH ₂ O ad 100 ml
10x SDS gel running buffer (pH 8.3)	0.25 M Tris 2M glycine 1% SDS pH adjusted to 8.3 using HCl ddH ₂ O ad 1000 ml
3x reducing buffer (pH 6.75)	65 mM Tris 20% (v/v) glycerol 10% (v/v) 2-mercaptoethanol 4% SDS 0.1% bromophenol blue pH adjusted to 6.75 using HCl ddH ₂ O ad 1000 ml
Coomassie staining solution	1g Coomassie brilliant blue G250 in 200 ml methanol 1g Coomassie brilliant blue R250 in 200 ml ddH ₂ O 40 ml acetic acid
Coomassie destaining solution	150 ml acetic acid 500 ml methanol ddH ₂ O ad 2000 ml
Resolving gel (12.5%)	6.25 ml acrylamid/BIS (30%) 5.00 ml lower gel buffer (pH 8.8) 30 µl TEMED 30 µl APS (40% w/v) ddH ₂ O ad 15.0 ml
Stacking gel (4%)	1.33 ml acrylamid/BIS (30%) 3.00 ml upper gel buffer (pH 6.7) 20 µl TEMED 20 µl APS (40% w/v) ddH ₂ O ad 10.0 ml
Protein transfer buffer	50 mM Tris 0.196 M glycine 20% (v/v) methanol pH adjusted to 8.3 using HCl
Tris buffered saline (TBS)	20 mM Tris 150 mM NaCl pH adjusted to 7.4 using HCl
TBS Tween (TBST)	TBS 0.05 % (v/v) Tween

3.1.4 Media

3.1.4.1 Media for cell culture

Medium	Supplier/Composition
Dulbecco's modified eagle medium (DMEM)	Gibco
DMEM GlutaMax-I (4.5 g/l glucose)	Gibco
DMEM Hepes	Gibco
freezing medium	4 ml rat Schwann cell medium 4 ml FBS 2 ml DMSO
trypsin/collagenase mixture	10 ml DMEM 1.2 ml trypsin 1.2 ml collagenase (0.6%)
fetal bovine serum gold (FBS gold)	PAA laboratories
rat Schwann cell medium	DMEM 10% (v/v) FBS 1% (v/v) glutamine 1% (v/v) pen/strep
rat Schwann cell proliferation medium (used only for preparation of primary Schwann cell cultures)	Rat Schwann cell medium 2 μ M forskolin 100 μ g/ml BPE
complement lysis mix (used only for preparation of primary Schwann cell cultures)	1.6 ml DMEM 0.4 ml mouse anti Thy1.1 antibody (1:10 diluted in DMEM)
DRG culture medium	DMEM + GlutaMax-I 10% (v/v) FBS 0.1 μ g/ml NGF 1% pen/strep
DRG differentiation medium	DRG culture medium 0.05 mg/ml ascorbic acid

3.1.4.2 Media for the cultivation of *E.coli*

Medium	Composition
Luria Broth medium (LB)	1.0% (w/v) bacto trypton 0.5% (w/v) yeast extract 0.5% (w/v) NaCl ddH ₂ O ad 1000 ml
LB agar	1.5% (w/v) bactoagar in LB
LB with ampicillin	50 µg/ml ampicillin in LB
LB with canamycin	50 µg/ml canamycin in LB
LB agar with ampicillin	50 µg/ml ampicillin in LB agar
LB agar with canamycin	50 µg/ml canamycin in LB agar
SOC medium	2% trypton 0.5% yeast extract 0.6% NaCl 2.5 mM KCl 10 mM MgCl ₂ 20 mM glucose ddH ₂ O ad 1000 ml

3.1.5 Antibiotics

Antibiotic	Supplier
penicillin/streptomycine, 5000 U/ml	Gibco
ampicillin (stock 50 mg/ml)	Roche
kanamycin (stock 50 mg/ml)	Sigma
hygromycin B (stock 50 mg/ml)	Calbiochem

3.1.6 Enzymes

Enzyme	Supplier
collagenase	Sigma
restriction endonucleases	Roche
restriction endonucleases	New England Biolabs
RNAse A	QIAGEN
RNAse free DNase	QIAGEN
RNAsin	Applied Biosystems
T4 DNA ligase	Roche
shrimp alkaline phosphatase	Roche
T4 polynucleotide kinase	New England Biolabs

3.1.7 DNA molecular weight standards

Marker	Supplier
1 kb molecular weight standard	Gibco
100 bp molecular weight standard	Promega

3.1.8 Synthetic oligonucleotides

Synthetic oligonucleotides used as PCR amplification primers were synthesized by MWG Biotech and 100 pmol/ μ l stock solutions were prepared by dissolving in ddH₂O. Cy3-labelled siRNAs (5 nmole) were synthesized by Ambion. 100 pmol/ μ l stock solutions were prepared by dissolving in ddH₂O and 5 μ l aliquots were stored at -80°C.

3.1.9 Transfection reagents

Transfection reagent	Supplier
FuGENE HD	Roche
siPORT NeoFx	Ambion

3.1.10 Vectors

Vectors	Supplier
pSUPER	OligoEngine
pMACS-CD14.1	Miltenyi Biotec
pIRES2-EGFP	Clontech
pcDNA3.1/hyg	Invitrogen
pSUPERkip1	see 3.2.2.1
pSUPERkip2.1	see 3.2.2.1
pSUPERkip2.3	see 3.2.2.1
pcDNA3.1/hyg-citrine	see 3.2.2.3

3.1.11 Kits

Reagent	Supplier
BrdU immunofluorescence assay kit	Roche
Plasmid mini kit	QIAGEN
EndoFree Plasmid maxi kit	QIAGEN
QIAquick gel extraction kit	QIAGEN
RNEasy mini kit	QIAGEN
miRVana miRNA isolation kit	Ambion
Shrimp alkaline DNA dephosphorylation kit	Roche
High Capacity cDNA reverse transcription kit	Applied Biosystems
GeneAmp High fidelity PCR system	Applied Biosystems
Gene Chip one cycle target labelling and control reagent kit	Affymetrix
Vectastain elite ABC complex kit	Vector

3.1.12 Technical devices and software

Technical device/software	Supplier
Array assist 5.0 software	Affymetrix
ABI 310 automatic sequencer	Applied Biosystems
ABI 7000 real time PCR system	Applied Biosystems
ABI 7900 real time PCR system	Applied Biosystems
AxioCam HRc	Zeiss
Axioplan 2	Zeiss
Concentrator 5301	Eppendorf
Diana II software	Raytest
Diana II transilluminator	Raytest
E.A.S.Y. RH transilluminator	Herolab
EBA 12R table top centrifuge	Hettich
Elisa reader MRX	Dynex
HAT Minitron shaker incubator	Infors
Heraeus Hera Safe incubator	Heraeus
INTENSILIGHT fluorescence lamp	Nikon
Lucia 4.21 software	Lucia software
New Brunswick Excella E24 incubator	New Brunswick
Nikon Digital Sight Camera System	Nikon
Nikon eclipse TE200 microscope	Nikon
NIS elements AR30 software	Nikon
Power Pac200 Power supply	BioRad
Primer express software	Applied Biosystems
RC5B Plus centrifuge	Sorvall
SE 250 Mighty small gel system (10x8 cm)	Hoefer

Technical device/software	Supplier
Table top centrifuge 5417C	Eppendorf
Thermomixer comfort	Eppendorf
TransBlot SD blot system	BioRad
Trio Thermoblock	Biometra
Varity 96 Well Fast Thermocycler	Applied Biosystems

3.2 Molecular biological methods

3.2.1 Cloning procedures

3.2.1.1 Agarose gel electrophoresis

Agarose gel electrophoresis was conducted in order to separate DNA fragments by size. Depending on the size of the fragments designated to be separated, 0.3 – 2 % agarose gels were prepared by dissolving agarose in 1x TAE buffer and boiling of the solution in a microwave oven. After cooling down, ethidium bromide was added to a final concentration of 0.5 µg/ml. The solution was poured into the gel rack and a comb was inserted on one side of the rack. After the gels became solid, they were transferred into a tank. The comb was removed and the tank was filled with 1x TAE buffer. DNA blue marker was added to the probes and the probes as well as molecular weight standards (100 bp molecular weight standard, Promega; 1 kb molecular weight standard, Gibco) were pipetted into the slots of the gel. Current was applied and electrophoresis was performed at 80-120 volts (~5 V/cm distance between the electrodes) for approximately 30-60 minutes. The separated DNA fragments were detected using a UV light device (Herolab or Raytest) and documented using a CSC camera.

3.2.1.2 Digestion of plasmids using restriction endonucleases

Restriction digest has been performed to fragmentize DNA. Therefore, DNA, restriction endonucleases and buffers were mixed in an Eppendorf tube. 1-5 units of restriction endonucleases per µg DNA were used and digestion was performed for at least one hour according to the temperature specifications of the supplier. When DNA had to be digested using two different enzymes and buffering conditions, DNA was purified from agarose gels with the QIAquick gel extraction kit (QIAGEN) after the first digestion and the second digestion was accomplished with the purified digested DNA in order to assure optimal buffering conditions.

3.2.1.3 Purification of DNA fragments using the QIAquick gel extraction kit

After digestion, PCR amplification or phosphorylation of DNA, DNA fragments were purified using the QIAquick gel extraction kit (QIAGEN) according to the specifications of the supplier. DNA was eluted with 30 μ l ddH₂O.

3.2.1.4 Dephosphorylation of plasmids

In order to minimize the risk of religation following plasmid restriction, dephosphorylation of plasmids was performed using shrimp alkaline phosphatase (Roche Applied Diagnostics) according to the specifications of the supplier. The digested DNA, shrimp alkaline phosphatase and phosphatase buffer were mixed in a 0.5 ml Eppendorf tube and phosphatase reaction was performed in a thermocycler at 37°C for 40 minutes. Prior to ligation, phosphatase was heat inactivated at 65°C for 10 minutes.

3.2.1.5 Annealing of oligonucleotides

Oligonucleotides to be annealed for the generation of pSUPER vector constructs (see 3.2.2.1) were dissolved in ddH₂O to a final concentration of 3 mg/ml. 1 μ l of each oligonucleotide was mixed with 48 μ l annealing buffer and the mixture was kept at 90°C for 4 minutes. The solution was then incubated at 70°C for 10 minutes and cooled down stepwise in 10° steps to 4°C.

3.2.1.6 Phosphorylation of annealed oligonucleotides

Since chemically synthesized oligonucleotides are not phosphorylated, phosphorylation of 5'-ends is required for subsequent ligation with digested and dephosphorylated plasmids. For phosphorylation, 2 μ l of the annealed oligonucleotides were mixed with 1 μ l T4 polynucleotide kinase buffer, 1 μ l of 10 mM ATP (end concentration 1 mM), 1 μ l T4 polynucleotide kinase and ddH₂O ad 10 μ l. The mixture was incubated at 37°C for 30 minutes and the polynucleotide kinase was heat inactivated at 70°C for 10 minutes.

3.2.1.7 Ligation of plasmid and insert

Ligation of DNA fragments was performed using the Rapid DNA phosphorylation kit (Roche Applied Diagnostics) according to the specifications of the supplier. Dephosphorylated plasmids and phosphorylated DNA fragments were typically

applied in a 1:3 ratio and mixed together with T4-DNA ligase and buffers. Ligation was performed at room temperature for at least 5 minutes or at 16°C over night.

3.2.1.8 Transformation of plasmids into *E.coli*

Transformation of *E.coli* strains with ligated plasmid DNA was performed using the heat shock method. One Shot TOP10 chemically competent cells (Invitrogen) and SURE2 chemically competent cells (Stratgene) were used according to the specifications of the supplier. Competent cells were thawed on ice and mixed with maximal 1/10 volume of DNA. Cells were kept on ice for 30 minutes and heat shock was applied for 30 seconds at 42°C. After the heat shock, 250 µl (One Shot TOP10 cells) or 900 µl (SURE2 cells) of SOC medium was pipetted onto the cells and cells were incubated for one hour in a shaker incubator at 37°C and 225 rpm. Cells were streaked on prewarmed selective agar plates and incubated at 37°C in an incubator oven over night.

3.2.2 Generation of vector constructs

Cloning has either been performed with *E.coli* One Shot TOP10 chemically competent (Invitrogen) cells or SURE2 supercompetent cells (Stratagene). The success of each cloning step was controlled by sequencing of the plasmid DNA using Sanger dideoxy mediated DNA sequencing with an ABI 310 automatic sequencer.

3.2.2.1 pSUPER vector constructs

The pSUPER vector system was used to suppress the gene expression of p27kip1 and p57kip2 by introduction of gene specific double-stranded RNA according to the manual of the provider (Oligoengine). Oligonucleotides were designed which included a 19 nt sequence from the mRNA transcript aimed to be suppressed. Sequence specificity was checked using BLASTn (NCBI database) to exclude the risk of unexpected downregulation of related genes. The designed oligonucleotide included the 19 nt target sequence in sense and antisense orientation, separated by a 9 nt spacer sequence. Further a 3' poly-T sequence as well as 5' BglIII and 3' HindIII restriction sites were part of the oligonucleotide sequence. The forward and reverse oligonucleotides were annealed, phosphorylated and inserted into BglIII and HindIII digested pSUPER. Following oligonucleotides were used for the generation of the vector constructs:

Primer	Sequence
kip1_sense	GAT CCC CGG TGC CGG CGC AGG AGA GCT TCA AGA GAG CTC TCC TGC GCC GGC ACC TTT TTG GAA A
kip1_antisense	AGC TTT TCC AAA AAG GTG CCG GCG CAG GAG AGC TCT CTT GAA GCT CTC CTG CGC CGG CAC CGG G
kip2_1_sense	GAT CCC CCA GGT CCC TGA GCA GGT CTT TCA AGA GAA GAC CTG CTC GGG ACC TGT TTT TGG AAA
kip2_1_antisense	AGC TTT TCC AAA AAC AGG TCC CTG AGC AGG TCT TCT CTT GAA AGA CCT GCT CAG GGA CCT GGG G
kip2_3_sense	GAT CCC CGG ACG AGG AGC CGG TGG AGT TCA AGA GAC TCC ACC GGC TCC TCG TCC TTT TTG GAA A
kip2_3_antisense	AGC TTT TCC AAA AAG GAC GAG GAG CCG GTG GAG TCT CTT GAA CTC CAC CGG CTC CTC GTC CGG G

3.2.2.2 rp57kip2-IRES2-EGFP

The pIRES2-EGFP vector (Invitrogen) contains an internal ribosome entry site (IRES) between the multiple cloning site and the EGFP coding region, allowing the translation of both the gene of interest and the EGFP gene from a single bicistronic mRNA. For cloning of rp57kip2-IRES2-EGFP, total rat mRNA was reverse transcribed using oligo dT(16) primers and the resulting cDNA of p57kip2 was amplified using primers which generate an EcoRI-EcoRI fragment of rat p57kip2. pIRES2-EGFP was digested with EcoRI and the PCR product was ligated with the digested plasmid and transformed into *E.coli* TOP10 One Shot Competent cells (Invitrogen). Following primers were used for the cloning of rat p57kip2 cDNA:

Primer	Sequence
rp57kip2_fwd1	TAG TGA ATT CAG CCA GCA GAA CAG CAT G
rp57kip2_rev1	TAG TCT TAA GGG TCT AAA CTA ACT CAT C

3.2.2.3 pcDNA3.1-HygB-citrine

The pcDNA3.1-HygB-citrine vector was used for cotransfection experiments and allows the selection of the transfected cells with hygromycin B and their identification

via citrine expression. Coexpression of citrine and hygromycin B resistance genes was achieved by the integration of a NheI/NotI citrine cDNA fragment (Griesbeck *et al.*, 2001) into the multiple cloning site of the pcDNA3-HygB expression vector (Invitrogen Ltd., Paisley, UK). The ligated vector construct was transformed into *E.coli* TOP10 One Shot Competent cells (Invitrogen).

3.2.3 Isolation of nucleic acids

3.2.3.1 Isolation of plasmid DNA (plasmid mini preparation)

After transformation of plasmids into *E.coli* strains, single colonies were picked with a sterile toothpick and transferred into a 14 ml polypropylene round bottom falcon tube (Becton Dickinson). The tubes were filled with 3 ml LB medium containing ampicillin or canamycin dependent on the plasmid resistance and incubated for 16 h in a shaker incubator at 37°C and 225 rpm. After incubation, 1.5 ml of the bacteria enriched LB medium was transferred into an Eppendorf tube and pelleted by short centrifugation at maximum speed in an Eppendorf table top centrifuge. The supernatant was aspirated and pellets were resuspended in 300 µl resuspension buffer (QIAGEN, buffer P1). Afterwards, resuspended bacteria were lysed for 5 minutes in 300 µl lysis buffer (QIAGEN, buffer P2). Lysis was stopped by addition of 300 µl icecold neutralization buffer (QIAGEN, buffer P3). After incubation for 10 minutes on ice, the solution was centrifuged for 15 minutes at 4°C and maximum speed, the supernatant was transferred into fresh tubes and mixed with 0.7 volumes of 2-propanol. The solution was vortexed and centrifuged for 30 minutes at 4°C and maximum speed. The supernatant was discarded and plasmid DNA pellets were washed with 900 µl 70 % ethanol. After centrifugation for 5 minutes at room temperature and maximum speed, supernatant was discarded and pellets were air dried until they had a glassy appearance. Pellets were dissolved in 50 µl ddH₂O and plasmid DNA was stored at -20°C.

3.2.3.2 Isolation of plasmid DNA (plasmid mini preparation) using the plasmid miniprep kit (QIAGEN)

All steps for plasmid DNA isolation using the plasmid miniprep kit (QIAGEN) were carried out in accordance to the protocol of the supplier (QIAGEN). Plasmid DNA was dissolved in 50 µl ddH₂O and stored at -20°C.

3.2.3.3 Isolation of plasmid DNA (plasmid maxi preparation)

Since endotoxins are known to interfere with transfection efficiency, the endofree plasmid maxi kit (QIAGEN) was used in order to isolate endotoxin free plasmid DNA. All steps for plasmid DNA isolation were carried out in accordance to the protocol of the supplier (QIAGEN). Plasmid DNA was dissolved in 500 μ l ddH₂O, aliquoted and stored at -20°C. Whenever possible, DNA concentration was adjusted to 1 μ g/ μ l.

3.2.3.4 Generation of glycerol stocks

In order to store transformed bacteria, 50% glycerol stocks were prepared prior to plasmid maxi preparation. Therefore, 500 μ l of bacteria enriched (log phase or stationary phase) LB medium was mixed with 500 μ l glycerol and immediately frozen using dry ice. Transformed bacteria were stored at -80°C.

3.2.3.5 Preparation of RNA

3.2.3.5.1 Preparation of total RNA using the RNeasy Mini Kit

All steps for total RNA isolation using the RNeasy Mini Kit (QIAGEN) were carried out in accordance to the protocol of the supplier. Cells were lysed in 350 μ l RLT buffer and stored at -20°C for short terms until RNA preparation. Cells were sheared using QIAshredder in order to solubilize the extract prior to RNA preparation. Genomic DNA was removed on column using RNase free DNase (QIAGEN). RNA was dissolved in 30 μ l nuclease free ddH₂O and stored at -20°C.

3.2.3.5.2 Preparation of total RNA using Trizol®-reagent

Total RNA of rat sciatic nerves (P0, P1, P4, P6, P14, P28, P90) was extracted using the Trizol®-reagent. Therefore, nerves were cut into pieces and put into 700 μ l Trizol®-reagent. Homogenization of nerves was done for 30 seconds using a Polytron Power Homogenizer and the homogenate was incubated for at least 5 minutes at room temperature. The homogenate was mixed with 140 μ l chloroform, vigorously shaken and centrifuged for 15 minutes at 12.000 rpm and 4°C. Of the three phases which were thus generated, the upper aqueous phase (approximately 500 μ l) was carefully pipetted into a new Eppendorf tube. Each tube was mixed with 1.1 μ l glycogen and 350 μ l 2-propanol, vortexed and incubated for 30 minutes at room temperature to allow precipitation of RNA. Samples were centrifuged for 10 minutes at 12.000 rpm and 4°C, supernatants were discarded and RNA pellets

were washed with 1 ml ethanol (75% in ddH₂O). Samples were again centrifuged for 10 minutes at 10.000 rpm and 4°C and supernatants were discarded carefully. After drying of the RNA pellets, RNA was dissolved with 30 µl nuclease free ddH₂O and incubated for 10 minutes at 57°C to maximize the yield. Samples were stored at -20°C.

3.2.3.5.3 Preparation of miRNA using the miRVana kit

Since alcohol precipitation of small RNAs is inefficient, the miRVana microRNA isolation kit (Ambion) was used for this purpose. According to the specifications of the supplier, total RNA was prepared from cultured cells. Cells were lysed in 300 µl Lysis/Binding solution prior to RNA extraction procedure. RNA was eluted with 100 µl of pre-heated (95°C) nuclease free ddH₂O and stored at -20°C.

3.2.3.5.4 Photometric nucleic acid concentration determination

Concentration determination of plasmid DNA and total RNA was performed with a NanoDrop 1000 spectral photometer using 1.5 µl of undiluted probes. Plasmid DNA concentration was adjusted to 1 µg/µl for transfection purpose.

3.2.4 Reverse transcription

3.2.4.1 Reverse transcription of total RNA

Reverse transcription of total RNA was performed applying the high capacity reverse transcription kit (Applied Biosystems) according to the specifications of the supplier. For each reverse transcription, 500 ng of total RNA were used in 30 µl total reaction volume. Reaction mixtures were incubated in a thermocycler for 10 minutes at 25°C, 120 minutes at 37°C and 5 seconds at 85°C. cDNA was diluted to a total volume of 100 µl for quantitative real time PCR purpose. Composition of the mastermix was as follows:

Component	Quantity in 30 µl reaction
10x TaqMan high capacity RT buffer	3.0 µl
100 mM dNTP mix (with dTTP)	1.2 µl
Random hexamer primers	3.0 µl
RNAse inhibitor, 20 U/µl	1.5 µl
Multiscribe reverse transcriptase, 50 U/µl	1.5 µl
Total RNA	500 ng
LiChrosolv H ₂ O (Merck)	ad 30 µl

3.2.4.2 Reverse transcription of micro RNA

MicroRNAs were selectively reverse transcribed using TaqMan microRNA assays (Applied Biosystems) according to the manual of the supplier. For reverse transcriptions of miRNAs, 500 µg of total RNA were used in a total volume of 15 µl. Reaction mixtures were incubated in a thermocycler for 30 minutes at 16°C, 30 minutes at 42°C and 5 minutes at 85°C. Composition of the mastermix was as follows:

Component	Quantity in 15 µl reaction
100 mM dNTP mix (with dTTP)	0.15 µl
Multiscribe reverse transcriptase, 50 U/µl	1.00 µl
10x reverse transcription buffer	1.50 µl
RNAse inhibitor, 20 U/µl	0.19 µl
miRNA specific reverse transcription primer	3.00 µl
Total RNA	500 ng
Lichrosolv H ₂ O (Merck)	ad 15 µl

3.2.5 Amplification of DNA fragments via polymerase chain reaction (PCR)

In order to amplify DNA fragments destined for further cloning procedures, the GeneAmp High Fidelity PCR kit (Applied Biosystems) was used. This kit contains AmpliTaq polymerases and proprietary proof reading enzyme, ensuring high accuracy of amplification. PCR primers were chosen using the Primer Express software (Applied Biosystems) and suitable restriction sites were added 5' and 3' of the cDNA sequence. Following reaction mastermixes were prepared:

Component	Volume per reaction	Final concentration
forward primer	1 µl	300 nM
reverse primer	1 µl	300 nM
Template	TBD	0.1-0.75 µg
dATP, 10 mM	1 µl	200 µM
dCTP, 10 mM	1 µl	200 µM
dGTP, 10 mM	1 µl	200 µM
dTTP, 10 mM	1 µl	200 µM
GeneAmp High Fidelity 10x PCR buffer (incl. MgCl ₂)	5.0 µl	1x
GeneAmp High Fidelity enzyme mix	0.5 µl	2.5 U
ddH ₂ O	ad 50 µl	-

Following primers were used for the amplification of rat p57kip2 cDNA:

Primer	Sequence
rp57kip2_fwd1	TAG TGA ATT CAG CCA GCA GAA CAG CAT G
rp57kip2_rev1	TAG TCT TAA GGG TCT AAA CTA ACT CAT C

Following thermal cycling parameters were used for the amplification of rat p57kip2 cDNA:

Step	Initial	PCR cycle (30 cycles of)			Final
		Denature	Anneal	Extend	
Temp	94°C	94°C	55°C	72°C	72°C
Time	2 min	15 sec	1 min	2 min	7 min

The success of the amplification was verified by agarose gel electrophoresis. DNA fragments were excised from gels and purified using the QIAquick gel extraction kit. The accuracy of the amplification was controlled by sequencing with the ABI 310 sequencing device.

3.2.6 Automatic sequencing using the ABI 310 sequencing device

In order to sequence DNA fragments, the Sanger dideoxy method was applied in a PCR amplification protocol using fluorescent dye marked deoxyribonucleotides the integration of which leads to a stop of the polymerization reaction (Sanger *et al.*, 1977). Subsequent separation of PCR products and readout of the sequence analysis was performed using an ABI 310 automatic sequencer.

Highly purified DNA probes were used for sequencing reactions to assure optimal performance. Either 100-300 ng of PCR products or 0.5-1.0 µg of plasmid DNA were mixed with 4 µl BigDye Terminator sequencing master mix (Applied Biosystems), 2 µl primer solution (5 pmol/µl) and LiChroSolv H₂O (Merck) in a total volume of 20 µl for sequencing reactions (sequencing PCR reaction mix). Afterwards, 4 µl of the sequencing PCR reaction mix were mixed with 12 µl Hi-Di formamide (Applied Biosystems) and used in the ABI 310 sequencing device. The unidirectional amplification of DNA was performed in a thermocycler using following temperature profile:

Step	Initial	PCR cycle (30 cycles of)			Final
		Denature	Anneal	Extend	
Temp	94°C	94°C	55°C	60°C	72°C
Time	1 min	30 sec	15 sec	4 min	7 min

3.2.7 Quantitative real time PCR (qRT-PCR)

Quantitative real time PCR (qRT-PCR) is a method for the template DNA quantification in a mixture of cDNAs, which can be applied in order to compare the amount of cDNAs in different samples. Prior to the quantification, mRNA is reverse transcribed into cDNA using the high capacity reverse transcription kit (Applied Biosystems). PCR amplification and quantification in real time was performed using the Power Sybr Green Mastermix (Applied Biosystems) or the TaqMan master mix (Applied Biosystems) according to the manual of the supplier with primers at a final concentration of 0.30 pmol/μl with an ABI 7000 or ABI 9700 geneamp. The default two step amplification profile used was 40 cycles of 15 seconds at 95°C and 1 minute at 60°C. The primers used in this study were chosen using the Primer Express 2.0 software (Applied Biosystems). GAPDH and ODC were used as endogenous reference genes and quantification was done according to the $\Delta\Delta CT$ method (Applied Biosystems). Following primers were used for qRT-PCR:

qRT-PCR-primer	Sequence
GAPDH (reference)	fwd: GAA CGG GAA GCT CAC TGG C rev: GCA TGT CAG ATC CAC AAC GG
ODC (reference)	fwd: GGT TCC AGA GGC CAA ACA TC rev: GTT GCC ACA TTG ACC GTG AC
Bm2_1	fwd: CAC CCT GTA CGG CAA CGT CT rev: GCC TCA AAC CTG CAG ATG GT
cJun_2	fwd: GCT GGA AGA AGA GGG TGT TGC rev: GCT TTC CCA GTG GGC TGT C
CXCR4	fwd: CGT CGT GCA CAA GTG GAT CT rev: CAG TGG AAG AAG GCG AGG G
FHL2	fwd: AGC TCT ATG CCA ACA CCT GTG A rev: GCC AGT GGC GAT CCT TGT AG
Hic5_1	fwd: CTG ATG GCA TCG CTC TCT GA rev: TGA GGC CGG AAG ATG GTT C
integrin beta 4	fwd: CTCCAGCAGACGAAGTTCCG rev: GTCTTGCTTTTTCCAGCGT
Krox20	fwd: TTT TTC CAT CTC CGT GCC A rev: GAA CGG CTT TCG ATC AGG G
Krox24	fwd: CCC TGT TGA GTC CTG CGA TC rev: GGC GTG TAA GCT CAT CCG AG
L1	fwd: CCT TAA CCT GGG CCA AGT CC rev: CTC AAG CAC TGT GCT GGT CAG
Lgi4	fwd: TGG CCA AGT CAC TGT AGC AGG rev: TTG AAG CAC GCT GCG AAT AA

qRT-PCR-primer	Sequence
MAL	fwd: AGG AGG CCT TTG GTT ATC CC rev: GCA AAT GGC AGA TTT GGG TAC
MBP	fwd: CAA TGG ACC CGA CAG GAA AC rev: TGG CAT CTC CAG CGT GTT C
Nab1	fwd: GGCCAAAATGATTGGTCACAT rev: TTGTGTGGATCCTCGTCGC
Oct-6	fwd: GGC ACC CTC TAC GGT AAT GTG T rev: TTG AGC AGC GGT TTG AGC T
P0 (myelin protein zero)	fwd: CCC CAG TAG AAC CAG CCT CA rev: TCC AGG CCC ATC ATG TTC TT
p21Cip1	fwd: TTC TTC TGC TGT GGG TCA GGA rev: AAG GCT AAG GCA GAA GAT GGG
p27kip1	fwd: TGG ACC AAA TGC CTG ACT CGT rev: GGC CCT TTT GTT TTG CGA A
p57kip2_1	fwd: CAG GAC GAG AAT CAG GAG CTG A rev: TTG GCG AAG AAG TCG TTC G
p57kip2_3	fwd: GCA GGA CGA GAA TCA GGA GC rev: CTG GAA TCC CCG AGA GAG
p75-LNGFR	fwd: TAT CTG GAA GCC ATG TCT GCC rev: ATA GAC CAA TGG ACC AGC CCT
PINCH1 (Lims1)	fwd: CCC CTT CTG GAC ATG CAC AC rev: TCT CCA TCC CTT CCC CCT C
PINCH2 (Lims2)	fwd: AAT GCT GTT CGC TCC ATG CT rev: CGG CCG ATG ACA AAC TCA C
PMP22	fwd: GCG GAA CAC TTG ACC CTG AA rev: TCA TTT AAA CAT GTG GCC CCA
Prkr	fwd: ACT CTG CAG CAG TGG TTG GA rev: AGC CTT GTC CTC TTG ACT CCG
RDC1	fwd: ACA TCT TGA ACC TGG CCA TTG rev: CAG GGA TGG TGA TGA CGA CC
SDF-1 α	fwd: GGA AGA GCG AGA TCC ACC CT rev: GCA TGG TGG GAT GAA GAG GA
Sox2	fwd: CAC CAA TCC CAT CCA AAT T rev: GTT TTC TAG TCG GCA TCA CGG
Sox10	fwd: GCA GGC TGG ACA CTA AAC CC rev: GTG CGA GGC AAA GGT AGA CTG

3.2.8 SDS gel electrophoresis and Western Blot

Schwann cells were harvested and lysed in RIPA-buffer containing protease inhibitors. Protein concentration was determined using the detergent compatible DC protein assay (Biorad) and BSA as standard. SDS-PAGE was performed according to Laemmli (Laemmli *et al.*, 1970) using a SE 250 Mighty Small gel system (10x8 cm;

Hoefler Inc.). 20 µg of proteins were used per lane and proteins were separated with 12.5% resolving / 4% stacking gels. Either the separated proteins were visualized by staining with Coomassie Brilliant Blue (SERVA) or subsequently subjected to Western blotting. Western blotting was performed according to Towbin (Towbin *et al.*, 1979), using mouse-anti-P0 (Archelos *et al.*, 1993) and mouse-anti-MBP (Chemicon) antibodies at a dilution of 1:10000 and 1:3000, respectively. The separated proteins were blotted onto nitrocellulose membranes (Amersham Pharmacia) using a Trans Blot Semidry-Blot system (BioRad) at 0.8 A/cm². Unspecific binding of antibodies to the membrane was prevented by saturation in TBS containing 3% BSA at 4°C over night. Membranes were incubated with the primary antibody for 1 h at room temperature after rinsing with TBS containing 0.05% Tween. Membranes were again rinsed with TBS containing 0.05% Tween and visualisation of proteins was conducted using horseradish peroxidase conjugated goat anti-mouse antibodies at a dilution of 1:10000 (Southern Biotechnology, Alabaster, AL) and an ECL Western blot detection system (Amersham).

3.2.9 GeneChip array analysis

Two micrograms of total RNA from Schwann cells cotransfected with pcDNA3.1/hyg-citrine and either pSUPER or pSUPERkip2 were used to generate cRNA probes using the GeneChip one-cycle target labelling and Control Reagents Kits (Affymetrix). The labelled cRNAs were hybridized to GeneChip Rat Genome 230 2.0 Arrays (Affymetrix) according to the manufacturer's protocol prior to chip readout and signal digitalization. Data quality-verification and analysis was performed by means of ArrayAssist 5.0 software (Stratagene). The data pre-processing algorithms MAS5.0 (Affymetrix, 2001), MBEI (Li and Wong, 2001), PLIER (Affymetrix, 2005), RMA (Irizarry *et al.*, 2003) and GC-RMA (Wu *et al.*, 2003) were used for low-level analysis. After variance stabilisation (+16) and log-transformation (base 2) statistical analysis was carried out via t-test. The thresholds to consider genes to be regulated were > 1.5 (fold-change) and < 0.02 (p-values). Genes were considered as being significantly regulated if they met above threshold criteria after PLIER or GC-RMA analysis and at least according to one additional pre-processing algorithm.

3.2.10 Proteome analysis

In order to identify differentially expressed nuclear proteins, proteome analysis was applied in collaboration with Dr. Kai Stühler and Michael Grzendowski, Medical Proteom Center, Ruhr University Bochum.

Schwann cells were plated onto 10 cm Ø dishes at a density of 1.000.000 cells/dish. One day after plating, Schwann cells were cotransfected with pSUPER or pSUPERkip2 and the citrine expression plasmid pcDNA3.1/hyg-citrine in a 5:1 ratio. Two days following transfection, medium was changed into Schwann cell medium including 50 µg/ml hygromycin B. Medium was changed every second day. Cells were harvested at nine days post transfection (9dpT) and nuclear extracts were prepared using the NE-PER nuclear and cytoplasmic extract kit (Pierce) in presence of protease inhibitors. Nuclear pellets were stored at -80°C prior to subsequent proteome analysis.

400 µg of nuclear proteins were lysed by sonication and 8 pmol fluorescent dye (Cy3 and Cy5, respectively) was added per µg protein. The labelling reaction was stopped after 30 minutes on ice by adding of 1 µl 10 mM lysine per 400 pmol dye. Both preparations of labelled protein extracts were mixed and 10 µl DTT and 10 µl Ampholine were added per 100 µl cell lysate. Isoelectric focusing (IEF) was done using tube gels (20x1.5 cm) and applying a voltage gated gradient in an IEF chamber (produced at the Ruhr University Bochum). After IEF, the second dimension gel was performed on polyacrylamide gels (15.2% acrylamid, 1.3% bis-acrylamide) using a Desaphor VA 300 system. To this end, IEF tube gels were placed on top of the polyacrylamide gels (20x30x1.5 cm) and electrophoresis was run. The SDS gels were scanned using a Typhoon 9400 scanner at wavelengths specific for the fluorescent dyes. Gel spot detection and matching of gel spots were performed using the Differential In Gel Analysis (DIA) mode and Biological Variation Analysis (BVA) mode of DeCyder software. The intensities of the spots were normalized to an internal standard and significantly regulated proteins ($p < 0.05$; five experiments were performed) were cut out of the gel and digested with trypsin. MALDI-TOF MS was performed using an UltraFlex (Bruker Daltonik) system in order to identify trypsin digested proteins in accordance to the ProteinScape (Bruker) proteome database.

3.3 Cell culture methods

3.3.1 Coating of flasks and culture dishes

3.3.1.1 PDL coating of flasks and culture dishes

Flasks and culture dishes were coated with sterile filtered poly-D-lysine (PDL, 0.1 mg/ml in PBS) either over night at 4°C or for at least one hour at room temperature before cultivation with primary Schwann cells to allow adhesion. Flasks and culture dishes were washed three times with PBS in order to avoid contamination of the culture medium with residual PDL. Culture medium was filled into culture flasks and flasks were incubated at 37°C, 98 % humidity and 10 % CO₂ for equilibration.

3.3.1.2 Collagen type I coating of culture dishes

Culture dishes have been coated with rat tail collagen type I (BD Biosciences) to allow adhesion of DRG dissociation coculture cells. Collagen was prepared by 1:7 dilution of 3.12 mg collagen type I with 0.02 M acetic acid in 1 ml. Dishes were coated with collagen twice and kept for 1 hour at 37°C, 98 % humidity and 10 % CO₂. Afterwards, dishes were filled with DRG culture medium and kept in an incubator at the above specified conditions.

3.3.2 Culturing of primary rat Schwann cells

3.3.2.1 Preparation of primary rat Schwann cells

Primary rat Schwann cells were obtained from sciatic nerves of six P0 rats following the protocol of Brockes *et al.*, 1979. Impurities of the nerves were cleared using forceps, and nerves were reduced to small pieces and transferred into a 50 ml Falcon tube containing 50 ml DMEM. Tissue was centrifuged for 5 minutes at 2000 rpm and pellets were digested with 10 ml trypsin/collagenase mixture for 60 minutes at 37°C. Digestion was stopped with 10 ml Schwann cell medium and cells were centrifuged for 5 minutes at 1500 rpm. Pellets were carefully triturated in 1 ml Schwann cell medium and filled up with additional 10 ml Schwann cell medium. The cell homogenate was filtered through a 60 µm filter, filled up with Schwann cell medium ad 50 ml and centrifuged for 5 minutes at 1500 rpm. Pellets were homogenized in 1 ml Schwann cell medium, 4 ml Schwann cell medium were added and cells were transferred into an uncoated T25 culture flask. After 24 hours, 10 µM arabinosyl cytosine (Ara-C) was added to the culture medium. As a DNA replication inhibitor, Ara-C forms cleavage complexes with topoisomerase I resulting in fragmentation of

DNA of dividing cells. Thus Ara-C treatment selectively kills fibroblasts, while Schwann cells do not proliferate in absence of forskolin. Ara-C treatment was performed for 7 days, changing medium in a 2 day rhythm. Afterwards, complement lysis was carried out to eliminate resting fibroblasts. Therefore, cells were detached from the T25 flask with 3 ml trypsin. After 2 minutes at 37°C, trypsin reaction was stopped with 8 ml Schwann cell medium and cells were centrifuged for 5 minutes at 1800 rpm. The supernatant was discarded, the cell pellet was resuspended in 2 ml complement lysis mix including mouse anti Thy1.1 antibodies and cells were incubated for 20 minutes at 37°C. Complement lysis was afterwards blocked by addition of 7 ml Schwann cell medium and cells were pelleted by centrifugation for 5 minutes at 1800 rpm. The cells were resuspended in 5 ml Schwann cell proliferation medium and transferred into a PDL coated T25 flask. Medium was exchanged by Schwann cell proliferation medium. After growing to confluence (4-7 days after medium exchange), an additional complement lysis step was conducted and cells were transferred into a PDL coated T75 flask containing Schwann cell proliferation medium. After growing to confluence, cells were propagated and distributed into four PDL coated T75 flasks. For further cultivation, Schwann cell medium including 2 µM forskolin but without BPE was used and exchanged every second day.

3.3.2.2 Freezing of primary rat Schwann cells

Confluent grown rat Schwann cells were detached from the T75 flask surface using trypsin for 2 minutes at 37°C. Trypsin reaction was stopped with 30 ml Schwann cell medium and cells were centrifuged for 5 minutes at 1500 rpm. Cells were resuspended in 500 µl Schwann cell medium. Afterwards, 500 µl of freezing medium was added and cells were immediately frozen at -80°C. 24 hours after freezing of cells at -80°C, tubes containing cells were transferred into liquid nitrogen and stored until thawing.

3.3.2.3 Maintenance of rat Schwann cell cultures

Primary rat Schwann cells were thawed, transferred into 50 ml Schwann cell medium and centrifuged for 5 minutes at 1500 rpm. Supernatant was discarded, pellets were resuspended in 20 ml Schwann cell culture medium supplemented with

2 μ M forskolin and cells were transferred into T75 culture flask. Cells were cultured at 37°C, 98 % humidity and 10 % CO₂. Medium was changed every second day.

Propagation of cells was performed when they were grown to confluence. Therefore, cells were washed three times with PBS, 4 ml trypsin solution was applied and cells were incubated at 37°C for 2 minutes. When cells were detached from the flask surface, trypsin reaction was immediately stopped by application of 30 ml Schwann cell culture medium. The cells were centrifuged for 5 minutes at 1500 rpm and pellets were resuspended in 1 ml Schwann cell medium including 2 μ M forskolin. Afterwards, the cells were transferred either into two or three freshly prepared culture flasks containing Schwann cell culture medium including forskolin, depending on the confluency.

3.3.3 Culturing of rat dorsal root ganglion (DRG) dissociation cultures

3.3.3.1 Preparation of rat DRG dissociation cultures

Dorsal root ganglia (DRGs) were collected from E17 Wistar rats and collected in a culture dish filled with 2 ml DMEM+GlutaMAX-I. After collecting, DRGs were dissociated by incubation in 2.5 ml trypsin and 0.5 ml collagenase for 45 minutes in an incubator at 37°C, 98 % humidity and 5 % CO₂. Cells were transferred into a 50 ml falcon tube and resuspended in 50 ml DMEM+GlutaMAX-I / 10 % FCS and centrifuged for 10 minutes at 1500 rpm. The supernatant was discarded and cell pellets were resuspended in 200 μ l DRG culture medium. Approximately 150.000 cells were plated onto collagen type I coated 35 mm plastic dishes as drops. Dishes were filled up with 1 ml DRG medium 30 minutes later.

3.3.3.2 Maintenance of rat DRG dissociation cultures

The DRG culture medium was exchanged with DRG differentiation culture medium (including 0.05 mg/ml ascorbic acid) two days after preparation. Medium was afterwards refreshed by DRG differentiation medium every second day.

3.3.4 Transfection

3.3.4.1 Transfection of primary rat Schwann cells with plasmid DNA

Schwann cells were transfected with FuGENE HD (Roche). Therefore, Schwann cells were plated onto culture dishes the day before transfection and kept in an incubator at 37°C, 98 % humidity and 10 % CO₂. After 24 h, FuGENE HD was mixed with

serum free DMEM/Hepes medium and incubated for 10 minutes at room temperature. Afterwards, this transfection mixture was mixed with plasmid DNA and again incubated for 10 minutes at room temperature hence allowing the transfection complexes to form. The Schwann cell medium was exchanged and the transfection mixtures were dropwise pipetted onto the cells. Medium was exchanged after 24 h. Following plasmid DNA/FuGENE HD/DMEM/Hepes ratios were used:

Culture dish	Cell number per well	μg plasmid DNA per well	μl FuGENE HD per well	μl DMEM/Hepes per well	ml medium per well
12 Well	100.000	0.84	2.5	84	1.5
6 Well	300.000	2.00	6.0	200	3.0
10 cm \emptyset	1.000.000	6.00	18.0	600	10.0
15 cm \emptyset	1.500.000	18.00	54.0	1800	20.0

3.3.4.2 Transfection of rat Schwann cells with siRNAs

For short term experiments desiring high transfection efficiencies, Schwann cells were transfected with 150 pmol siRNAs per well using the siPORT NeoFx kit (Ambion). Therefore, Cy3-labelled siRNAs (Ambion) were dissolved in nuclease free ddH₂O to generate stock solutions with a concentration of 100 pmol/ μl . Stock solutions were aliquoted (5 μl aliquots) and kept at -80°C until use. 12 well plates were coated with PDL at least for 30 minutes prior transfection and washed three times with PBS. Per well, 3 μl siPORT NeoFx transfection solution was mixed with 47 μl serum free DMEM/Hepes and incubated for 10 minutes at room temperature. The siRNA aliquots were diluted with 95 μl ddH₂O to a concentration of 5 pmol/ μl . Of these solutions, 30 μl were mixed with 20 μl DMEM/Hepes per well. The siPORT NeoFx/DMEM/Hepes and the siRNA/DMEM/Hepes mixtures were mixed, resulting in 100 μl transfection mix including 100 pmol siRNA per well, and incubated at room temperature for 10 minutes to allow transfection complexes to form. During that period, Schwann cells were detached from culture flasks by treatment with trypsin. Cells were resuspended in Schwann cell medium, counted and cell numbers were adjusted to 100.000 cells per 900 μl Schwann cell medium. The transfection mixture was pipetted into the wells and 100.000 cells were plated per well. Cells were incubated for 24 hours in an incubator at 37°C, 98% humidity and 10% CO₂. Transfection efficiency was verified with a fluorescence microscope and cells were

either fixed with 4% PFA or lysed in 350 µl RLT buffer (QIAGEN) for subsequent analysis.

3.3.4.3 Selection of transfected cells using hygromycin B

Cells were cotransfected with a vector of interest and pcDNA3.1/Hyg-citrine in a 5:1 ratio in order to achieve a selection of transfected cells using hygromycin B (endconcentration 50 µg/ml) in long term experiments. Schwann cell medium was exchanged by selection medium (Schwann cell medium, 2 µM forskolin, 50 µg/ml hygromycin B) 24 h after transfection, and selection medium was refreshed every second day.

3.3.4.4 Selection of transfected cells via magnetic sorting

For short term experiments, Schwann cells were cotransfected with a vector of interest and the CD14.1 expression vector pMACS-CD14.1 (Miltenyi) in a 5:1 ratio and plated onto 10 cm Ø dishes prior to selection. Only transfected cells expressed CD14.1. 24 hours or 48 hours after transfection, cells were detached from the culture dishes by treatment with 1 ml trypsin. After two minutes at 37°C, the trypsin reaction was stopped with 200 µl FBS and cells were incubated with 100 µl anti-CD14.1-magnetic beads, allowing the beads to bind to the CD14.1 surface antigen. Cells were shaken on a shaker incubator for 10 minutes at 37°C and 150 rpm. Paramagnetic columns were put in a magnetic MACS multistand and equilibrated with 500 µl sterile filtered and air bubble free PBE. Additional 500 µl PBE were added to the cell probes and probes were loaded onto columns in 500 µl steps. Columns were washed for four times with 500 µl PBE. For elution of Schwann cells expressing the CD14.1 antigen, columns were removed from the magnetic MACS multistand and cells were eluted with 1000 µl PBE. Cells were pelleted by centrifugation for 5 minutes at 14.000 rpm and the cell pellets were lysed in 350 µl RLT buffer (QIAGEN).

3.3.4.5 Selection of transfected cells by fluorescence activated cell sorting (FACS)

Fluorescence activated cell sorting (FACS) was applied in order to achieve pure populations of transfected rat Schwann cells at 24 hours post transfection. Therefore, Schwann cells were plated onto PDL coated 10 cm Ø culture dishes at a density of

1.000.000 cells/dish. 24 hours after plating of cells, they were cotransfected either with pSUPER or pSUPERkip2 and the citrine expression plasmid pcDNA3.1/hyg-citrine in a 5:1 ratio. 24 hours post transfection, cells were detached from the surface of the dishes by treatment with 1 ml trypsin for 2 minutes at 37°C. Trypsin reaction was stopped by addition of 10 ml Schwann cell medium and cells were centrifuged for 5 minutes at 1500 rpm. The supernatant was discarded, cell pellets were washed with 10 ml PBS and again centrifuged for 5 minutes at 1500 rpm. The cell pellets were carefully resuspended in 1 ml PBS. Afterwards, 200 µl non-enzymatic cell dissociation solution (Sigma) was added to prevent adhesion of cells. Cells were kept on ice until FACsorting. In order to distinguish non fluorescent from fluorescent cells, a non-transfected negative control was run as calibrator allowing setting up a gate specific for citrine positive fluorescent cells. Fluorescent cells were directly sorted into 350 µl RLT buffer (QIAGEN) leading to direct lysis of cells and RNA protection. All FACsorting experiments were performed with a FACSAria cell sorting system (Becton Dickinson). FACsorting was done in the FACS-facility of the Heinrich-Heine University by Dipl. Biol. Klaus L. Meyer (Institute for functional genomics of microorganisms, Prof. Dr. J.H. Hegemann).

3.3.5 Immunocytochemistry and immunohistochemistry

Rat Schwann cells and dissociated DRG cocultures were fixed for 10 minutes at room temperature with 4 % paraformaldehyde prior to staining procedures. After fixation, cells were rinsed three times with PBS and preincubated for one hour with normal goat serum (10 % NGS in PBS). Stainings were performed with rabbit-anti-p57kip2 (Sigma), mouse-anti-p27kip1 (Abcam), mouse-anti-FLAG-Cy3 (Sigma), Phalloidine-TRITC (Sigma), mouse-anti-MBP (Sternberger Monoclonals) and mouse-anti-P0 (Archelos *et al.*, 1993) antibodies. Antibodies were incubated at 4°C over night in PBS containing 3% NGS. Cells were rinsed three times with PBS the next day and goat-anti-mouse-Alexa-488 (Jackson), goat-anti-rabbit-Alexa-594 (Jackson) were incubated for 2h at RT and used as secondary antibodies for signal visualization. Stainings of intracellular proteins were done in presence of 0.1% triton X-100, whereas stainings of surface antigens was done without triton supplement.

Immunostainings of sciatic nerves were performed with paraformaldehyde fixed and paraffin embedded tissue. Therefore, rat sciatic nerves were fixed with 4 % PFA for

two days at 4°C. Fixed tissue was rinsed with PBS and water was removed by incubation with ascending ethanol concentrations. Dehydrated nerves were incubated with methyl benzoate over night at room temperature and paraffin embedded the next day. Immunostainings were performed on 7 µm sections. Therefore, paraffin was removed from the sections by incubation in ethanol at descending concentrations, finally transferring them into PBS. For DAB stainings, sections were incubated in 0.3 % H₂O₂/PBS for 30 minutes and afterwards rinsed with PBS. After blocking in 3 % NGS, sections were incubated with the first antibody at 4°C over night. Following a washing step, sections were incubated with the biotinylated secondary antibody for 30 minutes at room temperature. After washing, sections were incubated with the ABC-elite-complex (Vectastain elite ABC kit standard, Vector) for 30 minutes, again followed by a washing step. Finally, sections were incubated for 10 minutes in DAB staining solution and washed prior covering and embedding.

Nuclei were stained with 4',6-diamidino-2-phenylindol (DAPI, Sigma) for both immunocytochemistry and immunohistochemistry.

Following antibodies were used for staining procedures:

Antibody	Supplier	Dilution
rabbit anti p57kip2	Sigma	1:200
mouse anti p27kip1	Abcam	1:100
mouse anti FLAG-Cy3	Sigma	1:100
phalloidine-TRITC	Sigma	1:1000
mouse anti MBP	Sternberger Monoclonals	1:500 (Western 1:1000)
mouse anti P0	Archelos <i>et al.</i> , 1993	1:1000 (Western 1:10000)
mouse anti S100	Abcam	1:100
mouse anti LIMK-1	BD Biosciences	1:200
goat anti mouse peroxidase conj.	Southern Biotechnology	1:10000
Alexa goat anti mouse IgG-488	Jackson	1:1000
Alexa goat anti mouse IgG-594	Jackson	1:1000
Alexa goat anti rabbit IgG-488	Jackson	1:1000
Alexa goat anti rabbit IgG-594	Jackson	1:1000

3.3.6 BrdU incorporation and determination of the proliferation rate

Investigations of the Schwann cell proliferation rate were performed using the BrdU-Labeling and Detection Kit I (Roche) according to the specifications of the supplier. Schwann cells were cotransfected either with pSUPER, pSUPERkip1 or

pSUPERkip2 and the CD14.1 expression plasmid pMACS-CD14.1 in a ratio of 5:1 prior to incorporation of bromodeoxyuridine (BrdU). After 24 hours, transfected cells were magnetically sorted and plated onto Lab-Tek chamber slides (Nunc) at a density of 30.000 cells per well. 24 hours after plating, medium was exchanged by BrdU labelling medium (Schwann cell medium containing 10 μ M BrdU labelling reagent) and cells were incubated with the BrdU labelling medium for 20 hours at 37°C. Cells were fixed with ethanol fixative for 20 minutes at -20°C and covered with anti BrdU working solution for 30 minutes at 37°C. After washing, cells were incubated with sheep anti mouse Ig-fluorescein working solution for additional 30 minutes at 37°C. Cell nuclei were stained with DAPI. The cells were covered with Fluoromount G and BrdU incorporation was examined using a fluorescence microscope.

3.3.7 Transplantation of transfected rat Schwann cells onto DRG cocultures

1.000.000 Schwann cells were plated onto 10 cm \varnothing dishes and transfected with pSUPER or pSUPERkip2 and pcDNA3.1/Hyg-citrine in a 5:1 ratio three days prior transplantation of cells. One day after transfection, Schwann cell medium was exchanged by selection medium including 50 μ g/ml hygromycin B. On day three post transfection, Schwann cells were detached from the surface of the dishes by treatment with 1 ml trypsin for 2 minutes at 37°C. Trypsin reaction was stopped by addition of 10 ml Schwann cell medium and cells were pelleted by centrifugation for 5 minutes at 1500 rpm. Cell pellets were resuspended in 1 ml DRG medium and approximately 100.000 cells/cm² were dispersed dropwise on 7 days old DRG cocultures.

4. RESULTS

4.1 p57kip2 is dynamically expressed by Schwann cells during the postnatal development of the PNS

In an attempt to identify Schwann cell specific factors that might account for their plastic behaviour, gene array screening experiments with RNA derived from sciatic nerves after nerve crush were performed. These experiments revealed a number of genes the expression of which were correlated with redifferentiation activities. One of the genes which was transiently downregulated was p57kip2, suggesting a function in nerve regeneration (Küry *et al.*, 2002).

DAB staining of young adult rat sciatic nerves using anti-p57kip2 antibodies (Fig. 10 A, B) revealed that the p57kip2 protein is not only confined to Schwann cells, but also expressed in axons. This expression is in accordance with earlier results (Küry *et al.*, 2002; Schmetsdorf *et al.*, 2007). Double immunofluorescent staining using antibodies against p57kip2 and the Schwann cell marker S100 revealed a colocalization of both proteins (Fig.10 C). Colocalization with nuclear DAPI staining demonstrated that p57kip2 is expressed in Schwann cell cytoplasm as well as in nuclei (Fig.10 C). To determine whether p57kip2 expression is also differentially regulated during PNS development, the Schwann cell specific expression profile of p57kip2 was investigated. Therefore, RNA of sciatic nerves at different timepoints of postnatal development (P1, P4, P10, P14, P28 and P90) was prepared. Quantitative RT-PCR measurements revealed high transcript levels of p57kip2 around birth (Fig. 10 D). During the early postnatal development, these transcript levels steadily declined and remained low at young maturity. This expression profile was surprising since proliferation of Schwann cells continues during the first postnatal days (Stewart *et al.*, 1993) and indicated that glial p57kip2 expression is most likely not involved in cell cycle control. However, as indicated above, transcript levels were still high enough to allow immunohistochemical investigations of peripheral nerves (Fig. 10 A-C).

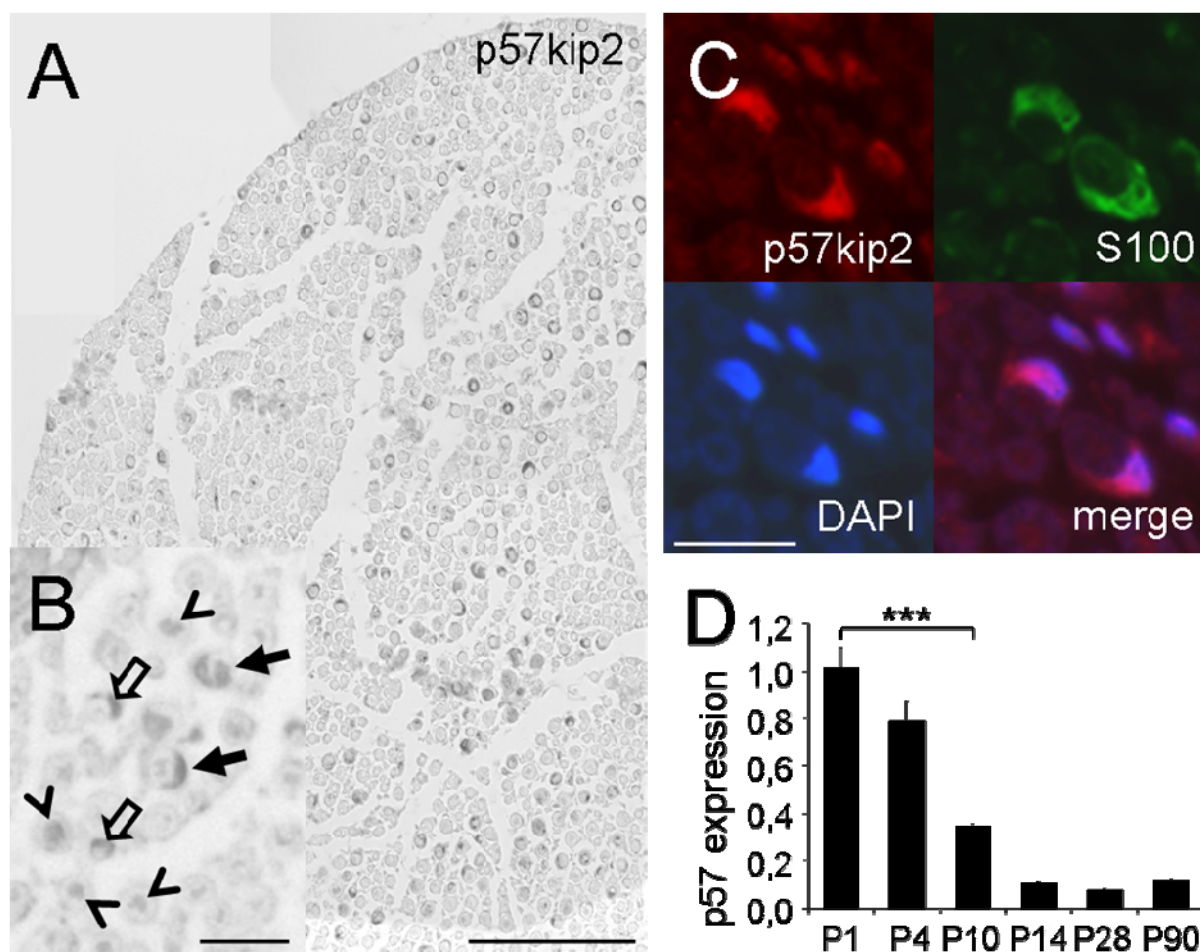


Fig. 10. p57kip2 is expressed by Schwann cells and axons of peripheral nerves. (A and B) Anti-p57kip2 immunostainings of young adult rat (P40) sciatic nerve cross sections. Shown is p57kip2 expression in axons and Schwann cells (arrows), in axons only (arrowheads) and in Schwann cells only (open arrows). (C) Anti-p57kip2 and anti-S100 double immunostaining demonstrated that p57kip2 is present in Schwann cell nuclei and cytoplasm. [Scale bars: 100 μ m (A) and 20 μ m (B, and C).] (D) Quantitative RT-PCR revealed downregulation of p57kip2 expression during postnatal nerve development. One representative measurement out of four different experiments is shown; GAPDH expression was used as reference, and data are mean values \pm SEM. *t*-test analysis demonstrated statistically significant regulation (***, $P < 0.001$).

4.2 Expression of p57kip2 and p27kip1 can be suppressed via vector mediated shRNA expression

The finding that p57kip2 expression is downregulated during the postnatal development prompted us to use a gene suppression approach in order to investigate its functional role in cultured primary rat Schwann cells. Therefore, pSUPER based suppression vector constructs were generated which specifically downregulate the expression of p57kip2 (H1-kip2; pSUPERkip2) and the related gene p27kip1 (H1-kip1; p27kip1). For each gene oligonucleotides were generated aiming at the expression of shRNAs under control of the H1 promoter (see 3.2.2.1). The oligonucleotides were chosen according to the specifications of the supplier (OligoEngine) and sequence specificity was controlled using NCBI Blastn analysis in order to exclude the risk of unspecific binding to further mRNAs. Both for p57kip2 and

p27kip1 at least two different suppression constructs were generated and tested in cell culture. In order to proof the functionality of these constructs, Schwann cells were cotransfected with the suppression vector construct and the selection vector pMACS-CD14.1. 24 hours after transfection, transfected cells were magnetically sorted using the MACS system (Miltenyi), RNA was isolated and the expression levels were determined by means of quantitative RT-PCR. This measurement revealed that the expression of both genes was strongly decreased (Fig. 11 A, B, C). p57kip2 could be suppressed to a level of 22% using the suppression variant pSUPERkip2_1 (Fig. 11 A). p57kip2 expression levels were higher when cells were transfected with the p57kip2 suppression variant pSUPERkip2_3 (Fig. 11 B). The variant pSUPERkip2_1, unless not stated otherwise designated H1-kip2, was used for all further suppression experiments. p27kip1 expression was decreased to a level of 30% using pSUPERkip1_4 compared with the control (Fig. 11 C). The use of other p27kip1 suppression constructs only led to a weakly diminished p27kip1 expression (Fig. 11 D), hence using pSUPERkip1_4 for further experiments, designated H1-kip1. In order to assess whether suppression of p57kip2 also leads to diminished protein levels, immunofluorescent staining of transfected Schwann cells was performed. Therefore, Schwann cells were cotransfected with pSUPER (H1) or H1-kip2 and the citrine expression vector pcDNA3.1/Hyg-citrine in a 5:1 ratio. Transfected cells were fixed after 48 hours and subjected to staining procedures. Fig. 11 E revealed that p57kip2 suppressed cells (green) only possessed basal nuclear p57kip2 levels (red) in comparison to untransfected cells, confirming the functionality of the suppression construct. Additionally, Fig. 11 E also showed that the expression of p57kip2 in cultured Schwann cells was high in the nucleus and low in the cytoplasm.

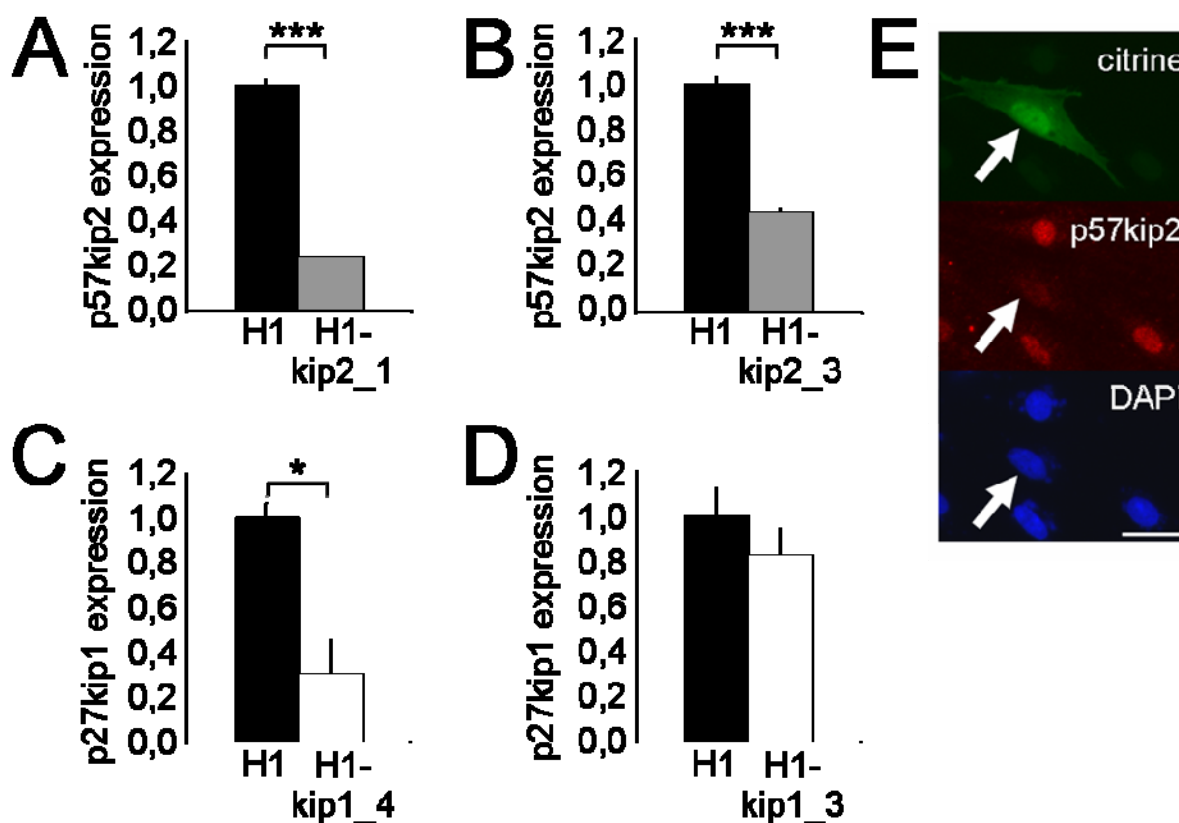


Fig. 11. Expression of p57kip2 and p27kip1 can be suppressed using pSUPER suppression constructs. (A and B) Quantitative RT-PCR measurements confirmed downregulation of p57kip2 after transfection with the suppression constructs H1-kip2_1 and H1-kip2_3 at transcription level. (E) Anti-p57kip2 immunostaining of cultured citrine expressing and p57kip2 suppressed Schwann cells confirmed downregulation of the p57kip2 protein upon transfection with H1-kip2_1. Nuclei were labelled by means of DAPI staining. [Scale bar: 20 μm.] (C and D) Quantitative RT-PCR measurement confirmed downregulation of p27kip1 gene expression levels using H1-kip1_4, while no significant downregulation could be reached using H1-kip1_3. One representative measurement out of four ((D) two) experiments is shown. GAPDH expression was used as reference, and data are mean values \pm SEM. *, $P < 0.05$; ***, $P < 0.001$ (t -test).

4.3 Suppression of p57kip2 leads to cell cycle exit

Members of the cip/kip family of genes are known to interfere with the progression through the cell cycle by binding to cyclin/CDK complexes and inhibition of CDK kinase activity. In order to assess whether suppression of p57kip2 affects the Schwann cell cycle, Schwann cells were cotransfected with H1 or H1-kip2 and the CD14.1 expression plasmid pMACS-CD14.1. 48 hours after transfection, transfected cells were isolated via magnetic sorting and plated onto LabTek chamber slides (Nunc). BrdU labelling was performed 24 hours later in order to determine the proliferation rate of transfected cells. The transfected cells were pulsed for 20 h by means of BrdU incorporation and processed for staining procedures. This revealed that the suppression of p57kip2 did not enhance the proliferation rate, but a more than 4-fold decreased proliferation rate was found (Fig. 12 A, B). The proliferation rate was decreased despite the presence of serum and the mitogen forskolin in the

Schwann cell medium. The observation that suppression of p57kip2 induces cell cycle arrest was in line with the postnatal downregulation of p57kip2 expression and supported that cell cycle inhibition is not the primary function for p57kip2 in glial cells.

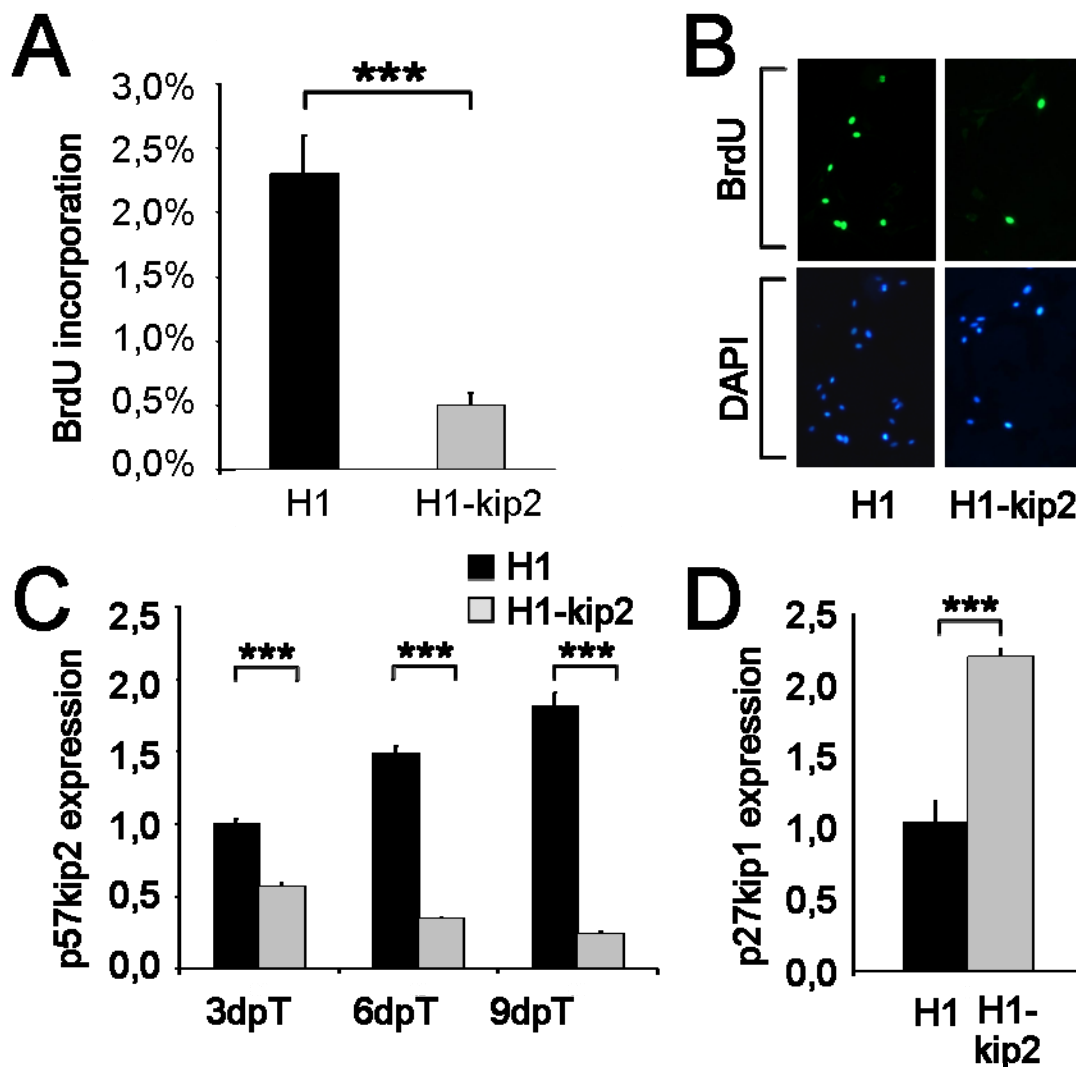


Fig. 12. Suppression of p57kip2 leads to a decrease in the proliferation rate. (A and B) Determination of the Schwann cell proliferation rate revealed a significant decrease of BrdU positive cells upon p57kip2 suppression (H1-kip2, A). (B) Anti-BrdU staining of p57kip2 suppressed and control transfected cells. Nuclei were marked by means of DAPI staining. (C) Quantitative RT-PCR measurement of p57kip2 levels in p57kip2 suppressed (H1-kip2) versus control transfected (H1) cells 3, 6 and 9 days post transfection revealed downregulation of p57kip2 in H1-kip2 transfected and upregulation in control transfected cells. (D) Suppression of p57kip2 was accompanied by upregulation of the related gene p27kip1 at 9dpT. (A, B, C, D) One representative measurement out of three (C) or four (A, B, D) different experiments is shown. GAPDH was used as reference (C, D), and data are mean values \pm SEM. *t*-test analysis demonstrated statistically significant decrease of the proliferation rate (A) as well as gene regulation (C, D) (***, $P < 0.001$).

Since the main interest was to explore long term cellular effects, Schwann cells were cotransfected with H1, H1-kip2 or H1-kip1 and pcDNA3.1/Hyg-citrine, allowing combined citrine expression and hygromycin selection. Transfected cells were selected by application of 50 μ g/ml hygromycin B Schwann cell medium. Quantitative

RT-PCR revealed that p57kip2 levels maintained suppressed even at 9 days post transfection (9dpT) in H1-kip2 transfected cells (Fig. 12 C). These measurements also revealed that p57kip2 levels steadily increased over time in control (H1) transfected cells (Fig. 12 C). Since control transfected cells continued to divide, this result underscored the finding that the role of p57kip2 in Schwann cells is not cell cycle associated (Heinen *et al.*, 2008a; Heinen *et al.*, 2008b). On the other hand, quantitative RT-PCR measurement of p27kip1 expression levels revealed that p27kip1 is induced upon suppression of p57kip2 (Fig. 12 D), suggesting that cell cycle exit in p57kip2 suppressed cells could be due to upregulation of further CKIs.

4.4 Long term suppression of p57kip2 leads to morphological changes

Regulation of the cell cycle exit is imperative for Schwann cell differentiation from precursors to myelinating Schwann cells. Further Schwann cell differentiation steps include morphological changes and alterations in the gene expression program. Surprisingly, the suppression of p57kip2 led to striking morphological changes, which started approximately at 3dpT and were most prominent at 9dpT (Fig. 13 A-B'). Interestingly, the morphologies of p57kip2 suppressed cells closely resembled those of premyelinating Schwann cells in cocultures (indicated by arrows in Fig. 16 C). In comparison to control transfected cells, p57kip2 suppressed cells elongated their processes. The Gaussian distribution of the protrusion lengths revealed that p57kip2 suppressed cells displayed a higher proportion of cells with longer protrusions (Fig. 13 D). The increase of the average protrusion length was more than three-fold (Fig. 13 E). Interestingly, in these cells also the somata were increased. Remarkably, the average protrusion length of p57kip2 suppressed Schwann cells was similar to the average protrusion length of rat Schwann cell protrusions during development at P16 (220 μm , Webster *et al.*, 1971).

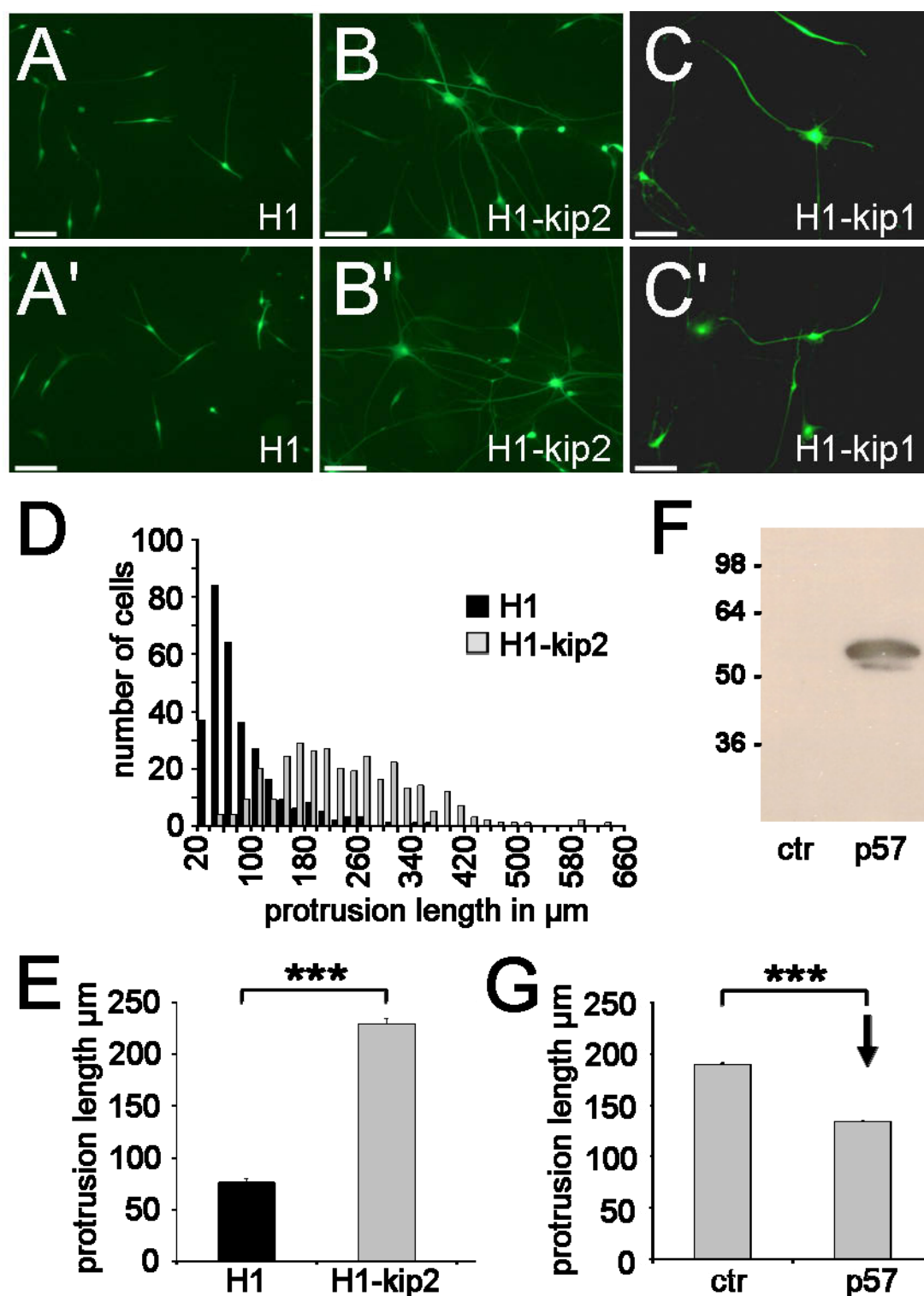


Fig. 13. Suppression of p57kip2 affects Schwann cell morphology. (A and B) Morphology and size were changed in p57kip2 suppressed Schwann cells at 9dpT. (D) Distribution of cells with different average protrusion lengths. (E) Quantification of the average protrusion lengths. (F) Western blot analysis demonstrated that p57kip2 protein levels increased in p57kip2 overexpressing Schwann cells (p57) in comparison to control (ctr) cells. (G) Overexpression of p57kip2 in growing (p57kip2 suppressed) Schwann cells led to significantly reduced average protrusion lengths. One representative measurement out of three (E) respectively two (G) experiments is shown. Data are mean values \pm SEM. ctr, control, empty expression vector; p57, p57kip2 expression vector; H1, pSUPER; H1-kip2, pSUPERkip2. ***, $P < 0.001$ (t -test). (C) Morphology and size of p27kip1 suppressed Schwann cells were also found to be changed.

Given that these morphological effects were a direct consequence of p57kip2 suppression, retransfection of p57kip2 suppressed cells with a p57kip2 expression plasmid was expected to revert the morphology. Therefore, the p57kip2 expression plasmid rp57kip2-IRES2-EGFP was introduced into p57kip2 suppressed cells. This expression plasmid led to high levels of p57kip2 expression, as revealed by quantitative RT-PCR (not shown) and Western blot analysis against p57kip2 (Fig. 13 F). Unfortunately, the only currently available antibody which is able to recognize the rat p57kip2 protein displayed a reduced sensitivity towards denatured p57kip2 protein and it was hence not possible to detect the endogenous protein on Western blots. Nevertheless, immunohisto- and cytochemistry could successfully be carried out. The specificity of which could be confirmed using p57kip2 suppressed cells (Fig. 11 E). For this reversion experiment, p57kip2 suppressed and citrine positive Schwann cells were selected with hygromycin B and retransfected at 5dpT either with the control plasmid pIRES (ctr) or the p57kip2 expression plasmid rp57kip2-IRES2-EGFP (p57). Retransfected cells could clearly be identified by staining against p57kip2, revealing cells overexpressing the p57kip2 protein (data not shown). Fig. 13 G shows that suppression of p57kip2 following pIRES transfection (ctr) led to an average protrusion length of 189 μm . In comparison, retransfection of p57kip2 suppressed Schwann cells with a p57kip2 expression plasmid (p57) significantly reduced the average protrusion length to 133 μm , suggesting that the morphological changes can either be reverted or counteracted. Nevertheless, since only morphological effects but not effects on the gene expression were investigated in the reversion experiment, it is still unclear whether the p57kip2 suppression induced differentiation is fully reversible.

Interestingly, also suppression of p27kip1 in rat Schwann cells led to morphological alterations (Fig. 13 C, C'). p27kip1 suppressed cells displayed a morphology which was similar to p57kip2 suppressed cells. The protrusions were elongated, but very thin. The appearance of p27kip1 suppressed cells was weak in contrast to p57kip2 suppressed cells and only few transfected cells survived 9dpT. However, since p57kip2 levels were found to be decreased upon p27kip1 suppression (data not shown), it is currently unsolved whether the morphological changes upon p27kip1 suppression were due to p27kip1 or due to an off target cross reaction which led to p57kip2 suppression.

In order to exclude the risk that shRNA induced unspecific downregulation of further genes (off target effects) account for the morphological alterations observed, Schwann cells were transfected with the p57kip2 suppression construct H1-kip2_3. Transfection with this plasmid led to the same morphological alterations observed with H1-kip2_1 transfected cells (data not shown). The fact that two different p57kip2 suppression constructs encoding for different RNA interfering sequences that are unique to the rat p57kip2 transcription sequence led to morphological transitions provided strong evidence that the effects described are specific for p57kip2 knockdown. Similarly, also knockdown of p57kip2 using siRNAs (Ambion) was performed. Schwann cells were plated onto 12 well plates at a density of 150.000 cells per well and transfected with 100 pmol siRNA per well using the siPORT NeoFx transfection reagent (Ambion). No morphological alterations were observed in these experiments, and measurements of the p57kip2 gene expression by quantitative RT-PCR revealed that p57kip2 gene expression levels were only weakly reduced at 1dpT, while no p57kip2 suppression was apparent at later timepoints (data not shown). Hence, the use of siRNAs was not sufficient in order to achieve long term suppression of p57kip2. These experiments as well as the fact that p57kip2 suppression induced morphological changes can (partially) be reverted indicated that ongoing, sustained suppression of p57kip2 is necessary to obtain and maintain the described morphological changes.

4.5 Suppression of p57kip2 leads to myelin gene induction

Cell cycle exit and morphological changes are imperative for the terminal differentiation of Schwann cells, which further includes the induction of myelin genes and the expression of myelin proteins and their presentation at the cell surface. In order to investigate the myelin gene expression profile of p57kip2 and p27kip1 suppressed rat Schwann cells, cells were transfected with the suppression constructs, selected using hygromycin B and RNA was prepared at 9dpT, the timepoint at which morphological alterations were most prominent. Quantitative RT-PCR measurements revealed that all myelin gene expression levels investigated (P0, MBP, PMP22 and MAL) were significantly induced upon suppression of p57kip2 (Fig. 14 A; Heinen *et al.*, 2008a). The induction could already be observed at 3dpT (data not shown) and the gene expression reached its maximum at 9dpT. The highest induction was found for the P0 gene, which is the most abundant peripheral

myelin protein. Importantly, immunofluorescent staining of non permeabilized Schwann cells against P0 (Fig. 14 D-E') as well as Western blot analysis of P0 and MBP (Fig. 14 F) revealed that control transfected cells were devoid of myelin proteins and that upon p57kip2 suppression myelin proteins were induced and presented at the Schwann cell surface. Expression of P0 was also found to be slightly induced when p57kip2 was suppressed using pSUPERkip2_3 (data not shown), again indicating that this induction is specific to p57kip2 gene knockdown.

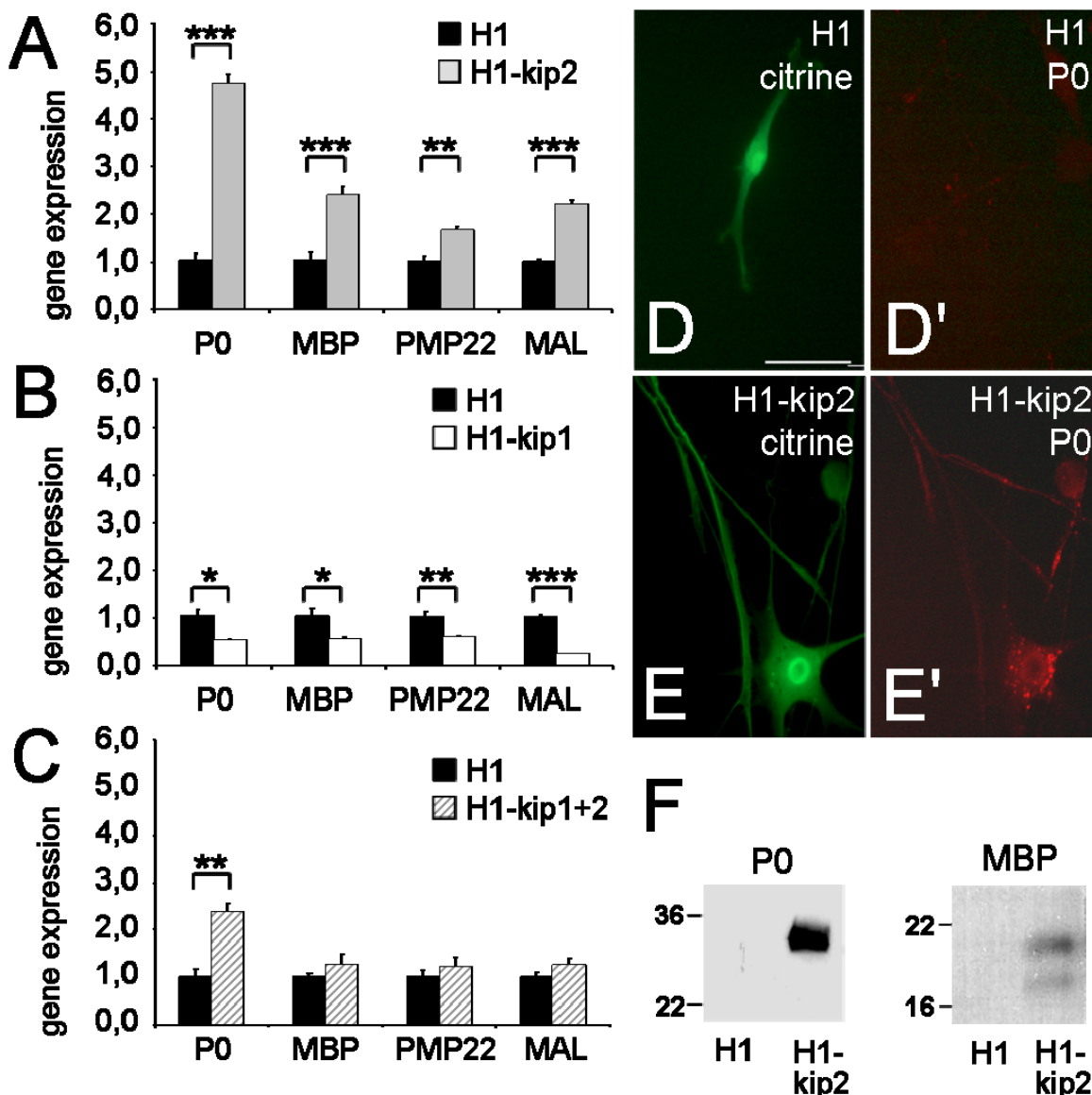


Fig. 14. Suppressed levels of p57kip2 expression lead to myelin induction. (A and B) Quantitative RT-PCR measurements revealed induced myelin gene expression in p57kip2 suppressed Schwann cells (A) and downregulated levels upon p27kip1 suppression at 9dpT. Double suppression of p57kip2 and p27kip1 (C) revealed inhibited induction of myelin genes. One representative experiment of five (A), three (B) and two (C), respectively, is shown. GAPDH expression was used as reference and data are mean values \pm SEM *, $P < 0.05$; **, $P < 0.01$; ***, $P < 0.001$ (t -test). (D-E') Immunostaining revealed P0 expression on p57kip2 suppressed Schwann cells [Scale bar: 50 μ m]. (F) Western blot analysis demonstrated induction of MBP and P0 in p57kip2 suppressed Schwann cells. H1, control transfected cells; H1-kip2, p57kip2 suppressed cells; H1-kip1, p27kip1 suppressed cells; H1-kip1+2, p27kip1 and p57kip2 suppressed cells.

In contrast to the induction of myelin genes in p57kip2 suppressed cells, p27kip1 suppression led to diminished levels of myelin genes (Fig. 14 B). Moreover, combined suppression of both p57kip2 and p27kip1 inhibited the induction of the myelin genes MBP, PMP22 and MAL, while a slight induction of P0 could be observed (Fig. 14 C). These results indicated that induction of myelin genes is restricted to p57kip2 suppression and that p27kip1 suppression inhibits p57kip2 suppression mediated myelin gene induction.

4.6 p57kip2 translocates LIMK-1 from the cytoplasm into Schwann cell nuclei

The described morphological alterations have to be seen in the context of protrusion extension during the normal Schwann cell differentiation, which features growth around and along axons. These alterations depend on cytoskeletal rearrangements, which have already been shown to be imperative for Schwann cell differentiation. Fernandez-Valle and colleagues showed that disruption of the actin polymerization by cytochalasin D (CD) inhibits myelination of DRG cocultures (Fernandez-Valle *et al.*, 1997), although a basal lamina has formed and neurons were healthy. At low doses, CD treated Schwann cells fail to express the myelin proteins CNP, MAG and P0, indicating that actin filament dynamics is imperative for Schwann cell growth. Because cytoskeletal dynamics depends on actin filament turnover and stabilization, actin filaments were stained using phalloidin-TRITC. This staining revealed that protrusions of p57kip2 suppressed rat Schwann cells consist of long actin filaments in elongated protrusions in comparison to the control (Fig. 15 A-B'), indicating that actin filament dynamically turnover was shifted towards polymerization. Actin filament turnover is regulated by LIMK-1 and cofilin. Binding of cofilin to actin filaments destabilizes them and leads to filament disassembly. LIMK-1 phosphorylates and inactivates cofilin, thus leading to a stabilization of actin filaments. Overexpression of LIMK-1 thus affects the intracellular equilibrium of actin polymerization and depolymerization. The ability of p57kip2 to bind LIMK-1 was shown to affect Rho dependent cytoskeletal dynamics (Besson *et al.*, 2004; Yokoo *et al.*, 2003).

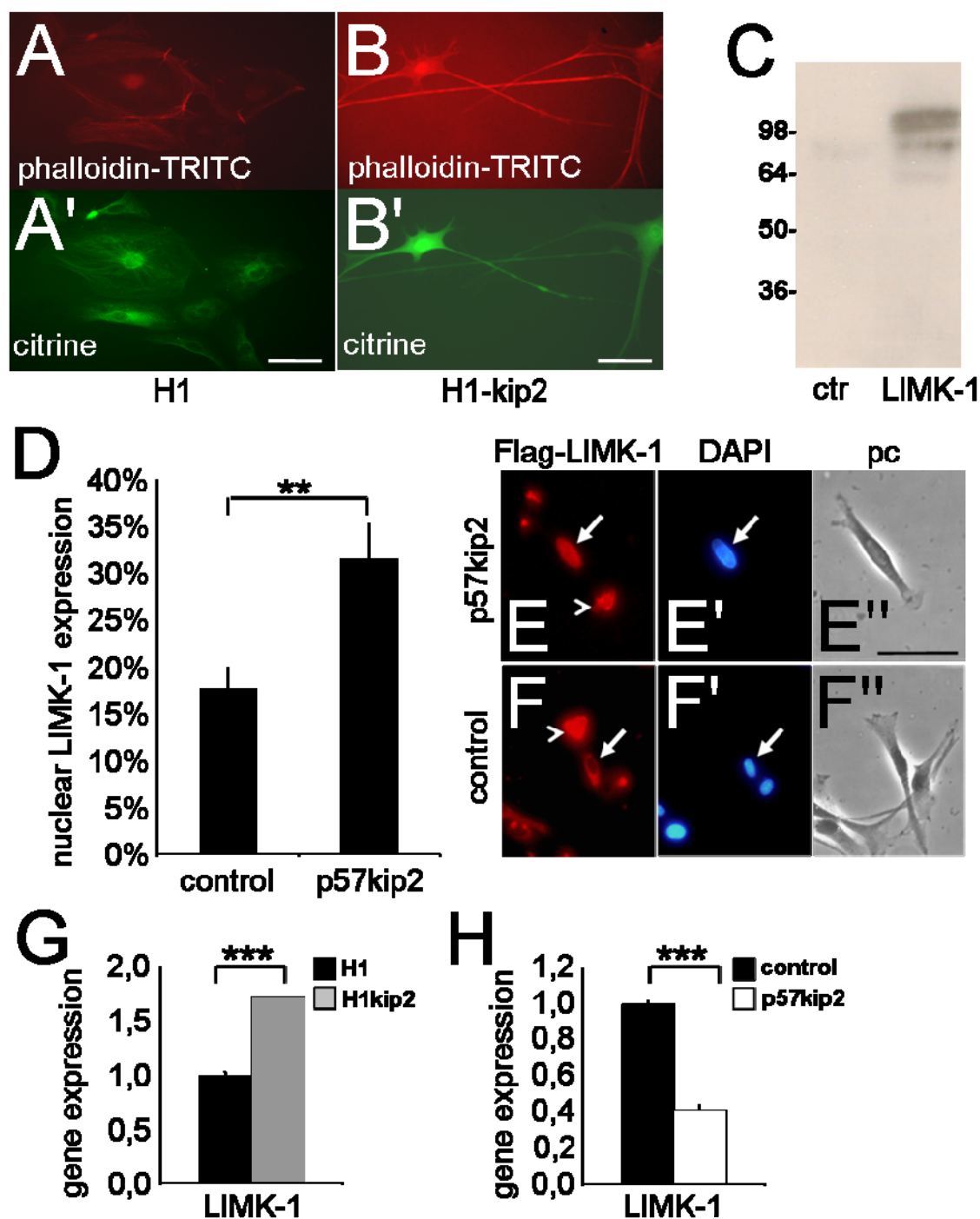


Fig. 15. Subcellular localisation of LIMK-1 in Schwann cells and translocation into nuclei. (A-B') Phalloidin-TRITC labelling of control transfected and p57kip2 suppressed Schwann cells revealed accumulation of long actin filaments. (C) Western blot analysis against LIMK-1 demonstrated that LIMK-1 can be overexpressed using p3xFLAG-LIMK-1. (D) Quantitative determination of transfected Schwann cells featuring nuclear LIMK-1 signals. Data are mean values \pm SEM; **, $P < 0.01$. (E, E', E'') The majority of control transfected cells exhibited Flag-tag labelled LIMK-1 expression perinuclearly (arrow) and at filopodial tips (arrowhead). (F, F', F'') Following overexpression of p57kip2, a significant increase in the number of Schwann cells with nuclear Flag-LIMK-1 expression (arrow) was observed. Nuclei were marked by means of DAPI staining. [Scale bars in (A-B') 100 μ m, in (E'') 50 μ m]. control, control transfected cells; p57kip2, p57kip2 overexpressing cells, pc, phase contrast. (G and H) Quantitative RT-PCR measurements of LIMK-1 expression levels in p57kip2 suppressed (G) and p57kip2 overexpressing (H) Schwann cells revealed that LIMK-1 is upregulated upon p57kip2 suppression and downregulated upon overexpression of p57kip2. One representative measurement out of two experiments is shown. GAPDH was used as reference and data are mean values \pm SEM. ***, $P < 0.001$ (*t*-test). H1, control transfected cells; H1-kip2, p57kip2 suppressed cells; control, control transfected cells; p57kip2, p57kip2 overexpressing cells.

In order to provide a proof of principle that an interaction of p57kip2 and LIMK-1 also occurs in Schwann cells, Schwann cells were cotransfected with the mouse LIMK-1 expression vector p3xFLAG-LIMK-1 (Yokoo *et al.*, 2003) together with the p57kip2 expression vector. Western blot using anti LIMK-1 antibodies showed that LIMK-1-FLAG can be successfully overexpressed in Schwann cells, while only minimal amounts of the endogenous protein could be found (Fig. 15 C). Immunofluorescent staining against FLAG revealed that LIMK-1 expression within Schwann cells is not confined to a single subcellular site, but can be found perinuclearly, in lamellipodia and also occasionally in nuclei (Fig 15 E-F”). However, upon overexpression of p57kip2, a significant higher proportion of LIMK-1 positive nuclei (18% control, 32% LIMK-1 positive nuclei for p57kip2 overexpressing cells) was found (Fig. 15 D), indicating that also in Schwann cells p57kip2 can bind to LIMK-1 and translocate LIMK-1 from the cytoplasm into the nucleus (Heinen *et al.*, 2008b). This suggests that under physiological conditions alterations of the p57kip2 protein levels directly influence the subcellular distribution of LIMK-1. Interestingly, the expression of LIMK-1 was found to be regulated depending on the cellular maturation status. Suppression of p57kip2 led to significantly elevated LIMK-1 levels (Fig. 15 G), while overexpression of p57kip2 led to downregulation of LIMK-1 levels (Fig. 15 H). Given that p57kip2 translocates LIMK-1, suppression of p57kip2 and subsequent upregulation of LIMK-1 is thought to enhance the LIMK-1 dependent stabilization of actin filaments in the cytoplasm.

4.7 Suppression of p57kip2 leads to accelerated *in vitro* myelination

The observed morphological alterations as well as the induction of myelin genes and proteins led to the question whether the myelination process was affected as well. Therefore, cocultures of DRG neurons and Schwann cells were established which allow the observation of the myelination process *in vitro*. In order to test a possible function for p57kip2 during the myelination process, Schwann cells were cotransfected either with H1 or H1-kip2 and the citrine expression vector pcDNA3.1/Hyg-citrine. Transfected cells were selected with hygromycin B, detached from the culture dishes at 3dpT and transplanted onto 10-14 days old DRG cocultures before endogenous *in vitro* myelination could be detected. Seven days after seeding of control transfected and p57kip2 suppressed Schwann cells, cocultures were fixed and processed for anti-MBP immunofluorescent staining.

Colocalization of MBP and citrine positive cells revealed that this short period was sufficient to induce the myelination of DRG axons by exogenous Schwann cells (Fig. 16 A-C). Several cells were found to be elongated and associated with axons, while few cells (marked by arrows in Fig. 16 C) were elongated, MBP negative premyelinating Schwann cells. Quantification of MBP positive internodes revealed that 58% of the p57kip2 suppressed cells (H1-kip2) were MBP positive, while only 17% of the control transfected cells (H1) were MBP positive (Fig.16 D). This result suggests that p57kip2 is an inhibitor of peripheral myelination and that suppression of p57kip2 accelerates *in vitro* myelination (Heinen et al., 2008a).

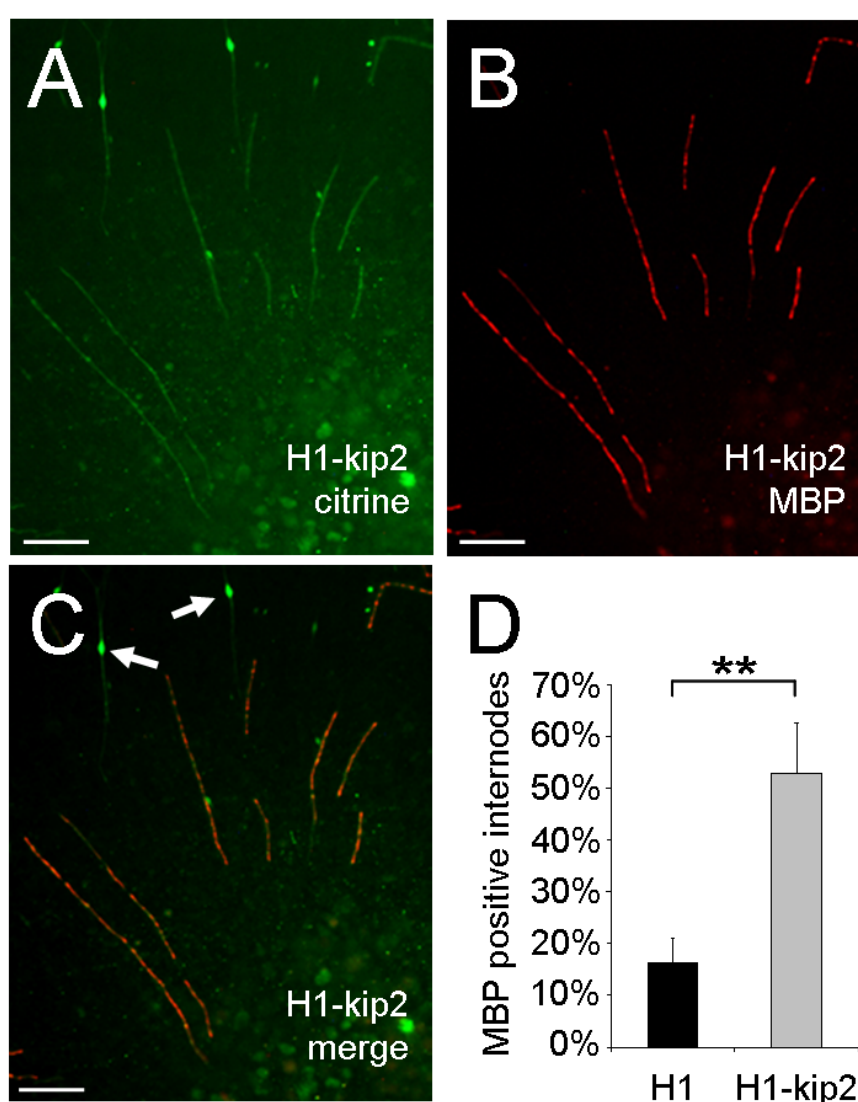


Fig. 16. *In vitro* myelination of DRG axons by p57kip2 suppressed Schwann cells. (A-C) Immunostaining revealed that p57kip2 suppressed Schwann cells (labelled by means of citrine expression) formed MBP positive internodes when seeded on DRG cocultures. Arrows mark elongated, premyelinating (MBP negative) Schwann cells [Scale bar: 100 μm]. (D) Quantification of the number of MBP positive control transfected versus p57kip2 suppressed Schwann cells. One representative experiment of two is shown. **, $P < 0.01$ (t-test). H1, control transfected cells; H1-kip2, p57kip2 suppressed cells.

4.8 GeneChip array analysis revealed that suppression of p57kip2 leads to a shift of the Schwann cell gene expression pattern

Suppression of p57kip2 led to striking morphological alterations and induction of myelin genes, both of which are associated with the induction of terminal Schwann cell differentiation. These alterations were expected to be accompanied by transitions in the gene expression program. In order to describe the transcriptome of *in vitro* differentiating Schwann cells, GeneChip array analysis of p57kip2 suppressed Schwann cells was performed using Rat Genome 230 2.0 arrays (Affymetrix), which allow the simultaneous expression analysis of 30,000 transcripts. Therefore, Schwann cells were cotransfected with H1 or H1-kip2 and the citrine expression plasmid pcDNA3.1/Hyg-citrine. Transfected cells were either sorted at 1dpT by FACS using the citrine expression as selection marker following direct lysis of sorted cells, or they were selected using hygromycin B and lysed at 9dpT. For GeneChip array analysis, 2 µg of total RNA were used for the generation of labelled cRNA probes, and cRNAs were hybridized to the rat arrays. Data were processed using the algorithms MAS5.0 (Affymetrix, 2001), MBEI (Li and Wong, 2001), PLIER (Affymetrix, 2005), RMA (Irizarry *et al.*, 2003) and GC-RMA (Wu *et al.*, 2003). Genes were considered to be significantly differentially regulated when a fold change of more than 1.5 (1dpt: 1.2) and a p-value smaller than 0.02 was reached (see section 3.2.9). Data analysis revealed that upon knockdown of p57kip2 392 genes were differentially regulated at 1dpT and a total of 3928 genes were differentially regulated at 9dpT. Of the regulated genes, 161 were up- and 231 were downregulated at 1dpT, while 1781 were up and 2147 were downregulated at 9dpT. Interestingly, 58 genes were overlapping and differentially regulated at both timepoints. Some of these genes were dynamically regulated within the two timepoints. However, this early impact on gene expression and the high number of regulated genes indicated a shift in the gene expression pattern of p57kip2 suppressed Schwann cells. The following sections describe this shift in greater detail.

4.9 p57kip2 suppression does not induce the interferon response defence reaction

Application of double stranded RNA (dsRNA) onto mammalian cells can induce an unspecific defence reaction, the so called interferon (IFN) response. In the natural context, the IFN response is caused by viral affection of cells and induces the

expression of interferon genes which lead to the defence reaction against viruses and to transcriptional silencing of genes. Induction of the IFN response was thought to be restricted to dsRNA longer than 30 nt, but by applying GeneChip array analysis, Bridge and colleagues have shown that it can also be induced following transfection with vectors for short hairpin loop RNA dependent knockdown of genes (Bridge *et al.*, 2003; Sledz *et al.*, 2003; Sledz *et al.*, 2004). Since such a response can affect the morphology as well as gene expression, it was strongly suggested to measure the expression of IFN responsive genes before attributing particular effects to p57kip2 suppression. Thus the results of the GeneChip array experiments were used in order to control the expression of these genes. Of 55 genes known to be affected by the IFN response, 50 genes could be detected, while five genes were not present on the array (Table 1). This analysis revealed that seven genes were upregulated and four were downregulated at 1dpT, while five genes were upregulated and six downregulated at 9dpT. Of note, the IFN-inducible double-stranded RNA-dependent protein kinase (Prkr), one of the major IFN response regulator genes, was not regulated at 1dpT and even repressed at 9dpT. This together with the overall low number of slightly induced IFN responsive genes supported our conclusion that IFN response does not account for the observed effects and that they are therefore a specific consequence of p57kip2 knockdown.

GenBank accession#	gene	expression	regulation 1dpT	regulation 9dpT
NM_001014786	interferon, alpha-1 precursor	present	-	-
NM_019127	interferon, beta-1	present	-	-
NM_138880	interferon, gamma	present	-	-
NM_053390	interleukin 12a	present	-	-
NM_022611	interleukin 12b	present	-	-
NM_138913	2',5'-oligoadenylate synthetase 1	present	-	-
NM_144752	2',5'-oligoadenylate synthetase 2	present	-	-
XM_342872	Jak1	present	up	-
NM_031514	Jak2	present	up	-
NM_012855	Jak3	present	down	-
XM_233741	Similar to tyrosine kinase TYK2	present	-	-
NM_032612	Stat1	present	-	-
NM_001011905	Stat2	present	down	-
NM_012747	Stat3	present	-	-
NM_001012226	Stat4	absent	-	-
NM_017064	Stat5a	present	-	-
NM_022380	Stat5b	present	up	-
NM_012591	interferon regulatory factor 1	present	up	-
NM_001106314	interferon induced transmembrane protein	absent	-	-
NM_012554	enolase 1	present	-	-
NM_139325	enolase 2-gamma	present	down	up
NM_001024753	IFIT2	present	down	-
NM_053535	ectonucleotide pyrophosphatase/phosphodiesterase 1	present	up	-
NM_057104	ectonucleotide pyrophosphatase/phosphodiesterase 2	present	-	up
NM_019370	ectonucleotide pyrophosphatase/phosphodiesterase 3	present	-	-
NM_001012744	ectonucleotide pyrophosphatase/phosphodiesterase 5	present	-	-
XM_224853	ectonucleotide pyrophosphatase/phosphodiesterase 6	present	-	-
XM_573552	secreted phosphoprotein-1	present	-	-
NM_053769	dual specificity phosphatase 1	present	-	-
NM_001012089	dual specificity phosphatase 2	present	-	-
NM_022199	dual specificity phosphatase 4	present	-	-
NM_133578	dual specificity phosphatase 5	present	-	up
NM_053883	dual specificity phosphatase 6	present	-	down
NM_001037973	dual specificity phosphatase 9	absent	-	-
NM_001025650	dual specificity phosphatase 11	present	-	-
NM_022248	dual specificity phosphatase 12	present	-	-
NM_001007006	dual specificity phosphatase 13	present	-	-
XM_575070	dual specificity phosphatase 14	present	-	down
NM_001108598	dual specificity phosphatase 15	absent	-	-
NM_001013128	dual specificity phosphatase 18	present	-	-
XM_230039	dual specificity phosphatase 19	present	-	-
XM_341523	dual specificity phosphatase 22	present	-	-
XM_215117	interferon induced transmembrane protein 1	present	-	-
NM_030833	interferon induced transmembrane protein 2	present	-	-
XM_341957	interferon induced transmembrane protein 3	present	-	down
NM_001024755	ubiquitin-conjugating enzyme E2L 6	present	-	down
NM_172222	complement component 2	present	-	-
NM_001013170	tryptophanyl-tRNA synthetase	present	-	-
NM_198741	major histocompatibility complex, class II, DM alpha	present	-	down
NM_198740	major histocompatibility complex, class II, DM beta	present	-	-
NM_001013925	NY-REN-18 antigen	absent	-	-
XM_342487	similar to NY-REN-41 antigen	present	up	up
XM_579659	Best5 protein	present	-	up
NM_019335	interferon-inducible double stranded RNA dependent protein kinase	present	-	down

Table 1. Suppression of p57kip2 does not induce an interferone response. This list contains genes with known implication in the interferone response. Genes present on the gene chip are marked by “present”, while absent genes are marked by “absent”. Genes which were found to be downregulated in p57kip2 suppressed cells are marked by “down”, genes which were found to be upregulated are marked by “up” and genes the expression of which did not change are marked by “-”.

4.10 GeneChip array analysis revealed the expression of possible off target genes in p57kip2 suppressed cells

The oligonucleotide sequences which were used for suppression vector construct generation were aligned against all currently known rat sequences by Blastn (basic local alignment search tool) search in order to assure specificity of the target p57kip2 sequences. We therefore compared the 30,000 transcripts provided by the Rat Genome 230 2.0 chip with the 19 nt p57kip2 target sequence integrated into the pSUPER vector (CAGGTCCCTGAGCAGGTCT) and verified whether possible overlaps exist using the DAVID knowledgebase (Sherman *et al.*, 2007). Expression of genes comprising high similarity to the target sequence was investigated by analysis of the GeneChip array data. This revealed that in addition to the p57kip2 sequence further 52 transcripts present on the chip were partially overlapping with the target sequence (Table 2). Of these genes, six were found to be downregulated and two upregulated at 1dpT, while 12 were found to be downregulated and four upregulated at 9dpT. None of the downregulated genes is known to possess a function during peripheral nerve development. However, only two of the genes downregulated at 1dpT were also downregulated at 9dpT, namely “basophil leukaemia expressed sequence” (94% query coverage; 1.27 fold and 2.45 fold downregulation at 1dpT and 9dpT, respectively) and “protein phosphatase 1, regulatory subunit 10” (94% query coverage; 1.68 fold and 1.56 fold downregulation at 1dpT and 9dpT, respectively). Whether the downregulation of these genes is due to an unspecific off target effect or a secondary consequence of p57kip2 knockdown, will be elucidated elsewhere. Currently there is no indication that our suppression strategy is unspecific.

GenBank accession # / locus	Gene	regulation 1dpT	regulation 9dpT	query coverage
NM_172327	aryl-hydrocarbon receptor-interacting protein	-	down	68%
BX883048	Basophil leukemia expressed sequence Bles05 mRNA, partial Sequence	down	down	94%
NM_001037775	carbohydrate sulfotransferase 12 (predicted)	-	up	73%
AF100154	Cysteine conjugate beta lyase	-	-	73%
BX883048	DEAH (Asp-Glu-Ala-His) box polypeptide 16	-	-	94%
NM_138710	Disabled homolog 2 (Drosophila) interacting protein	-	-	68%
BX883047	discoidin domain receptor family, member 1	-	-	100%
BX883047	E030032D13RIK gene	-	-	100%
BC087740	fasciculation and elongation protein zeta 1 (zygin I)	-	-	73%
NM_001008295	FIP1-like 1	-	down	73%
BX883048	flotillin 1	-	-	94%
BX883047	general transcription factor II H, polypeptide 4	-	-	100%
BX883048	guanine nucleotide binding protein-like 1	down	-	94%
BX883047	HCR (a-helix coiled-coil rod homolog)	up	-	100%
BX883048	hypothetical protein FLJ13158	-	down	94%
BX883048	hypothetical protein MGC15854	-	-	94%
BX883048	immediate early response 3	down	up	94%
BX883048	mediator of DNA damage checkpoint 1	-	down	94%
BX883048	MHC class I RT1.O type 149 processed pseudogene	-	-	94%
NM_181823	MIRO2 protein	-	-	73%
BX883048	mitochondrial ribosomal protein S18B	down	-	94%
NM_012607	neurofilament, heavy polypeptide	-	-	68%
BX883048	nurim (nuclear envelope membrane protein)	-	-	94%
AF138789	piccolo (presynaptic cytomatrix protein)	-	-	78%
AF136584	polo-like kinase 3 (Drosophila)	-	-	73%
	PREDICTED: Rattus norvegicus similar to peptidylglycine alpha-amidating monooxygenase COOH-terminal interactor; peptidylglycine alpha-amidating monooxygenase COOH-terminal interactor protein-1 (predicted) (RGD1309847_predicted), mRNA	-	-	68%
XR_009191.1	(predicted) (RGD1309847_predicted), mRNA	-	-	68%
BX883048	proline-rich polypeptide 3	-	-	94%
BX883048	protein phosphatase 1, regulatory subunit 10	down	down	94%
	Rattus norvegicus microtubule associated serine/threonine kinase 2 (predicted) (Mast2_predicted), mRNA	-	up	78%
NM_001108005.1	(predicted) (Mast2_predicted), mRNA	-	up	68%
NM_001107657.1	Rattus norvegicus myosin X (predicted) (Myo10_predicted), mRNA	-	up	68%
	Rattus norvegicus similar to DKFZP434P1750 protein (predicted) (RGD1311490_predicted), mRNA	-	-	68%
NM_001081980.1	(RGD1311490_predicted), mRNA	-	-	68%
	Rattus norvegicus ubiquitin specific protease 29 (predicted) (Usp29_predicted), mRNA	-	-	68%
NM_001108465.1	(Usp29_predicted), mRNA	-	-	68%
BX883047	RT1 class I, CE5	-	-	100%
BX883048	RT1 CLASS I, T24, gene 2	up	-	94%
BX883048	RT1 class Ib gene, H2-TL-like, grc region (N1)	-	-	94%
BX883048	RT1 CLASS IB GENE, H2-TL-LIKE, GRC region (N3)	-	down	94%
BX883047	RT1 class Ib, locus Aw2	-	-	100%
BX883048	RT1 CLASS IB, LOCUS BM1	-	down	94%
BX883048	RT1 CLASS IB, LOCUS H2-Q-like, GRC region	-	-	94%
BX883048	RT1 class Ib, locus S3	-	-	94%
	similar to ataxin 2-binding protein 1 isoform 1; hexaribonucleotide binding protein 1	-	down	68%
XM_213535	similar to KIAA0947 protein (predicted)	-	-	100%
XM_225143	Similar to KIAA1790 protein (Lrrk)	-	-	94%
XM_218760	Similar to periodic tryptophan protein 1 homolog; periodic tryptophan protein 1 homolog (S. cerevisiae)	-	down	73%
XM_343186	SIMILAR TO RIKEN CDNA 2610110G12	-	-	94%
NM_001014030	Similar to RIKEN cDNA 4930538D17	-	-	73%
BX883047	similar to TL antigen	-	-	100%
AF106937	SNF1-like kinase	-	-	73%
BX883047	Transcribed locus	down	-	100%
BX883047	transcription factor 19	-	down	100%
BX883048	tubulin, beta 5	-	down	94%
BX883047	valyl-tRNA synthetase 2-like	-	-	100%

Table 2. Regulation of possible off targets in p57kip2 suppressed cells. Listed are genes with high sequence similarity to the oligonucleotide sequence used for knockdown of p57kip2. The query coverage revealed the highest percentage of a partial overlap with the knockdown sequence. Genes which were found to be downregulated in p57kip2 suppressed cells are marked by “down”, genes which were found to be upregulated are marked by “up” and genes the expression of which did not change are marked by “-”.

4.11 p57kip2 suppression induced shift in gene expression resembles the *in vivo* gene expression associated with Schwann cell differentiation

Several genes are known to be differentially regulated during the development of peripheral nerves, including myelin genes, transcription factors and adhesion molecules. The array analysis revealed that most of these well described genes were also differentially regulated in p57kip2 suppressed Schwann cells. In order to validate the obtained results, quantitative RT-PCR was performed with p57kip2 suppressed Schwann cells at 9dpT (Fig. 17) and compared with *in vivo* expression data obtained from early developing nerves at P0, P6 and P28 (Fig. 18). This analysis revealed that differential expression of most genes in p57kip2 suppressed cells is in accordance to their expression profile during peripheral nerve development, underscoring the postulated function for p57kip2 as an inhibitor of peripheral myelination. Interestingly, among the genes investigated only p57kip2 was found to possess such a strong downregulation during postnatal peripheral nerve development. The members of the cip/kip family of genes, p21cip1 and p27kip1, were found to be biphasically regulated during sciatic nerve development. p27kip1 was upregulated early during development and downregulated at P28, while p21cip1 initially was downregulated and induced later on. These data indicate that Schwann cell cycle control is complex and will be discussed further below in greater detail.

Promyelinating markers, inhibitors of myelination and myelin genes:

In vivo myelination is initiated by downregulation of the promyelinating markers Oct-6 and Krox24, downregulation of the differentiation inhibitors Sox2 and c-Jun and the transient induction of Krox20 and Sox10 (Fig. 18). In p57kip2 suppressed Schwann cells we observed suppression of these promyelinating markers upon downregulation of p57kip2, whereas an induction of Krox20 was not detected (Fig. 17). Interestingly, while Sox2 levels were found to decline in p57kip2 suppressed Schwann cells, c-Jun levels increased. This suggests that p57kip2 suppression induced maturation of Schwann cells is independent from c-Jun regulation. Nevertheless, in line with the *in vivo* regulation, Sox10 upregulation as well as Krox24 downregulation were found in p57kip2 suppressed Schwann cells. Nab1 expression levels were induced in p57kip2 suppressed cells, which is in accordance with its *in vivo* regulation. Nab proteins act as cofactors and were shown to be necessary for Krox20 dependent

induction of myelin genes (Le *et al.*, 2005). Induction of myelin gene expression levels (P0, MBP, PMP22 and MAL) was also in accordance to the *in vivo* data.

Adhesion molecules and receptors:

Induction of myelination depends on interactions of cell adhesion molecules (integrins) with components of the extracellular matrix (laminins) as well as autocrine and paracrine signalling. In this regard, induction of the Lgi4 gene, which encodes a secreted protein and was shown to be necessary for peripheral nerve myelination (Bermingham *et al.*, 2005), was an important finding. Since only a weak induction could *in vivo* be observed, it remains to be demonstrated whether cells other than Schwann cells express this ligand as well. Another interesting gene is integrin- β 4, the expression of which was shown to be axon dependent and induced during peripheral nerve development (Feltri *et al.*, 1994). During this, integrin- β 4 is coexpressed with the myelin protein PMP22, and absence of integrin- β 4 was shown to alter the Schwann cell basal lamina, revealing the functional importance (Amici *et al.*, 2006). Interestingly, integrin- β 4 was found to be robustly induced in p57kip2 suppressed Schwann cells, suggesting that its expression can be uncoupled from axonal contact. Importantly, integrin- β 1, the expression of which is not regulated during postnatal peripheral nerve development, was also not regulated in p57kip2 suppressed cells, revealing specific differentiation associated gene induction among integrins. In contrast to the *in vivo* data, the cell adhesion molecules L1 and p75-LNGFR were found to be upregulated in p57kip2 suppressed cells, suggesting that their downregulation depends on axonal signals and is hence p57kip2 independent.

Activation of the alpha chemokine receptor CXCR4 by its ligand SDF1 was shown to increase the number of dying Schwann cells in culture (Küry *et al.*, 2003), suggesting that this interaction matches the number of Schwann cells in the nerve. During peripheral nerve development, CXCR4 was strongly downregulated, which is in line with the above postulation, while SDF1 levels decline only weakly. On the other hand, levels of the newly identified SDF1 receptor RDC1 (also referred to as CXCR7), were found to increase both during peripheral nerve development as well as in p57kip2 suppressed cells, suggesting different functions for both receptors. Downregulation of CXCR4 as well as upregulation of RDC1 in p57kip2 suppressed Schwann cells is therefore in accordance with the *in vivo* data. In contrast to this an upregulation of SDF1 could be observed. This does not correspond to the *in vivo*

expression profile. It remains to be shown whether this is due to the absence of axonal signals or whether *in vivo* other cells than Schwann cells additionally contribute to SDF1 expression. Nevertheless, these observations suggested a function for SDF1/RDC1 signalling during peripheral nerve development and *in vitro* maturation.

LIM domain encoding genes:

Since LIM domain containing proteins can bind to p57kip2 and this interaction is thought to affect the equilibrium between cytoplasmic and nuclear expression of these interaction partners, we were particularly interested in their expression and regulation. Among all genes the expression of which were validated by quantitative RT-PCR, induction of the LIM domain encoding gene PINCH2 was highest *in vitro* and *in vivo*, suggesting a specific function during Schwann cell differentiation. The highly related gene PINCH1 was also found to be induced, but induction was more modest. Interestingly, the degree of induction of PINCH1 and PINCH2 was very similar during peripheral nerve development and upon p57kip2 suppression. Levels of ROCK1 as well as its downstream effector LIMK-1 were found to decrease during peripheral nerve development, while an increase of LIMK-1 expression levels could be observed in p57kip2 suppressed Schwann cells, suggesting that LIMK-1 expression *in vivo* does not directly depend on p57kip2 expression. Nevertheless, since ROCK1 and LIMK-1 are almost ubiquitously expressed *in vivo*, other cell types are likely to contribute to the expression profile. The four and a half LIM domain protein 2 (Fhl2) is a crucial component of focal adhesions. Fhl2 is known to affect gene expression, migration and cell survival. Its overexpression is associated with stimulation of proliferation and glioma formation (Li *et al.*, 2008). Fhl2 was found to be downregulated both *in vivo* as well as *in vitro*, suggesting that FHL2 downregulation contributes to changes in Schwann cell morphology or cell cycle exit. Another constituent of focal adhesions, the LIM domain containing protein Hic-5, was shown to be slightly downregulated in p57kip2 suppressed cells as well as in the natural context. Interestingly, Hic-5 was shown to possess a function regarding activation of the Rho/ROCK signalling cascade (Tumbarello *et al.*, 2007) and as a scaffold protein within integrin signalling. Further to this, Hic-5 was shown to heterooligomerize with PINCH, suggesting that Hic-5 coordinates adhesion with cellular activities (Mori *et al.*,

2006). Taking together, GeneChip array analysis revealed a shift of Schwann cell related genes towards differentiation.

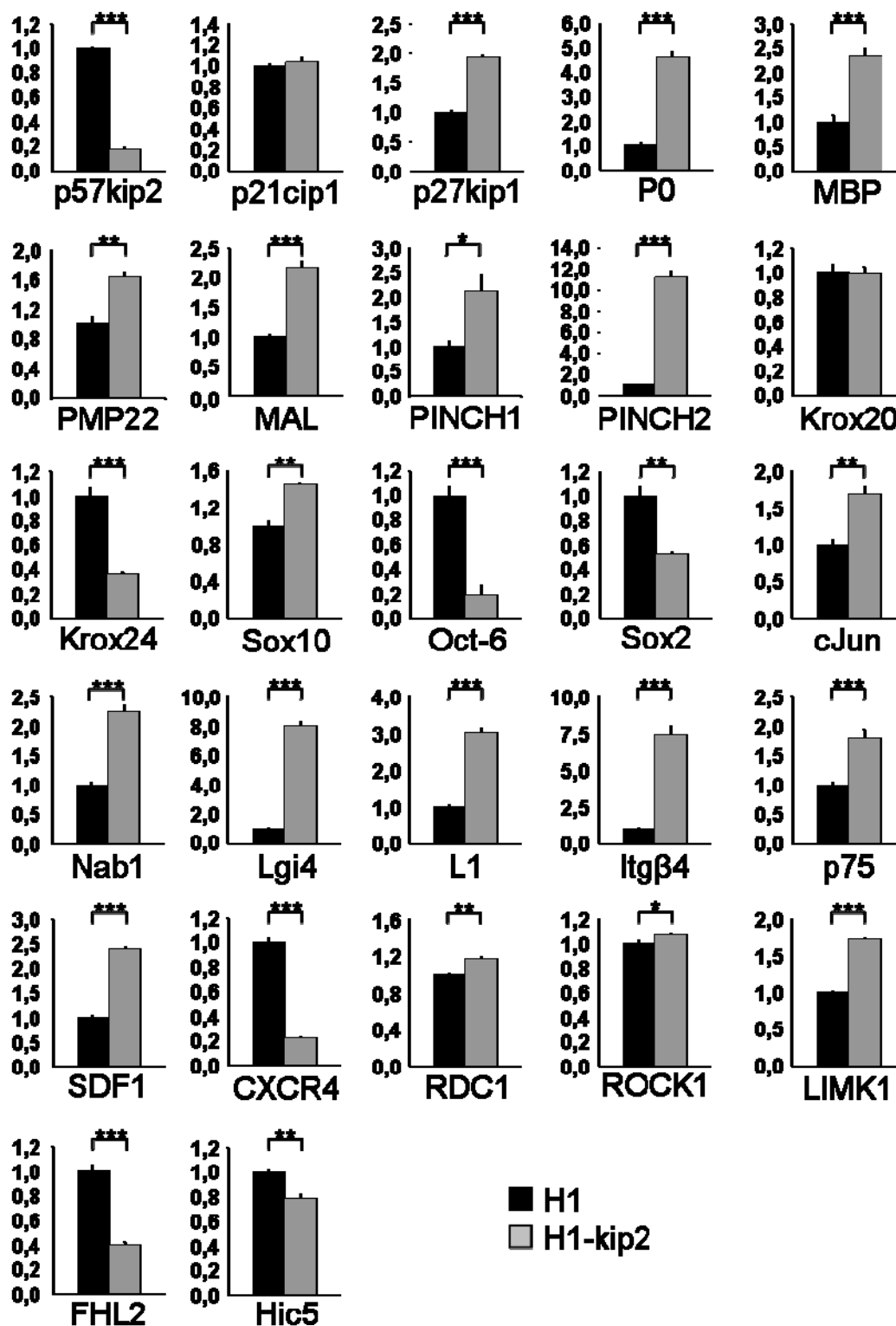


Fig. 17. Regulation of Schwann cell related genes in p57kip2 suppressed cells. Quantitative RT-PCR measurement was used to validate GeneChip array expression data of Schwann cell related genes in p57kip2 suppressed cells versus control transfected cells at 9dpT. For each gene one representative measurement out of three experiments is shown. GAPDH expression was used as reference, and data are mean values \pm SEM. *t*-test *, $P < 0.05$; **, $P < 0.01$; ***, $P < 0.001$. H1, control transfected cells; H1-kip2, p57kip2 suppressed cells.

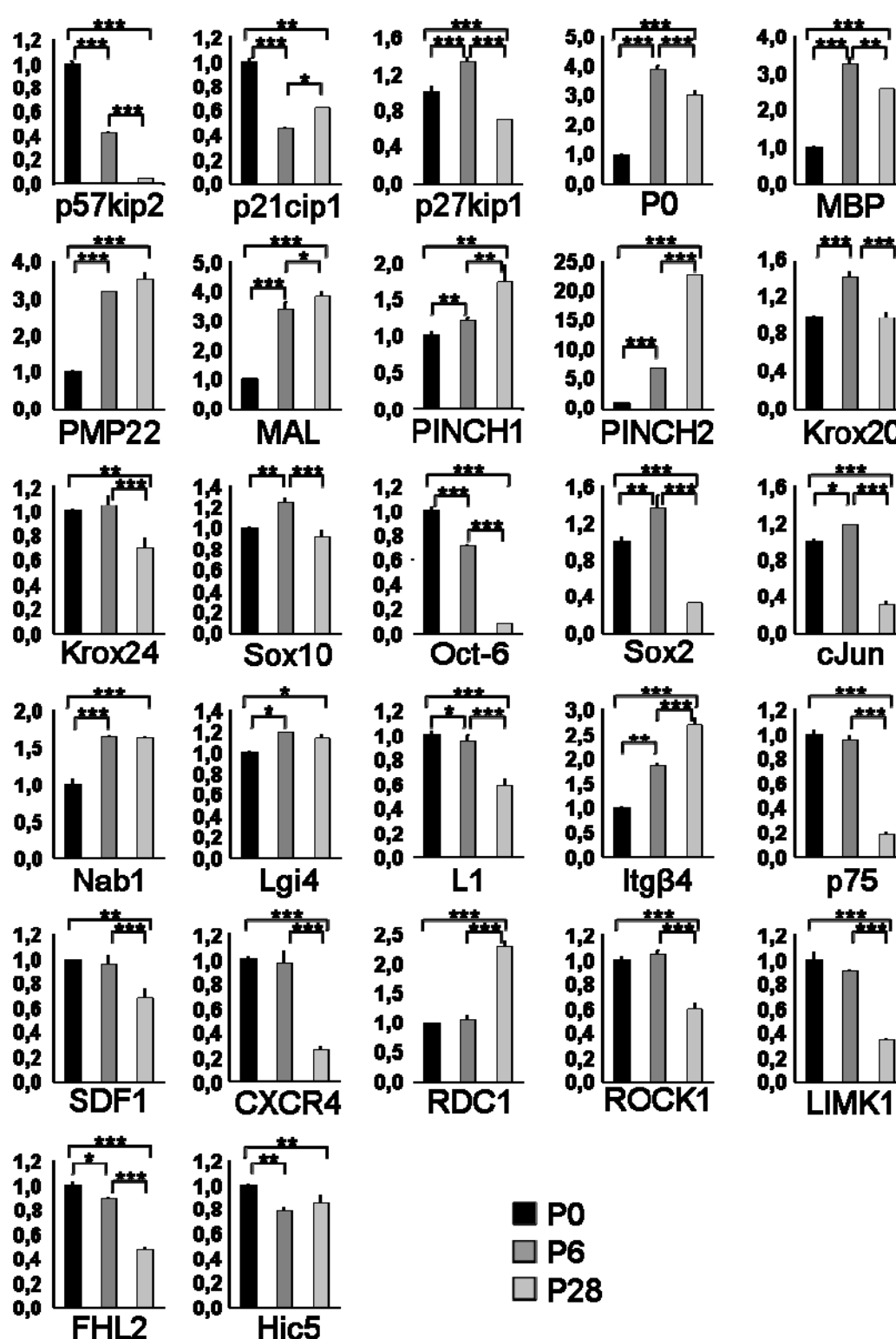


Fig.18. Regulation of Schwann cell related genes during peripheral nerve development. Quantitative RT-PCR measurement revealed the expression profile of Schwann cell related genes during early postnatal development at postnatal days P0 (black bars), P6 (dark grey bars) and P28 (light grey bars). GAPDH expression was used as reference, and data are mean values \pm SEM. *t*-test *, $P < 0.05$; **, $P < 0.01$; ***, $P < 0.001$.

4.12 GeneChip array analysis revealed changes in cell cycle associated gene expression

Although p57kip2 expression has initially be shown as negative regulator of the cell cycle, suppression of p57kip2 was accompanied by cell cycle exit. Schwann cell proliferation must therefore be controlled by other CKIs. In order to shed light on the genes involved in p57kip2 suppression induced cell cycle exit, expression levels of cyclins, CDKs and CKIs as well as other cell cycle related genes were investigated. The array data obtained from Schwann cells at 1dpT and 9dpT revealed a complex pattern of cell cycle related gene expression (Table 3; Heinen *et al.*, 2008b). Interestingly, of 100 cell cycle related genes investigated, 28 were upregulated at the early timepoint, while only 10 genes were upregulated at the late timepoint. In contrast to this, 10 genes were downregulated at the early timepoint and 31 genes were downregulated at the late timepoint. The fact that many regulations were observed at 1dpT suggests that cell cycle exit is a direct consequence of p57kip2 suppression and probably not only an indirect consequence of Schwann cells being allowed to differentiate. In addition, expression of some of the regulated genes differed between the two timepoints, implicating cdk4 and cyclin D1, both of which were shown to be involved in the control of Schwann cell proliferation (Atanasoski *et al.*, 2001; Atanasoski *et al.*, 2008). These genes were induced at the early timepoint and subsequently downregulated at the second timepoint during p57kip2 dependent Schwann cell differentiation. Such a similar profile was observed for many cyclins investigated, including cyclin A2, cyclin L1 and cyclin B1, suggesting that downregulation of cyclins is an indication for terminal differentiation onset. Interestingly, cdk2 and cdk6 expression was unchanged in p57kip2 suppressed cells, which is in agreement with recent observations that their inactivation does not affect Schwann cell proliferation *in vivo* (Atanasoski *et al.*, 2008).

Regarding CKI expression, p18INK4c and cdkn3 were induced one day after Schwann cell differentiation was initiated, whereas at the late timepoint p21cip1 and p27kip1 were found to be induced. While until now no reports describe a function for p18INK4c or cdkn3 in Schwann cell proliferation control, the induction of p21cip1 and p27kip1 is in line with recent results. Atanasoski and colleagues have shown that p21cip1 expression is attributed to Schwann cell cycle exit (Atanasoski *et al.*, 2006). Further reports revealed that p27kip1 expression is upregulated during peripheral nerve development and downregulated following peripheral nerve injury (Tikoo *et al.*,

2000; Shen *et al.*, 2008). In addition, it has been shown that p27kip1 expression inhibits Schwann cell proliferation (Iacovelli *et al.*, 2007), suggesting that both CKIs share redundant functions. Of note, p18INK4c, p27kip1 and p57kip2 have been shown to be important components of the intrinsic timer that controls the differentiation of oligodendrocytes (Dugas *et al.*, 2007; Tokumoto *et al.*, 2002). The expression of p16INK4a, which is attributed to injury induced Schwann cell proliferation (Atanasoski *et al.*, 2006), was found to be downregulated at 9dpT, while no regulation was found at 1dpT. On the other hand, p19INK4d was downregulated one day after Schwann cell differentiation was initiated, implying that the CKI function of this gene is not involved in p57kip2 suppression induced Schwann cell differentiation. These findings indicate that the decision to exit the cell cycle along the differentiation process is dynamic and complex and can thus not be confined to a single cell cycle associated gene.

GeneBank accession #	Gene	regulation 1dpT	regulation 9dpT
cyclin, CDK, CKI, Pak			
NM_012766	cyclin D3	-	-
NM_022267	cyclin D2	down	up
NM_001107171	similar to cyclin T2	-	down
NM_001105998	cyclin I	-	-
NM_053702	cyclin A2	up	down
NM_052981	cyclin H	up	-
NM_001100474	cyclin F	-	-
NM_012923	cyclin G1	-	-
NM_053662	cyclin L1	up	down
NM_171991	cyclin B1	up	down
NM_001100472	cyclin C	-	up
NM_171992	cyclin D1	up	down
NM_001108657	core-binding factor; cyclin D-related	-	down
NM_031030	cyclin G associated kinase	down	down
NM_001013204	cyclin D-type binding-protein 1	up	up
NM_001011942	cyclin M2	-	-
NM_001011949	cyclin A1	-	-
NM_053593	Cdk4	up	down
XM_342638	Cdk6	-	-
NM_001113751	Cdk2-associated protein 1	up	-
XM_215467	Cdk7	-	down
NM_199501	Cdk2	-	-
NM_080885	Cdk5	-	down
NM_001007743	Cdk9	-	down
NM_053891	Cdk5, regulatory subunit 1	-	-
NM_022799	Nucks1	down	-
NM_001106758	similar to Cdk2-interacting protein	up	-
NM_001109936	Cdk10	-	-
NM_145721	Cdk5 regulatory subunit associated protein 1	-	-
XM_575844	Cdk5 regulatory subunit associated protein 2	up	-
NM_024488	Cdk5 regulatory subunit associated protein 3	-	-
NM_001107404	Cdk5 and Abl enzyme substrate 1	-	-
NM_001106028	Cdkn3	up	down
NM_031550	Cdkn2a (p16INK4a)	-	down
NM_001033757	Cdkn1c (p57kip2)	down	down
NM_031762	Cdkn1b (p27kip1)	-	up
NM_131902	Cdkn2c (p18INK4c)	up	down
NM_130812	Cdkn2b (p15INK4b)	-	-
NM_001009719	Cdkn2d (p19INK4d)	down	-
NM_080782	Cdkn1a (p21cip1)	-	up
NM_017198	Pak1	-	-
NM_053306	Pak2	-	down
NM_019210	Pak3	-	-
NM_001106238	Pak4	-	-
NM_001106498	Pak6	down	-
cell cycle related			
NM_032080	Gsk3b	-	-
NM_021578	TGF-beta1	-	up
NM_031131	TGF-beta2	-	-
NM_013174	TGF-beta3	-	-
NM_031132	TGFR2	down	up

Table 3.
(described on p. 97)

GeneBank accession #	Gene	regulation 1dpT	regulation 9dpT
cell cycle related, continued			
NM_012775	TGFR1	-	up
NM_019191	Smad2	-	-
NM_013095	Smad3	-	-
NM_019275	Smad4	up	-
XM_001071121	retinoblastoma 1	-	-
NM_133381	Crebbp	-	-
NM_030989	Trp53	up	-
NM_001108327	Prkdc	-	down
NM_001106821	Atm	-	-
NM_053677	Chek2	-	-
XM_001065279	similar to 14-3-3 protein sigma	-	-
NM_024127	Gadd45a	-	up
XM_001080736	budding uninhibited by benzimidazoles 1 homolog	up	down
NM_001106594	MAD2-like 1	up	down
NM_031683	Smc11	up	-
XM_001067790	extra spindle poles like 1	up	down
NM_022391	pituitary tumor-transforming 1	up	down
NM_001080147	anaphase-promoting complex subunit 5	-	-
NM_171993	cdc20	up	down
NM_013052	Ywhah	up	-
NM_133571	cdc25a	-	down
NM_133572	cdc25b	-	down
NM_001108074	fizzy/cell division cycle 20 related 1	up	-
NM_001108404	cdc14 cell division cycle 14 homolog B	down	-
NM_017100	polo-like kinase 1	up	down
NM_001033690	Orc6l	-	down
NM_199092	Orc4l	up	-
NM_001025282	Orc3l	-	-
NM_177931	Orc1l	-	down
NM_001014186	Orc5l	-	down
NM_001012003	Orc2l	up	-
NM_017287	Mcmd6	-	down
XM_344048	Mcmd4	down	down
NM_001107873	Mcmd2	-	-
XM_001070728	Mcmd3	-	down
NM_001106170	Mcmd5	-	-
NM_001004203	Mcmd7	-	-
NM_001108352	cdc7	-	-
XM_231388	Dbf4	-	-
RGD:1593939	E2F2	-	-
XM_574892	E2F5	up	-
NM_031094	Rbl2	-	-
XM_001067833	similar to Retinoblastoma-like protein 1	up	-
XM_001081495	Hdac5	up	up
NM_053448	Hdac3	-	-
XM_228753	Hdac6	-	-
XM_001079831	Abl1	-	-

Table 3, continued. Regulation of cell cycle related genes in p57kip2 suppressed cells. GeneChip array analysis revealed that a number of cell cycle associated genes were differentially regulated upon p57kip2 suppression at 1dpT and 9dpT. Genes which were found to be downregulated in p57kip2 suppressed cells are marked by “down”, genes which were found to be upregulated are marked by “up” and genes the expression of which did not change are marked by “-”.

4.13 2D gel electrophoresis revealed nuclear proteins which are differentially regulated in p57kip2 suppressed Schwann cells

The changes in the gene expression pattern shown by GeneChip array analysis prompted us to investigate the nuclear proteome of p57kip2 suppressed cells at 9dpT in order to identify differentially regulated transcription factors and nuclear LIM

domain proteins. Therefore, Schwann cells were cotransfected with H1 or H1-kip2 together with the hygromycin resistance plasmid pcDNA3.1/hyg lacking citrine expression. Transfected cells were enriched using hygromycin B selection. Since nuclear events most likely account for the observed effects on gene expression, cells were harvested at 9dpT and nuclei were prepared using the NE-PER nuclear and cytoplasmic extract kit (Pierce). Proteins of the two cell populations (control and p57kip2 suppressed cells) were labelled with Cy3 and Cy5 dye and separated using 2D gel electrophoresis. Following normalization, differentially expressed protein spots were excised and identified by mass spectrometry. Labelling of proteins, 2D gel electrophoresis and analysis of results was done in collaboration with Dr. Kai Stühler, (Medical Proteome Center, Ruhr University Bochum). Five experiments were performed in order to assure statistical significance. Analysis of these experiments revealed that 55 significantly regulated protein spots could be identified which corresponded to 32 different proteins (Table 4). Expression of the nuclear proteins lamins and nucleoporin revealed successful enrichment of nuclear fractions. Interestingly, protein regulation was in accordance to the GeneChip array data. Among the proteins of interest regarding Schwann cell differentiation, we detected differentially expressed septins. These cytoskeletal associated proteins were shown to be involved in dendritic spine formation (Xie *et al.*, 2007) and were shown to be part of myelin fractions (Taylor *et al.*, 2004). PLP null mutant myelin was shown to lack distinct septin isoforms (Werner *et al.*, 2007), suggesting a function during glial cell myelination. Interestingly, our analysis of the differentiating Schwann cell proteome showed that septins are also expressed in the nucleus, revealing additional functions. Another important protein which was shown to be upregulated in p57kip2 suppressed cells was the SWI/SNF-related matrix associated actin dependent regulator of chromatin. SWI/SNF proteins are known to affect DNA methylation and to promote the transcriptional activation. We also found the serine protease inhibitor precursor serpin H1 to be differentially regulated in p57kip2 suppressed cells. The expression of the serine protease inhibitor nexin-1 for example was shown to be crucial for nerve regeneration (Lino *et al.*, 2007). Taking together, these results reveal promising candidates the expression of which can be attributed to Schwann cell differentiation.

Proteins downregulated upon p57kip2 suppression

accession	protein	protein regulation	gene regulation
IPI00366190.3	similar to Lamin-B2	-3,83	down
IPI00212724.1	Type A/B hnRNP p38	-3,03	down
IPI00421500.9	Heterogeneous nuclear ribonucleoprotein A1	-2,83	down
IPI00212724.1	Type A/B hnRNP p38	-2,76	down
IPI00562850.1	59 kDa protein (Ptpb1)	-2,35	down
IPI00231555.1	Isoform PYBP1 of Polypyrimidine tract-binding protein 1	-2,19	absent
IPI00231555.1	Isoform PYBP1 of Polypyrimidine tract-binding protein 1	-2,07	absent
IPI00231555.1	Isoform PYBP1 of Polypyrimidine tract-binding protein 1	-2,07	absent
IPI00212724.1	Type A/B hnRNP p38	-2,02	down
IPI00358211.3	similar to Heterogeneous nuclear ribonucleoproteins A2/B1	-2,01	absent
IPI00212969.2	32 kDa protein (Hnrpa2b1)	-1,98	absent
IPI00364061.4	Hnrpl protein	-1,89	down
IPI00230941.5	Vimentin	-1,89	-
IPI00208304.1	Septin-2	-1,88	-
IPI00364061.4	Hnrpl protein	-1,82	absent
IPI00366789.2	similar to retinoblastoma binding protein 4	-1,81	down
IPI00189770.1	Nucleoporin p54	-1,79	down
IPI00188909.2	Collagen alpha-1(I) chain precursor	-1,72	down
IPI00204703.5	Serpin H1 precursor	-1,72	down
IPI00231555.1	Isoform PYBP1 of Polypyrimidine tract-binding protein 1	-1,69	absent
IPI00231555.1	Isoform PYBP1 of Polypyrimidine tract-binding protein 1	-1,66	absent
IPI00212969.2	32 kDa protein (Hnrpa2b1)	-1,61	absent
IPI00372854.4	similar to heterogeneous nuclear ribonucleoprotein H3 isoform a	-1,53	down
IPI00200920.1	Khsrp Far upstream element-binding protein 2	-1,52	-

Proteins upregulated upon p57kip2 suppression

IPI00209148.3	Splice Isoform 1 of Heterogenous nuclear ribonucleoprotein M	3,19	up
IPI00204899.2	Septin 7	2,74	up
IPI00201060.4	Lamin-A	2,73	-
IPI00201060.4	Lamin-A	2,69	-
IPI00201060.4	Lamin-A	2,53	-
IPI00201060.4	Lamin-A	2,48	-
IPI00201060.4	Lamin-A	2,47	-
IPI00201060.4	Lamin-A	2,32	-
IPI00204899.1	Septin 7	2,28	up
IPI00207355.3	Heat shock-related 70 kDa protein 2	2,18	up
IPI00201060.4	Lamin-A	2,14	-
IPI00201060.4	Lamin-A	2,14	-
IPI00551729.1	Eef1a1 Elongation factor 1-alpha 1	2,14	-
IPI00201060.4	Lamin-A	2,06	-
IPI00212622.1	Trifunctional enzyme subunit alpha, mitochondrial precursor	2,04	absent
IPI00365286.3	similar to Vinculin	2	-
IPI00551729.1	50 kDa protein	1,91	absent
IPI00363719.3	Heterogeneous nuclear ribonucleoprotein D-like	1,91	-
IPI00201060.4	Lamin-A	1,84	-
IPI00551729.1	Eef1a1 Elongation factor 1-alpha 1	1,8	-
IPI00201060.4	Lamin-A	1,74	-
IPI00555259.4	Matrin-3	1,71	-
IPI00370384.3	similar to Alpha-centractin	1,7	absent
IPI00758469.1	Isoform 2 of Polypyrimidine tract-binding protein 2	1,64	-
IPI00464718.1	Ddx5 gene	1,63	absent
IPI00364061.4	Hnrpl protein	1,61	absent
IPI00393081.3	similar to SWI/SNF-related matrix-associated actin-dependent regulator of chromatin c2 isoform b isoform 2	1,59	up
IPI00758469.1	Isoform 2 of Polypyrimidine tract-binding protein 2	1,59	-
IPI00201060.4	Lamin-A	1,57	-
IPI00201060.4	Lamin-A	1,55	-
IPI00208304.1	Septin-2	1,54	-

Table 4. Differential expression of nuclear proteins in p57kip2 suppressed cells. 2 d gele electrophoresis revealed a number of nuclear proteins which were differentially expressed in comparison to control transfected cells at 9dpT. The fold change of protein expression is shown in the column “protein regulation”. The expression of some of these proteins was in accordance to the GeneChip array data, shown in the column “gene expression”. Genes which were found to be downregulated in p57kip2 suppressed cells are marked by “down”, genes which were found to be upregulated are marked by “up” and genes the expression of which did not change are marked by “-”. “Absent” marks genes which were not listed in the GeneChip array.

5. DISCUSSION

Schwann cells and oligodendrocytes, the myelinating glial cells of the PNS and CNS, respectively, share similar functions. They ensheath axons by radially wrapping around them and thus generate myelin internodes which electrically insulate axons from the environment. Furthermore these cells account for the uptake of residual glutamate and allow the rapid repolarization of axons after action potentials. Another important function of these cells is the supply of axons with nutrients, and a recent publication has shown that Schwann cells also provide polyribosomes to axons in order to control axonal protein synthesis (Court *et al.*, 2008), thus revealing the close interactions between these two cell types. This is also reflected by the fact that axons degenerate when glial cells get lost, for example following autoimmune attack against myelin, as it occurs during the disease processes of multiple sclerosis (MS) and Guillain-Barre syndrome. On the other hand, loss of axons also leads to the dedifferentiation and degeneration of glial cells. In this case, Schwann cells reveal a remarkable plasticity which allows them to dedifferentiate, reenter the cell cycle and remyelinate newly sprouting axons. Thus, Schwann cells support the regeneration of peripheral nerves (Son and Thompson, 1995). This is in striking contrast to, oligodendrocytes, which lack the capacity to regenerate and die following loss of axons. Hence regeneration as well as axonal protection and restoration in the CNS is a result of resident precursor cell activation and remains therefore limited. This suggests that intrinsic inhibitors exist the expression of which interferes with the regeneration in the CNS, while they are dynamically regulated following PNS injury or demyelinating disease processes.

Another important difference between Schwann cells and oligodendrocytes is the fact that oligodendroglial precursor cells spontaneously differentiate in cell culture, while Schwann cells have so far been regarded as blocked in their differentiation (Abney *et al.*, 1981; Morrison *et al.*, 1991). It was postulated that an intrinsic timer mechanism controls the timepoint to exit the oligodendroglial cell cycle leading to terminal differentiation, including induction of the CKIs p18INK4c and p27kip1 (Tokumoto *et al.*, 2002). Since Schwann cell proliferation *in vitro* is not controlled by such a timer mechanism, it seems that the induction of cell cycle inhibitors and thus also terminal differentiation is blocked and depends on the activation of intracellular signalling cascades by extracellular receptor/ligand interactions with axons.

This thesis provides for the first time evidence that the *in vitro* differentiation of Schwann cells can be uncoupled from axonal signalling by suppression of the CKI p57kip2 (Heinen *et al.*, 2008a; Heinen *et al.*, 2008b). It was shown that p57kip2 is strongly downregulated during postnatal peripheral nerve development. Suppression of p57kip2 by means of vector based RNAi surprisingly led to cell cycle exit and striking morphological alterations in cultured primary immature Schwann cells. Determination of gene expression levels by quantitative RT-PCR as well as Western blot analysis revealed an increase in the gene and protein levels of important myelin components. It could also be shown that transplantation of DRG cocultures with p57kip2 suppressed Schwann cells accelerated the *in vitro* myelination process. Additionally, analysis of the transcriptome revealed a shift in the gene expression program towards terminal differentiation of Schwann cells, and nuclear proteome research revealed promising candidate proteins which were differentially expressed in nuclei of p57kip2 suppressed Schwann cells and could therefore be implied in this differentiation process. All together these results strongly suggest that p57kip2 is an intrinsic inhibitor of myelinating Schwann cell differentiation and that suppression of p57kip2 is necessary to overcome the differentiation blockade to allow maturation uncoupled from axonal signals.

5.1 The role of intrinsic myelination inhibitors

During embryonic development of the peripheral nervous system, Schwann cell precursors are in close contact with several axons. In this early phase of development, axonal signals control proliferation and survival of these cells, functions which are thought to be mediated through Nrg1/erbB2 signalling (Nave and Salzer, 2005). Interestingly, the same signalling pathway, together with additional laminin/integrin signalling events, also contributes to the terminal differentiation during later developmental stages, including the decision to segregate and myelinate axons and the control of the myelin thickness (Taveggia *et al.*, 2005). Nevertheless, both Nrg1 as well as laminins are not able to induce *in vitro* myelination of pure Schwann cell cultures. This finding raised the assumption that Schwann cell differentiation is blocked and that myelination depends on direct contact between Schwann cells and axons in order to release this blockade. Thus intrinsic inhibitors of myelination are thought to exist the expression of which must be reduced during the postnatal development to allow myelination. On the other hand, taking into account

that Schwann cells de- and redifferentiate following nerve injury, these inhibitors are also expected to be differentially regulated as a consequence of axonal degeneration. Hence axonal signals repress these inhibitors, and axonal signalling therefore has to be maintained throughout lifetime in order to prevent demyelination.

Up to date, only few proteins were shown to inhibit myelination *in vivo*. The expression of c-Jun, Notch and Sox2 is repressed during postnatal development of sciatic nerves and reexpression was shown to promote the regeneration after nerve injury (Parkinson *et al.*, 2008; Le *et al.*, 2005). Furthermore it has been suggested that Id proteins inhibit myelination, since their expression is also repressed during myelination. Since repression neither of c-Jun, Notch or Sox2 nor of Id proteins leads to the induction of Schwann cell *in vitro* differentiation, it is currently unclear whether Id regulations are functionally involved in important inhibitory mechanisms. In this context, our observation of p57kip2 suppression induced Schwann cell differentiation is a surprising result. Interestingly, while suppression of p57kip2 led to downregulation of Sox2, upregulation of c-Jun was observed (Fig. 17), suggesting that at least *in vitro* p57kip2 suppression induced Schwann cell differentiation is independent from c-Jun. It would therefore be interesting to investigate whether suppression of both p57kip2 and Sox2 or p57kip2 and c-Jun could further accelerate the cultured Schwann cell differentiation. On the other hand, among all known inhibitors of Schwann cell differentiation, p57kip2 is the only one the expression of which was found to be strongly decreased as early as postnatal day six (Fig. 18). In contrast to this, both c-Jun as well as Sox2 levels were slightly increased at this timepoint, which is in line with their proliferation promoting function. This expression profile also suggests that the late downregulation of, for example, Sox2 is likely a secondary consequence of lowered p57kip2 levels.

As a member of the cip/kip family of CKIs, p57kip2 is primarily considered to negatively interfere with the G1/S transition of the cell cycle (Lee *et al.*, 1995; Matsuoka *et al.*, 1995). However, it has also been shown that CKIs can act independent from their cell cycle inhibitory function, for example as regulators of neural differentiation (Dyer *et al.*, 2000; Joseph *et al.*, 2003; Ohnuma *et al.*, 1999). The finding that p57kip2 expression is dynamic following crush lesion and during development of peripheral nerves (Küry *et al.*, 2002) as well as according to the *in vitro* observations described in this thesis strongly suggest a differentiation and regeneration associated function for this protein. This assumption is also supported

by the finding that p57kip2 is dynamically expressed in experimental autoimmune encephalomyelitis (EAE) affected rats. EAE is an animal model for multiple sclerosis and is characterized by phases of myelin degeneration followed by phases of partial functional recovery. We could demonstrate that within this disease process downregulation of p57kip2 is correlated with functional recovery (Kremer, D., Zimmermann, K., Heinen, A., Jadasz, J., Jander, S., Hartung, H.P., and Küry, P., manuscript submitted). Moreover it could be shown that p57kip2 is downregulated during spontaneous *in vitro* differentiation of oligodendrocyte precursor cells and that additional suppression of p57kip2 accelerates their maturation process, strongly suggesting that downregulation of p57kip2 is a general prerequisite for myelinating glial cell maturation. Hence p57kip2 is expected to be a negative determinant of myelinating glial cell differentiation. This raises the question how the regulation of a single molecule is able to affect a number of divergent functions such as cell cycle exit, morphological changes and gene expression.

5.2 p57kip2 expression and cell cycle control

Proliferation of Schwann cells can still be observed within the first postnatal weeks (Stewart *et al.*, 1993). The finding that p57kip2 is downregulated even at this early postnatal timepoint implies that its function is most likely not involved in the control of Schwann cell cycle exit. However, there are further observations supporting this notion: Whereas suppression of p57kip2 led to a significant decrease of the proliferation rate, we observed that p57kip2 expression levels were found to steadily increase in control transfected cells without inhibition of the cell cycle (Fig. 12C). Since CKI are known to act redundantly, it can be assumed that further CKIs account for the cell cycle exit observed in differentiating cells. This assumption was confirmed by GeneChip array analysis, which revealed the dynamic expression of several CKIs upon p57kip2 suppression even as early as one day after transfection, indicating that the decision to exit the cell cycle is not solely dependent on a single factor (Heinen *et al.*, 2008b). This is in accordance to previously published results, including functions for p16INK4a, p21cip1 and p27kip1 regarding Schwann cell cycle control both during development and regeneration (Atanasoski *et al.*, 2006; Shen *et al.*, 2008). The array data additionally revealed a potential function of p18INK4c and cdkn3, which were so far not reported in this context. However, since so far only two timepoints (1dpT and 9dpT) were investigated, it cannot be excluded that further CKIs account for the cell

cycle exit, the expression of which are transiently upregulated within this period. Therefore, a detailed temporal analysis of CKI expression profiles and the timing of cell cycle exit in response to p57kip2 suppression is likely to shed more light on that particular issue. In addition, protein expression levels and subcellular distributions of cell cycle associated proteins remain to be determined.

The complex pattern of CKI expression was also reflected by the analysis of their postnatal expression profiles. Surprisingly, p21cip1 levels were found to be decreased at postnatal day six but increased later on again. On the other hand, p27kip1 expression was found to increase early and to decrease at the late timepoint. This suggests that, at least among the detailed investigated CKIs, p27kip1 induction is necessary for cell cycle exit, while late induction of p21cip1 maintains Schwann cells in an arrested state, a speculation which is supported by the finding that both genes are rapidly downregulated upon peripheral nerve injury (Atanasoski *et al.*, 2006; Shen *et al.*, 2008).

5.3 p57kip2's influence on cell morphology

Suppression of p57kip2 was found to induce striking morphological changes, including increases in protrusion length as well as soma size. The described alterations have to be seen in the context of protrusion extension during postnatal development and maturation of these cells. Since two different p57kip2 suppression constructs led to similar morphological alterations and since they were partially reversible by overexpression of p57kip2, these effects were found to be specific to p57kip2 knockdown and not a consequence of side effects caused by the gene suppression strategy. The finding that changes in morphology were accompanied by accumulation of long actin filaments supported the assumption that these are due to changes of the actin filament equilibrium. Indeed, cytoskeletal rearrangements have been shown to be crucial for Schwann cell differentiation, since disruption of actin polymerization using cytochalasin D leads to morphological alterations and inhibits the myelination of DRG cocultures (Fernandez-Valle *et al.*, 1997). We however also observed p27kip1 dependent morphological changes. These cells nevertheless displayed only similar morphologies but no myelin induction. Furthermore, p27kip1 reduction appeared to reduce cell viability. Whether this is due to an effect of p27kip1 acting on Rho signalling other than p57kip2 or an (unspecific) side effect needs to be shown.

Previous reports revealed that p57kip2 consists of at least four different domains (Lee *et al.*, 1995). One of these domains, the so called proline rich region, was shown to bind to LIM domain containing proteins and is unique among all members of the cip/kip family of genes. The particular interaction of p57kip2 and LIM domains was revealed to affect the subcellular localization of LIMK-1 (Yokoo *et al.*, 2003), a downstream effector of the Rho cascade. As LIMK-1 phosphorylates and inactivates cofilin, which is an important modulator of actin filament disassembly, changes in the p57kip2 concentration are thought to have an influence on actin filament stability. Since both p57kip2 and p27kip1 are known to affect the cytoskeleton by interference of the Rho signalling cascade through interactions with different binding partners (Besson *et al.*, 2008), this finding supports the assumption that morphological alterations in p57kip2 suppressed cells are due to changes in actin filament stability.

In this thesis, p57kip2 overexpression was shown to reciprocally result in higher levels of nuclear LIMK-1 expression, providing a proof of principle that interactions of these two proteins also occur in Schwann cells. Whether this leads to a loss of cytoplasmic or to a gain of nuclear LIMK-1 functions remains to be shown in future experiments. The finding that suppression of p57kip2 raised the levels of LIMK-1 expression *in vitro* could not be confirmed by the *in vivo* expression data, since LIMK-1 levels are downregulated during postnatal development, suggesting that p57kip2 does not directly influence LIMK-1 levels. Therefore it is likely that the ubiquitous expression of LIMK-1 in other cells than Schwann cells *in vivo* contribute to the changes in the LIMK-1 gene expression. Nevertheless, it is assumed that upregulation of LIMK-1 upon p57kip2 suppression amplifies the cytoplasmic activity of the kinase.

According to our current model (Fig. 19; Heinen *et al.*, 2008b), LIMK-1 is shifted from the cytoplasm to the nucleus due to the presence of high p57kip2 levels such as in Schwann cells of early postnatal nerves. This in turn leads to increased cofilin activity and subsequent actin filament depolymerization, hence limiting Schwann cell growth. The finding that p57kip2 is able to translocate LIMK-1 suggests that alterations in p57kip2 levels could directly affect the subcellular distribution of LIM domain containing binding partners. Hence it is assumed that high p57kip2 levels lead to the accumulation of further potential LIM domain containing binding partners, which might affect the expression of Schwann cell differentiation related gene

expression (Fig. 19A). Upon p57kip2 suppression or under physiological circumstances where p57kip2 levels are downregulated, such as during peripheral nerve development or in response to injury, less LIMK-1 is translocated (Fig. 19B). This leads to elevated levels of phosphorylated and inactive cofilin which in turn promotes actin filament polymerization and stabilization. On the other hand, it can be assumed that the nuclear concentration of further potential p57kip2 binding partners is also reduced upon p57kip2 suppression, allowing terminal differentiation of Schwann cells.

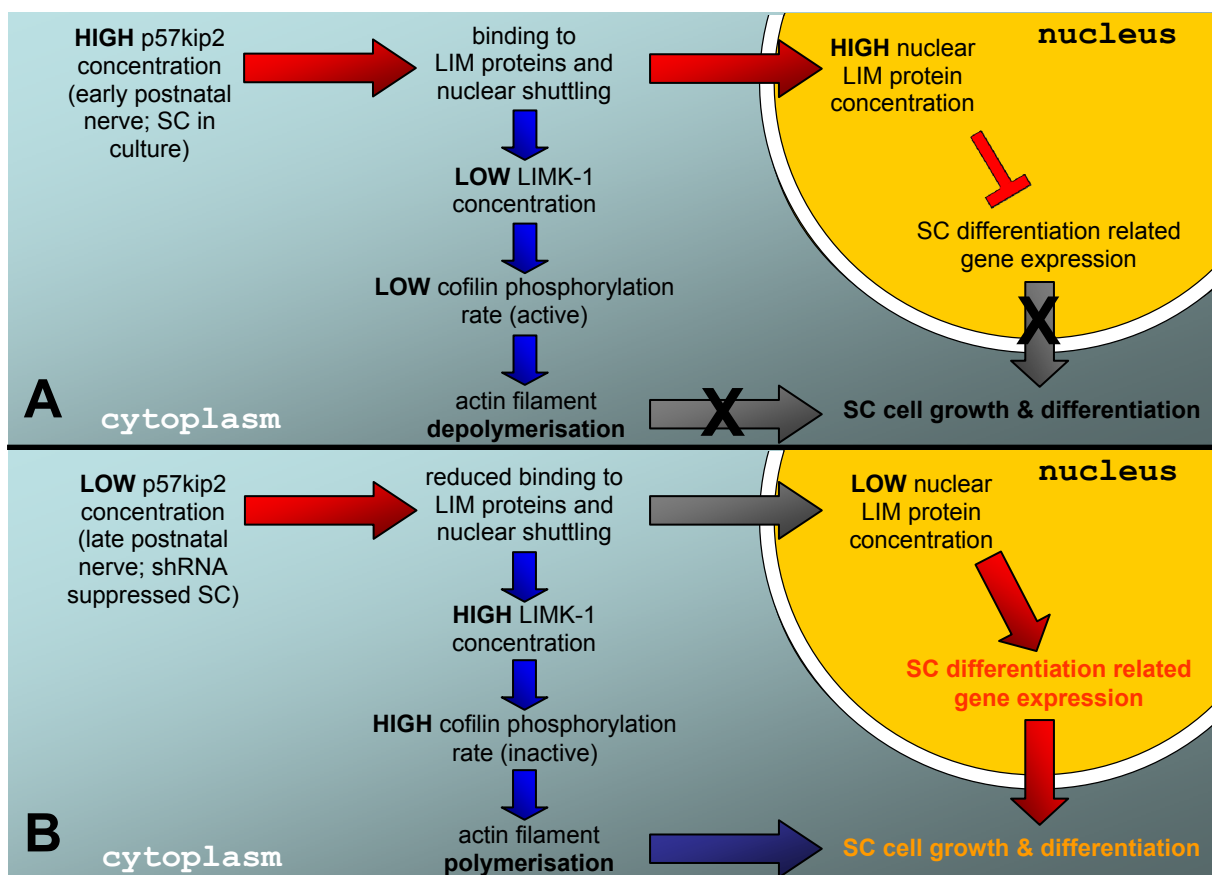


Fig. 19. Proposed mode of action for p57kip2 regulated Schwann cell differentiation. (A) Schwann cells of early postnatal nerves or in culture exhibit high p57kip2 levels which lead to increased LIM protein nuclear translocation. Reduced cytoplasmic levels of LIMK-1 result in low cofilin phosphorylation rates and subsequently favour actin filament depolymerisation. Whether high nuclear LIM protein concentrations can negatively affect differentiation related gene expression is a matter of speculation, but serves an explanation for the observed changes in gene expression. (B) Upon suppression of p57kip2 in cultured cells or during postnatal development, the shuttling of LIM domain proteins to the nucleus is reduced. Increased cytoplasmic LIMK-1 levels lead to cofilin phosphorylation and inactivation which in turn stabilizes actin filament assembly. Low nuclear LIM protein concentrations are thought to promote Schwann cell differentiation related gene expression. The combination of both processes is thought to be necessary in order to allow Schwann cell differentiation to proceed.

However, until now no direct evidence for an interaction of p57kip2 and LIMK-1 in Schwann cells and no direct evidence that this interaction influences the cofilin activity in these cells could be established. Furthermore, no additional LIM

domain containing binding partners for p57kip2 have so far been identified. Additionally, there is no evidence that LIM domain containing proteins affect the Schwann cell gene expression in terms of terminal differentiation. The identification of further p57kip2 binding partners and the detailed description of their functions thus awaits future investigations. In order to identify novel p57kip2 interaction partners, the full length protein p57kip2 or its proline rich region could be overexpressed in fusion with a tag peptide (His, Myc, TAP). Upon binding to cytoplasmic or nuclear protein extracts, p57kip2 interacting proteins could be identified by means of affinity purification and subsequent mass spectrometry.

5.4 p57kip2 suppression induces terminal differentiation of Schwann cells

Suppression of p57kip2 was shown to induce the expression of myelin genes and proteins. This thesis provides additional evidence that knockdown of p57kip2 also accelerates *in vitro* myelination of DRG cocultures, indicating that p57kip2 suppressed Schwann cells readily form myelin. Given that *in vitro* differentiation of Schwann cells could not be shown before, this was a surprising result. GeneChip array analysis revealed widespread alterations in Schwann cell gene expression upon suppression of p57kip2, which start at 1dpT. Interestingly, most of the genes the expression of which were validated by quantitative RT-PCR were found to be regulated similar to the natural postnatal development profile. Whether these are primary changes in Schwann cell morphology inducing secondary gene regulatory events or whether these are parallel processes based on different p57kip2 binding partners remains to be elucidated. The fact that both suppression of p57kip2 and p27kip1 induce morphological changes, but only p57kip2 suppression also induces terminal differentiation, suggests that these processes are acting in parallel. It thus seems that p57kip2 inhibits the myelination program by binding to hitherto unknown specific transcription factors or LIM domain proteins.

One interesting LIM domain containing protein regarding control of cell morphology and, possibly, also gene expression is PINCH. As part of the IPP complex, PINCH connects extracellular signalling via integrins with the actin cytoskeleton, and it is believed that the IPP complex functions as an organizer of adhesion signals and intracellular molecular signal transduction (Mori *et al.*, 2006). PINCH associates with integrin linked kinase (ILK), the overexpression of which was shown to affect Rho mediated cytoskeletal dynamics (Khyrul *et al.*, 2004). Moreover,

since PINCH was shown to shuttle between nucleus and cytoplasm (Campana *et al.*, 2003), it is also believed that PINCH has nuclear functions which remain to be elucidated. It is currently unknown whether and how PINCH proteins interfere with or regulate transcription or posttranscriptional events. Measurement of PINCH1 and PINCH2 expression in both p57kip2 suppressed Schwann cells as well as during peripheral nerve development revealed them to be induced. PINCH2 experienced the strongest induction among all validated genes, which might indicate that it is important for glial maturation. Thus our results suggest that PINCH expression is repressed by p57kip2. Whether this repression is direct or indirect and whether PINCH has a functional role during peripheral nerve development will be determined by future experiments.

Myelin gene induction was found to be mediated without affecting Krox20 expression in Schwann cells, a transcription factor which is known to play a vital role regarding Schwann cell terminal differentiation. It was furthermore postulated that upregulation of Krox20 is necessary to overcome intrinsic inhibition of terminal differentiation (LeBlanc *et al.*, 2007; Topilko *et al.*, 1994; Parkinson *et al.*, 2008). Krox20 was found to be transiently upregulated during peripheral nerve development. However, no induction of Krox20 could be observed in p57kip2 suppressed cells. The upregulation of myelin genes therefore is thought to be mediated by induction of Sox10 and the Krox20 cofactors Nabs, given that Nab cofactors are the active components of Krox20 transcription complexes. Nevertheless, the expression of Nab proteins was shown to be crucial for peripheral myelin induction (Le *et al.*, 2005). Interestingly, Nabs were shown to associate with the nucleosome and deacetylase complex (NuRD), and this interaction affects Schwann cell differentiation (Srinivasan *et al.*, 2006). The NuRD complex includes histone deacetylases (HDAC), which repress the activation of target gene promoters they are recruited to by chromatin remodelling. Nab interaction with Krox20 and the NuRD complex and subsequent recruitment to target genes could thus epigenetically control the expression of a high number of genes and explain why p57kip2 knockdown leads to a complete shift in the Schwann cell gene expression program. In this regard it is important to mention that also p57kip2 expression was shown to be controlled by the NuRD complex (Topark-Ngarm *et al.*, 2006), suggesting that the same epigenetic changes account for the downregulation of p57kip2 during development. Whether Nab or other

transcriptional repressors control the expression of p57kip2 remains yet to be solved and is subject of future investigations.

5.5 Biomedical relevance of p57kip2 expression

Misexpression of p57kip2 has been attributed to the formation of several tumours, hence a tumour suppressor function for p57kip2 was proposed, which is clearly linked to its function in the cell cycle. Further point mutations of p57kip2 were found to induce the Beckwith Wiedemann syndrome, which is characterized by abnormalities including gigantism and enlarged organs, and once more can directly be linked to cell cycle control.

The finding that p57kip2 is dynamically regulated following nerve crush (Küry *et al.*, 2002) and the observation that p57kip2 downregulation correlates with regeneration in the diseased, demyelinating central nervous system following EAE (Kremer, D., Zimmermann, K., Heinen, A., Jadasz, J., Jander, S., Hartung, H.P., and Küry, P., manuscript submitted) suggests that p57kip2 has important implications in disease processes. These findings are of biomedical relevance, since the peripheral nervous system and the central nervous system differ fundamentally regarding their regenerative potential. Successful nerve regeneration depends on the generation of a growth permissive environment. This is achieved by dedifferentiating and redifferentiating Schwann cells within the degenerating distal nerve segment. This adaptive behaviour actively promotes axonal regeneration (Son and Thompson, 1995). Such a behaviour is not observed with oligodendrocytes, which degenerate as a consequence of trauma or disease (Hisahara *et al.*, 2003). Importantly, successful Schwann cell mediated CNS regeneration indicated that a fundamental difference in nerve repair is based on different myelinating glial cell responses (Li and Raisman, 1997; Woodhoo *et al.*, 2007). Nevertheless, the observation that increasing levels of p57kip2 constitute the differentiation associated timer preceding oligodendrocyte differentiation (Dugas *et al.*, 2007) suggests that p57kip2 does not exert other or additional functions in the differentiation of CNS myelinating glial cells. We on the other hand have now gathered evidence that oligodendrocyte precursor cell maturation similarly depends on decreasing p57kip2 expression levels (Kremer, D., Zimmermann, K., Heinen, A., Jadasz, J., Jander, S., Hartung, H.P., and Küry, P., manuscript submitted). It remains to be proven to what degree differential p57kip2

expression contributes to this plasticity and whether it represents the main determinant for glial cell (de)differentiation.

Demyelination is not only a consequence of trauma or autoimmune diseases. Several demyelinating diseases were shown to depend on dysregulation of myelin components. For example, the PNS demyelinating disease Charcot-Marie-Tooth (CMT1a) is caused by a duplication of the PMP22 gene, while HNPP (hereditary neuropathy with liability to pressure palsies) is caused by too low levels of PMP22 expression. Knowledge of the p57kip2 gene regulation could be a helpful therapeutic tool in order to treat such peripheral demyelinating diseases or to promote myelin restoration after traumatic injury. Current experiments therefore aim at the understanding of how p57kip2 levels can be modulated *in vitro* either pharmacologically or by microRNA mediated posttranscriptional control. Among interesting candidates for p57kip2 regulators are histone deacetylase (HDAC) activators and HDAC inhibitors, which allow the epigenetic control of gene expression and have been shown to be part of a complex which controls p57kip2 expression (Topark-Ngarm *et al.*, 2006). Of note, HDAC inhibitors were shown to selectively upregulate p57kip2 levels (Cucciolla *et al.*, 2008), while HDAC activators can be expected to downregulate p57kip2 levels. It will be thus be of particular interest to see whether for example valproic acid (VPA) as a HDAC inhibitor can modulate p57kip2 expression in cultured cells or even *in vivo*. The latter can be easily tested as VPA is currently used in order to treat schizophrenia.

Another yet unsolved issue is the elucidation of p57kip2 *in vivo* functions during development and nerve regeneration. Unfortunately, gene knockout of p57kip2 was found to result in severe developmental defects which lead to perinatal death of p57kip2^{-/-} mice (Yan *et al.*, 1997; Zhang *et al.*, 1997; Takahashi *et al.*, 2000). It was suggested that the unique protein domain structure and thus loss of interactions with several p57kip2 binding partners accounts for this lethal phenotype. Thus loss of p57kip2 expression cannot be compensated by other CKIs. Unfortunately, the early death of p57kip2 knockout animals precludes the analysis of its functions during postnatal peripheral nerve development or during regeneration. In order to analyse the *in vivo* functions of this gene, several alternative attempts have to be considered, including the generation of p57kip2 knockdown mice. This is a promising attempt, since knockdown of p57kip2 did not result in total loss of gene expression nor protein expression, hence mild defects are expected. The generation

of such p57kip2 knockdown is currently performed in collaboration with Prof. Ulrich R  ther (Heinrich Heine University, D  sseldorf). On the other hand, the generation of conditional p57kip2 knockout mice could help solving this problem. In this regard it would be conceivable to generate mice with a floxed p57kip2 allele. These mice could then be used with P0-Cre transgenic mice in order to achieve Schwann cell specific knockout of p57kip2 during postnatal development. Another elegant attempt in order to assess the *in vivo* role of p57kip2 during development and disease could be mediated via breeding with tamoxifen inducible Cre mice (Decker *et al.*, 2006). Tamoxifen injection could then lead to a focal loss of p57kip2 expression at a timepoint and tissue of choice, which would allow additional investigations of p57kip2 functions during CNS development. Finally, a yet different approach in order to modulate *in vivo* p57kip2 levels can be achieved by transduction of sciatic nerves using lentiviruses (Perrin-Tricaud *et al.*, 2007). To this end, we are currently establishing vectors for the lentiviral mediated p57kip2 knockdown which will then be used in order to transduce nerves. This is done in collaboration with Dr. Nicolas Tricaud (ETH, Z  rich).

5.6 Concluding remarks and open questions

Data presented in this thesis demonstrate that p57kip2 is a negative regulator of myelinating Schwann cell differentiation. It has been shown that suppression of p57kip2 gene expression levels by means of vector based RNA interference leads to cell cycle exit, morphological changes as well as induction of myelination. Moreover, these alterations could be shown to be accompanied by a shift in the gene expression program of the transfected cells towards differentiation and also to differential nuclear protein expression.

In the presented study, suppression of p57kip2 levels mimicked the postnatal downregulation of p57kip2. However, it is currently unsolved what signals mediate this downregulation *in vivo*, both during development and regeneration of peripheral nerves. Since *in vivo* as well as in coculture axonal signals are necessary to initiate the terminal differentiation program, it is conceivable that signalling via Nrg1/erbB2 or, alternatively, signalling via integrin receptors and the IPP complex mediate the downregulation of p57kip2. Since Schwann cell specific p57kip2 transcriptional regulators apart from Mash2 are unknown, their identification awaits future experiments.

On the other hand, p57kip2 target molecules are also yet unknown. It is still unclear, whether the observed effects in p57kip2 suppressed cells are due to the release of binding partners and/or due to altered subcellular localization. Nevertheless, the high number of regulated genes upon p57kip2 suppression could imply that epigenetic mechanisms account for the onset of terminal Schwann cell differentiation similar to what has recently been shown for oligodendrocytes (Shen *et al.*, 2008). Hence the identification of p57kip2 binding partners and the investigation of their specific functions regarding Schwann cell differentiation are part of future projects.

As to which concerns investigations of p57kip2's *in vivo* role in PNS and CNS, alternative strategies have to be established. Using such approaches, we will finally be able to decide whether this gene is a true master gene of myelinating glial cell genesis.

6. REFERENCES

- Abney, E. R., P. P. Bartlett and M. C. Raff (1981). "Astrocytes, ependymal cells, and oligodendrocytes develop on schedule in dissociated cell cultures of embryonic rat brain." *Dev Biol* **83**(2): 301-10.
- Adlkofer, K., R. Martini, A. Aguzzi, J. Zielasek, K. V. Toyka and U. Suter (1995). "Hypermyelination and demyelinating peripheral neuropathy in Pmp22-deficient mice." *Nat Genet* **11**(3): 274-80.
- Amici, S. A., W. A. Dunn, Jr., A. J. Murphy, N. C. Adams, N. W. Gale, D. M. Valenzuela, G. D. Yancopoulos and L. Notterpek (2006). "Peripheral myelin protein 22 is in complex with alpha6beta4 integrin, and its absence alters the Schwann cell basal lamina." *J Neurosci* **26**(4): 1179-89.
- Andrews, S. C., M. D. Wood, S. J. Tunster, S. C. Barton, M. A. Surani and R. M. John (2007). "Cdkn1c (p57Kip2) is the major regulator of embryonic growth within its imprinted domain on mouse distal chromosome 7." *BMC Dev Biol* **7**: 53.
- Arber, S., F. A. Barbayannis, H. Hanser, C. Schneider, C. A. Stanyon, O. Bernard and P. Caroni (1998). "Regulation of actin dynamics through phosphorylation of cofilin by LIM-kinase." *Nature* **393**(6687): 805-9.
- Archelos, J. J., K. Roggenbuck, J. Schneider-Schaulies, C. Linington, K. V. Toyka and H. P. Hartung (1993). "Production and characterization of monoclonal antibodies to the extracellular domain of P0." *J Neurosci Res* **35**(1): 46-53.
- Arroyo, E. J. and S. S. Scherer (2000). "On the molecular architecture of myelinated fibers." *Histochem Cell Biol* **113**(1): 1-18.
- Atanasoski, S., M. Boentert, L. De Ventura, H. Pohl, C. Baranek, K. Beier, P. Young, M. Barbacid and U. Suter (2008). "Postnatal Schwann cell proliferation but not myelination is strictly and uniquely dependent on cyclin-dependent kinase 4 (cdk4)." *Mol Cell Neurosci* **37**(3): 519-27.
- Atanasoski, S., D. Boller, L. De Ventura, H. Koegel, M. Boentert, P. Young, S. Werner and U. Suter (2006). "Cell cycle inhibitors p21 and p16 are required for the regulation of Schwann cell proliferation." *Glia* **53**(2): 147-57.
- Atanasoski, S., S. Shumas, C. Dickson, S. S. Scherer and U. Suter (2001). "Differential cyclin D1 requirements of proliferating Schwann cells during development and after injury." *Mol Cell Neurosci* **18**(6): 581-92.
- Auld, D. S. and R. Robitaille (2003). "Glial cells and neurotransmission: an inclusive view of synaptic function." *Neuron* **40**(2): 389-400.

- Bermingham, J. R., Jr., H. Shearin, J. Pennington, J. O'Moore, M. Jaegle, S. Driegen, A. van Zon, A. Darbas, E. Ozkaynak, E. J. Ryu, J. Milbrandt and D. Meijer (2006). "The claw paw mutation reveals a role for Lgi4 in peripheral nerve development." *Nat Neurosci* **9**(1): 76-84.
- Besson, A., S. F. Dowdy and J. M. Roberts (2008). "CDK inhibitors: cell cycle regulators and beyond." *Dev Cell* **14**(2): 159-69.
- Besson, A., M. Gurian-West, X. Chen, K. S. Kelly-Spratt, C. J. Kemp and J. M. Roberts (2006). "A pathway in quiescent cells that controls p27Kip1 stability, subcellular localization, and tumor suppression." *Genes Dev* **20**(1): 47-64.
- Besson, A., M. Gurian-West, A. Schmidt, A. Hall and J. M. Roberts (2004). "p27Kip1 modulates cell migration through the regulation of RhoA activation." *Genes Dev* **18**(8): 862-76.
- Bondurand, N., M. Girard, V. Pingault, N. Lemort, O. Dubourg and M. Goossens (2001). "Human Connexin 32, a gap junction protein altered in the X-linked form of Charcot-Marie-Tooth disease, is directly regulated by the transcription factor SOX10." *Hum Mol Genet* **10**(24): 2783-95.
- Bornstein, G., J. Bloom, D. Sitry-Shevah, K. Nakayama, M. Pagano and A. Hershko (2003). "Role of the SCFSkp2 ubiquitin ligase in the degradation of p21Cip1 in S phase." *J Biol Chem* **278**(28): 25752-7.
- Boyle, M. E., E. O. Berglund, K. K. Murai, L. Weber, E. Peles and B. Ranscht (2001). "Contactin orchestrates assembly of the septate-like junctions at the paranode in myelinated peripheral nerve." *Neuron* **30**(2): 385-97.
- Bridge, A. J., S. Pebernard, A. Ducraux, A. L. Nicoulaz and R. Iggo (2003). "Induction of an interferon response by RNAi vectors in mammalian cells." *Nat Genet* **34**(3): 263-4.
- Britsch, S., D. E. Goerich, D. Riethmacher, R. I. Peirano, M. Rossner, K. A. Nave, C. Birchmeier and M. Wegner (2001). "The transcription factor Sox10 is a key regulator of peripheral glial development." *Genes Dev* **15**(1): 66-78.
- Brockes, J. P., K. L. Fields and M. C. Raff (1979). "Studies on cultured rat Schwann cells. I. Establishment of purified populations from cultures of peripheral nerve." *Brain Res* **165**(1): 105-18.
- Bunge, M. B., R. P. Bunge and G. D. Pappas (1962). "Electron microscopic demonstration of connections between glia and myelin sheaths in the developing mammalian central nervous system." *J Cell Biol* **12**: 448-53.
- Bunge, M. B., A. K. Williams, P. M. Wood, J. Uitto and J. J. Jeffrey (1980). "Comparison of nerve cell and nerve cell plus Schwann cell cultures, with particular emphasis on basal lamina and collagen formation." *J Cell Biol* **84**(1): 184-202.

- Butt, A. M., A. Duncan, M. F. Hornby, S. L. Kirvell, A. Hunter, J. M. Levine and M. Berry (1999). "Cells expressing the NG2 antigen contact nodes of Ranvier in adult CNS white matter." *Glia* **26**(1): 84-91.
- Campana, W. M., R. R. Myers and A. Rearden (2003). "Identification of PINCH in Schwann cells and DRG neurons: shuttling and signaling after nerve injury." *Glia* **41**(3): 213-23.
- Casaccia-Bonnet, P., R. Tikoo, H. Kiyokawa, V. Friedrich, Jr., M. V. Chao and A. Koff (1997). "Oligodendrocyte precursor differentiation is perturbed in the absence of the cyclin-dependent kinase inhibitor p27Kip1." *Genes Dev* **11**(18): 2335-46.
- Chen, L. M., D. Bailey and C. Fernandez-Valle (2000). "Association of beta 1 integrin with focal adhesion kinase and paxillin in differentiating Schwann cells." *J Neurosci* **20**(10): 3776-84.
- Chen, Z. L. and S. Strickland (2003). "Laminin gamma1 is critical for Schwann cell differentiation, axon myelination, and regeneration in the peripheral nerve." *J Cell Biol* **163**(4): 889-99.
- Coats, S., W. M. Flanagan, J. Nourse and J. M. Roberts (1996). "Requirement of p27Kip1 for restriction point control of the fibroblast cell cycle." *Science* **272**(5263): 877-80.
- Court, F. A., W. T. Hendriks, H. D. Macgillivray, J. Alvarez and J. van Minnen (2008). "Schwann cell to axon transfer of ribosomes: toward a novel understanding of the role of glia in the nervous system." *J Neurosci* **28**(43): 11024-9.
- Cucciolla, V., A. Borriello, M. Criscuolo, A. A. Sinisi, D. Bencivenga, A. Tramontano, A. C. Scudieri, A. Oliva, V. Zappia and F. Della Ragione (2008). "Histone deacetylase inhibitors upregulate p57Kip2 level by enhancing its expression through Sp1 transcription factor." *Carcinogenesis* **29**(3): 560-7.
- Decker, L., C. Desmarquet-Trin-Dinh, E. Taillebourg, J. Ghislain, J. M. Vallat and P. Charnay (2006). "Peripheral myelin maintenance is a dynamic process requiring constant Krox20 expression." *J Neurosci* **26**(38): 9771-9.
- Deng, C., P. Zhang, J. W. Harper, S. J. Elledge and P. Leder (1995). "Mice lacking p21CIP1/WAF1 undergo normal development, but are defective in G1 checkpoint control." *Cell* **82**(4): 675-84.
- Denicourt, C. and S. F. Dowdy (2004). "Cip/Kip proteins: more than just CDKs inhibitors." *Genes Dev* **18**(8): 851-5.
- Denicourt, C., C. C. Saenz, B. Datnow, X. S. Cui and S. F. Dowdy (2007). "Relocalized p27Kip1 tumor suppressor functions as a cytoplasmic metastatic oncogene in melanoma." *Cancer Res* **67**(19): 9238-43.

- Desmazieres, A., L. Decker, J. M. Vallat, P. Charnay and P. Gilardi-Hebenstreit (2008). "Disruption of Krox20-Nab interaction in the mouse leads to peripheral neuropathy with biphasic evolution." *J Neurosci* **28**(23): 5891-900.
- Dong, Z., A. Brennan, N. Liu, Y. Yarden, G. Lefkowitz, R. Mirsky and K. R. Jessen (1995). "Neu differentiation factor is a neuron-glia signal and regulates survival, proliferation, and maturation of rat Schwann cell precursors." *Neuron* **15**(3): 585-96.
- Dugas, J. C., A. Ibrahim and B. A. Barres (2007). "A crucial role for p57(Kip2) in the intracellular timer that controls oligodendrocyte differentiation." *J Neurosci* **27**(23): 6185-96.
- Duncan, I. D., J. P. Hammang and S. A. Gilmore (1988). "Schwann cell myelination of the myelin deficient rat spinal cord following X-irradiation." *Glia* **1**(3): 233-9.
- Duncan, I. D., J. P. Hammang, S. Goda and R. H. Quarles (1989). "Myelination in the jimpy mouse in the absence of proteolipid protein." *Glia* **2**(3): 148-54.
- Dyer, M. A. and C. L. Cepko (2000). "p57(Kip2) regulates progenitor cell proliferation and amacrine interneuron development in the mouse retina." *Development* **127**(16): 3593-605.
- el-Deiry, W. S., T. Tokino, V. E. Velculescu, D. B. Levy, R. Parsons, J. M. Trent, D. Lin, W. E. Mercer, K. W. Kinzler and B. Vogelstein (1993). "WAF1, a potential mediator of p53 tumor suppression." *Cell* **75**(4): 817-25.
- Etienne-Manneville, S. and A. Hall (2002). "Rho GTPases in cell biology." *Nature* **420**(6916): 629-35.
- Feltri, M. L., D. Graus Porta, S. C. Previtali, A. Nodari, B. Migliavacca, A. Casseti, A. Littlewood-Evans, L. F. Reichardt, A. Messing, A. Quattrini, U. Mueller and L. Wrabetz (2002). "Conditional disruption of beta 1 integrin in Schwann cells impedes interactions with axons." *J Cell Biol* **156**(1): 199-209.
- Feltri, M. L., S. S. Scherer, R. Nemni, J. Kamholz, H. Vogelbacker, M. O. Scott, N. Canal, V. Quaranta and L. Wrabetz (1994). "Beta 4 integrin expression in myelinating Schwann cells is polarized, developmentally regulated and axonally dependent." *Development* **120**(5): 1287-301.
- Fernandez-Moran, H. and J. B. Finean (1957). "Electron microscope and low-angle x-ray diffraction studies of the nerve myelin sheath." *J Biophys Biochem Cytol* **3**(5): 725-48.
- Fernandez-Valle, C., N. Fregien, P. M. Wood and M. B. Bunge (1993). "Expression of the protein zero myelin gene in axon-related Schwann cells is linked to basal lamina formation." *Development* **119**(3): 867-80.
- Fernandez-Valle, C., D. Gorman, A. M. Gomez and M. B. Bunge (1997). "Actin plays a role in both changes in cell shape and gene-expression associated with Schwann cell myelination." *J Neurosci* **17**(1): 241-50.

- Fernandez-Valle, C., L. Gwynn, P. M. Wood, S. Carbonetto and M. B. Bunge (1994). "Anti-beta 1 integrin antibody inhibits Schwann cell myelination." *J Neurobiol* **25**(10): 1207-26.
- Fernandez-Valle, C., Y. Tang, J. Ricard, A. Rodenas-Ruano, A. Taylor, E. Hackler, J. Biggerstaff and J. Iacovelli (2002). "Paxillin binds schwannomin and regulates its density-dependent localization and effect on cell morphology." *Nat Genet* **31**(4): 354-62.
- Fero, M. L., M. Rivkin, M. Tasch, P. Porter, C. E. Carow, E. Firpo, K. Polyak, L. H. Tsai, V. Broudy, R. M. Perlmutter, K. Kaushansky and J. M. Roberts (1996). "A syndrome of multiorgan hyperplasia with features of gigantism, tumorigenesis, and female sterility in p27(Kip1)-deficient mice." *Cell* **85**(5): 733-44.
- Figliola, R., A. Busanello, G. Vaccarello and R. Maione (2008). "Regulation of p57(KIP2) during muscle differentiation: role of Egr1, Sp1 and DNA hypomethylation." *J Mol Biol* **380**(2): 265-77.
- Friede, R. L. and R. Bischhausen (1980). "The precise geometry of large internodes." *J Neurol Sci* **48**(3): 367-81.
- Gaiano, N., J. S. Nye and G. Fishell (2000). "Radial glial identity is promoted by Notch1 signaling in the murine forebrain." *Neuron* **26**(2): 395-404.
- Garratt, A. N., S. Britsch and C. Birchmeier (2000). "Neuregulin, a factor with many functions in the life of a schwann cell." *Bioessays* **22**(11): 987-96.
- Garratt, A. N., O. Voiculescu, P. Topilko, P. Charnay and C. Birchmeier (2000). "A dual role of erbB2 in myelination and in expansion of the schwann cell precursor pool." *J Cell Biol* **148**(5): 1035-46.
- Gartel, A. L. and S. K. Radhakrishnan (2005). "Lost in transcription: p21 repression, mechanisms, and consequences." *Cancer Res* **65**(10): 3980-5.
- Gartel, A. L. and A. L. Tyner (1999). "Transcriptional regulation of the p21((WAF1/CIP1)) gene." *Exp Cell Res* **246**(2): 280-9.
- Geren, B. B. and F. O. Schmitt (1954). "The Structure of the Schwann Cell and Its Relation to the Axon in Certain Invertebrate Nerve Fibers." *Proc Natl Acad Sci U S A* **40**(9): 863-70.
- Ghislain, J. and P. Charnay (2006). "Control of myelination in Schwann cells: a Krox20 cis-regulatory element integrates Oct6, Brn2 and Sox10 activities." *EMBO Rep* **7**(1): 52-8.
- Ghislain, J., C. Desmarquet-Trin-Dinh, M. Jaegle, D. Meijer, P. Charnay and M. Frain (2002). "Characterisation of cis-acting sequences reveals a biphasic, axon-dependent regulation of Krox20 during Schwann cell development." *Development* **129**(1): 155-66.

- Giese, K. P., R. Martini, G. Lemke, P. Soriano and M. Schachner (1992). "Mouse P0 gene disruption leads to hypomyelination, abnormal expression of recognition molecules, and degeneration of myelin and axons." *Cell* **71**(4): 565-76.
- Gollan, L., D. Salomon, J. L. Salzer and E. Peles (2003). "Caspr regulates the processing of contactin and inhibits its binding to neurofascin." *J Cell Biol* **163**(6): 1213-8.
- Graham, V., J. Khudyakov, P. Ellis and L. Pevny (2003). "SOX2 functions to maintain neural progenitor identity." *Neuron* **39**(5): 749-65.
- Greenfield, S., S. Brostoff, E. H. Eylar and P. Morell (1973). "Protein composition of myelin of the peripheral nervous system." *J Neurochem* **20**(4): 1207-16.
- Griesbeck, O., G. S. Baird, R. E. Campbell, D. A. Zacharias and R. Y. Tsien (2001). "Reducing the environmental sensitivity of yellow fluorescent protein. Mechanism and applications." *J Biol Chem* **276**(31): 29188-94.
- Gu, Y., C. W. Turck and D. O. Morgan (1993). "Inhibition of CDK2 activity in vivo by an associated 20K regulatory subunit." *Nature* **366**(6456): 707-10.
- Gui, H., S. Li and M. P. Matise (2007). "A cell-autonomous requirement for Cip/Kip cyclin-kinase inhibitors in regulating neuronal cell cycle exit but not differentiation in the developing spinal cord." *Dev Biol* **301**(1): 14-26.
- Harper, J. W., G. R. Adami, N. Wei, K. Keyomarsi and S. J. Elledge (1993). "The p21 Cdk-interacting protein Cip1 is a potent inhibitor of G1 cyclin-dependent kinases." *Cell* **75**(4): 805-16.
- Hatada, I., J. Inazawa, T. Abe, M. Nakayama, Y. Kaneko, Y. Jinno, N. Niikawa, H. Ohashi, Y. Fukushima, K. Iida, C. Yutani, S. Takahashi, Y. Chiba, S. Ohishi and T. Mukai (1996). "Genomic imprinting of human p57KIP2 and its reduced expression in Wilms' tumors." *Hum Mol Genet* **5**(6): 783-8.
- Hatada, I. and T. Mukai (1995). "Genomic imprinting of p57KIP2, a cyclin-dependent kinase inhibitor, in mouse." *Nat Genet* **11**(2): 204-6.
- Hatada, I., H. Ohashi, Y. Fukushima, Y. Kaneko, M. Inoue, Y. Komoto, A. Okada, S. Ohishi, A. Nabetani, H. Morisaki, M. Nakayama, N. Niikawa and T. Mukai (1996). "An imprinted gene p57KIP2 is mutated in Beckwith-Wiedemann syndrome." *Nat Genet* **14**(2): 171-3.
- Heinen, A., D. Kremer, P. Gottle, F. Kruse, B. Hasse, H. Lehmann, H. P. Hartung and P. Küry (2008a). "The cyclin-dependent kinase inhibitor p57kip2 is a negative regulator of Schwann cell differentiation and in vitro myelination." *Proc Natl Acad Sci U S A* **105**(25): 8748-53.
- Heinen, A., D. Kremer, H. P. Hartung and P. Küry (2008b). "p57 kip2's role beyond Schwann cell cycle control." *Cell Cycle* **7**(18): 2781-6.
- Hengst, L. and S. I. Reed (1998). "Inhibitors of the Cip/Kip family." *Curr Top Microbiol Immunol* **227**: 25-41.

- Henry, E. W., E. M. Eicher and R. L. Sidman (1991). "The mouse mutation claw paw: forelimb deformity and delayed myelination throughout the peripheral nervous system." *J Hered* **82**(4): 287-94.
- Hildebrand, C. and S. G. Waxman (1984). "Postnatal differentiation of rat optic nerve fibers: electron microscopic observations on the development of nodes of Ranvier and axoglial relations." *J Comp Neurol* **224**(1): 25-37.
- Hisahara, S., H. Okano and M. Miura (2003). "Caspase-mediated oligodendrocyte cell death in the pathogenesis of autoimmune demyelination." *Neurosci Res* **46**(4): 387-97.
- Iacovelli, J., J. Lopera, M. Bott, E. Baldwin, A. Khaled, N. Uddin and C. Fernandez-Valle (2007). "Serum and forskolin cooperate to promote G1 progression in Schwann cells by differentially regulating cyclin D1, cyclin E1, and p27Kip expression." *Glia* **55**(16): 1638-47.
- Inoue, K., K. Shilo, C. F. Boerkoel, C. Crowe, J. Sawady, J. R. Lupski and D. P. Agamanolis (2002). "Congenital hypomyelinating neuropathy, central dysmyelination, and Waardenburg-Hirschsprung disease: phenotypes linked by SOX10 mutation." *Ann Neurol* **52**(6): 836-42.
- Irizarry, R. A., B. Hobbs, F. Collin, Y. D. Beazer-Barclay, K. J. Antonellis, U. Scherf and T. P. Speed (2003). "Exploration, normalization, and summaries of high density oligonucleotide array probe level data." *Biostatistics* **4**(2): 249-64.
- Jaegle, M., M. Ghazvini, W. Mandemakers, M. Piirsoo, S. Driegen, F. Levavasseur, S. Raghoenath, F. Grosveld and D. Meijer (2003). "The POU proteins Brn-2 and Oct-6 share important functions in Schwann cell development." *Genes Dev* **17**(11): 1380-91.
- Jaegle, M., W. Mandemakers, L. Broos, R. Zwart, A. Karis, P. Visser, F. Grosveld and D. Meijer (1996). "The POU factor Oct-6 and Schwann cell differentiation." *Science* **273**(5274): 507-10.
- Jessen, K. R., A. Brennan, L. Morgan, R. Mirsky, A. Kent, Y. Hashimoto and J. Gavrilovic (1994). "The Schwann cell precursor and its fate: a study of cell death and differentiation during gliogenesis in rat embryonic nerves." *Neuron* **12**(3): 509-27.
- Jessen, K. R. and R. Mirsky (2005). "The origin and development of glial cells in peripheral nerves." *Nat Rev Neurosci* **6**(9): 671-82.
- Joseph, B., A. Wallen-Mackenzie, G. Benoit, T. Murata, E. Joodmardi, S. Okret and T. Perlmann (2003). "p57(Kip2) cooperates with Nurr1 in developing dopamine cells." *Proc Natl Acad Sci U S A* **100**(26): 15619-24.
- Kawauchi, T., K. Chihama, Y. Nabeshima and M. Hoshino (2006). "Cdk5 phosphorylates and stabilizes p27kip1 contributing to actin organization and cortical neuronal migration." *Nat Cell Biol* **8**(1): 17-26.

- Khyrul, W. A., D. P. LaLonde, M. C. Brown, H. Levinson and C. E. Turner (2004). "The integrin-linked kinase regulates cell morphology and motility in a rho-associated kinase-dependent manner." *J Biol Chem* **279**(52): 54131-9.
- Kim, H. A., S. L. Pomeroy, W. Whoriskey, I. Pawlitzky, L. I. Benowitz, P. Sicinski, C. D. Stiles and T. M. Roberts (2000). "A developmentally regulated switch directs regenerative growth of Schwann cells through cyclin D1." *Neuron* **26**(2): 405-16.
- Kirschner, D. A. and C. J. Hollingshead (1980). "Processing for electron microscopy alters membrane structure and packing in myelin." *J Ultrastruct Res* **73**(2): 211-32.
- Kiyokawa, H., R. D. Kineman, K. O. Manova-Todorova, V. C. Soares, E. S. Hoffman, M. Ono, D. Khanam, A. C. Hayday, L. A. Frohman and A. Koff (1996). "Enhanced growth of mice lacking the cyclin-dependent kinase inhibitor function of p27(Kip1)." *Cell* **85**(5): 721-32.
- Knecht, A. K. and M. Bronner-Fraser (2002). "Induction of the neural crest: a multigene process." *Nat Rev Genet* **3**(6): 453-61.
- Koszowski, A. G., G. C. Owens and S. R. Levinson (1998). "The effect of the mouse mutation claw paw on myelination and nodal frequency in sciatic nerves." *J Neurosci* **18**(15): 5859-68.
- Kremer, D., Zimmermann, K., Heinen, A., Jadasz, J., Jander, S., Hartung, H.P., and Küry, P. p57kip2 is dynamically regulated in experimental autoimmune encephalomyelitis and functions as a negative regulator of postmitotic oligodendroglial differentiation. (manuscript submitted to *Proc. Natl. Acad. Sci. U. S. A.*)
- Kuhlbrodt, K., B. Herbarth, E. Sock, I. Hermans-Borgmeyer and M. Wegner (1998). "Sox10, a novel transcriptional modulator in glial cells." *J Neurosci* **18**(1): 237-50.
- Küry, P., F. Bosse and H. W. Müller (2001). "Transcription factors in nerve regeneration." *Prog Brain Res* **132**: 569-85.
- Küry, P., R. Greiner-Petter, C. Cornely, T. Jürgens and H. W. Müller (2002). "Mammalian achaete scute homolog 2 is expressed in the adult sciatic nerve and regulates the expression of Krox24, Mob-1, CXCR4, and p57kip2 in Schwann cells." *J Neurosci* **22**(17): 7586-95.
- Küry, P., H. Koller, M. Hamacher, C. Cornely, B. Hasse and H. W. Müller (2003). "Cyclic AMP and tumor necrosis factor-alpha regulate CXCR4 gene expression in Schwann cells." *Mol Cell Neurosci* **24**(1): 1-9.
- Laemmli, U. K. (1970). "Cleavage of structural proteins during the assembly of the head of bacteriophage T4." *Nature* **227**(5259): 680-5.

- Lajtha, A., J. Toth, K. Fujimoto and H. C. Agrawal (1977). "Turnover of myelin proteins in mouse brain in vivo." *Biochem J* **164**(2): 323-9.
- Le Douarin, N. M., M. A. Teillet and M. Catala (1998). "Neurulation in amniote vertebrates: a novel view deduced from the use of quail-chick chimeras." *Int J Dev Biol* **42**(7): 909-16.
- Le, N., R. Nagarajan, J. Y. Wang, T. Araki, R. E. Schmidt and J. Milbrandt (2005). "Analysis of congenital hypomyelinating Egr2^{Lo/Lo} nerves identifies Sox2 as an inhibitor of Schwann cell differentiation and myelination." *Proc Natl Acad Sci U S A* **102**(7): 2596-601.
- Le, N., R. Nagarajan, J. Y. Wang, J. Svaren, C. LaPash, T. Araki, R. E. Schmidt and J. Milbrandt (2005). "Nab proteins are essential for peripheral nervous system myelination." *Nat Neurosci* **8**(7): 932-40.
- Leblanc, S. E., R. Srinivasan, C. Ferri, G. M. Mager, A. L. Gillian-Daniel, L. Wrabetz and J. Svaren (2005). "Regulation of cholesterol/lipid biosynthetic genes by Egr2/Krox20 during peripheral nerve myelination." *J Neurochem* **93**(3): 737-48.
- LeBlanc, S. E., R. M. Ward and J. Svaren (2007). "Neuropathy-associated Egr2 mutants disrupt cooperative activation of myelin protein zero by Egr2 and Sox10." *Mol Cell Biol* **27**(9): 3521-9.
- Lee, M. H., I. Reynisdottir and J. Massague (1995). "Cloning of p57KIP2, a cyclin-dependent kinase inhibitor with unique domain structure and tissue distribution." *Genes Dev* **9**(6): 639-49.
- Lee, M. P., M. DeBaun, G. Randhawa, B. A. Reichard, S. J. Elledge and A. P. Feinberg (1997). "Low frequency of p57KIP2 mutation in Beckwith-Wiedemann syndrome." *Am J Hum Genet* **61**(2): 304-9.
- Lee, S. and D. M. Helfman (2004). "Cytoplasmic p21Cip1 is involved in Ras-induced inhibition of the ROCK/LIMK/cofilin pathway." *J Biol Chem* **279**(3): 1885-91.
- Legate, K. R., E. Montanez, O. Kudlacek and R. Fassler (2006). "ILK, PINCH and parvin: the tIPP of integrin signalling." *Nat Rev Mol Cell Biol* **7**(1): 20-31.
- Lemke, G. and R. Axel (1985). "Isolation and sequence of a cDNA encoding the major structural protein of peripheral myelin." *Cell* **40**(3): 501-8.
- Li, M., L. Pevny, R. Lovell-Badge and A. Smith (1998). "Generation of purified neural precursors from embryonic stem cells by lineage selection." *Curr Biol* **8**(17): 971-4.
- Li, M., J. Wang, S. S. Ng, C. Y. Chan, A. C. Chen, H. P. Xia, D. T. Yew, B. C. Wong, Z. Chen, H. F. Kung and M. C. Lin (2008). "The four-and-a-half-LIM protein 2 (FHL2) is overexpressed in gliomas and associated with oncogenic activities." *Glia* **56**(12): 1328-38.

- Li, R., S. Waga, G. J. Hannon, D. Beach and B. Stillman (1994). "Differential effects by the p21 CDK inhibitor on PCNA-dependent DNA replication and repair." *Nature* **371**(6497): 534-7.
- Li, Y. and G. Raisman (1997). "Integration of transplanted cultured Schwann cells into the long myelinated fiber tracts of the adult spinal cord." *Exp Neurol* **145**(2 Pt 1): 397-411.
- Lino, M. M., S. Atanasoski, M. Kvajo, B. Fayard, E. Moreno, H. R. Brenner, U. Suter and D. Monard (2007). "Mice lacking protease nexin-1 show delayed structural and functional recovery after sciatic nerve crush." *J Neurosci* **27**(14): 3677-85.
- Mager, G. M., R. M. Ward, R. Srinivasan, S. W. Jang, L. Wrabetz and J. Svaren (2008). "Active gene repression by the Egr2.NAB complex during peripheral nerve myelination." *J Biol Chem* **283**(26): 18187-97.
- Masaki, T., K. Matsumura, A. Hirata, H. Yamada, A. Hase, K. Arai, T. Shimizu, H. Yorifuji, K. Motoyoshi and K. Kamakura (2002). "Expression of dystroglycan and the laminin-alpha 2 chain in the rat peripheral nerve during development." *Exp Neurol* **174**(1): 109-17.
- Matsuoka, S., M. C. Edwards, C. Bai, S. Parker, P. Zhang, A. Baldini, J. W. Harper and S. J. Elledge (1995). "p57KIP2, a structurally distinct member of the p21CIP1 Cdk inhibitor family, is a candidate tumor suppressor gene." *Genes Dev* **9**(6): 650-62.
- Matsuoka, S., J. S. Thompson, M. C. Edwards, J. M. Bartletta, P. Grundy, L. M. Kalikin, J. W. Harper, S. J. Elledge and A. P. Feinberg (1996). "Imprinting of the gene encoding a human cyclin-dependent kinase inhibitor, p57KIP2, on chromosome 11p15." *Proc Natl Acad Sci U S A* **93**(7): 3026-30.
- Meier, C., E. Parmantier, A. Brennan, R. Mirsky and K. R. Jessen (1999). "Developing Schwann cells acquire the ability to survive without axons by establishing an autocrine circuit involving insulin-like growth factor, neurotrophin-3, and platelet-derived growth factor-BB." *J Neurosci* **19**(10): 3847-59.
- Melendez-Vasquez, C. V., J. C. Rios, G. Zanazzi, S. Lambert, A. Bretscher and J. L. Salzer (2001). "Nodes of Ranvier form in association with ezrin-radixin-moesin (ERM)-positive Schwann cell processes." *Proc Natl Acad Sci U S A* **98**(3): 1235-40.
- Meyer, D., T. Yamaai, A. Garratt, E. Riethmacher-Sonnenberg, D. Kane, L. E. Theill and C. Birchmeier (1997). "Isoform-specific expression and function of neuregulin." *Development* **124**(18): 3575-86.
- Michailov, G. V., M. W. Sereda, B. G. Brinkmann, T. M. Fischer, B. Haug, C. Birchmeier, L. Role, C. Lai, M. H. Schwab and K. A. Nave (2004). "Axonal neuregulin-1 regulates myelin sheath thickness." *Science* **304**(5671): 700-3.

- Mills, J., A. Niewmierzycka, A. Oloumi, B. Rico, R. St-Arnaud, I. R. Mackenzie, N. M. Mawji, J. Wilson, L. F. Reichardt and S. Dedhar (2006). "Critical role of integrin-linked kinase in granule cell precursor proliferation and cerebellar development." *J Neurosci* **26**(3): 830-40.
- Morgan, D. O. (1995). "Principles of CDK regulation." *Nature* **374**(6518): 131-4.
- Mori, K., M. Asakawa, M. Hayashi, M. Imura, T. Ohki, E. Hirao, J. R. Kim-Kaneyama, K. Nose and M. Shibamura (2006). "Oligomerizing potential of a focal adhesion LIM protein Hic-5 organizing a nuclear-cytoplasmic shuttling complex." *J Biol Chem* **281**(31): 22048-61.
- Morrison, S., L. S. Mitchell, M. S. Ecob-Prince, I. R. Griffiths, C. E. Thomson, J. A. Barrie and D. Kirkham (1991). "P0 gene expression in cultured Schwann cells." *J Neurocytol* **20**(9): 769-80.
- Morrison, S. J., S. E. Perez, Z. Qiao, J. M. Verdi, C. Hicks, G. Weinmaster and D. J. Anderson (2000). "Transient Notch activation initiates an irreversible switch from neurogenesis to gliogenesis by neural crest stem cells." *Cell* **101**(5): 499-510.
- Moya, F., M. B. Bunge and R. P. Bunge (1980). "Schwann cells proliferate but fail to differentiate in defined medium." *Proc Natl Acad Sci U S A* **77**(11): 6902-6.
- Nagahama, H., S. Hatakeyama, K. Nakayama, M. Nagata, K. Tomita and K. Nakayama (2001). "Spatial and temporal expression patterns of the cyclin-dependent kinase (CDK) inhibitors p27Kip1 and p57Kip2 during mouse development." *Anat Embryol (Berl)* **203**(2): 77-87.
- Nagahara, H., A. M. Vocero-Akbani, E. L. Snyder, A. Ho, D. G. Latham, N. A. Lissy, M. Becker-Hapak, S. A. Ezhevsky and S. F. Dowdy (1998). "Transduction of full-length TAT fusion proteins into mammalian cells: TAT-p27Kip1 induces cell migration." *Nat Med* **4**(12): 1449-52.
- Nagarajan, R., J. Svaren, N. Le, T. Araki, M. Watson and J. Milbrandt (2001). "EGR2 mutations in inherited neuropathies dominant-negatively inhibit myelin gene expression." *Neuron* **30**(2): 355-68.
- Nakayama, K., N. Ishida, M. Shirane, A. Inomata, T. Inoue, N. Shishido, I. Horii, D. Y. Loh and K. Nakayama (1996). "Mice lacking p27(Kip1) display increased body size, multiple organ hyperplasia, retinal dysplasia, and pituitary tumors." *Cell* **85**(5): 707-20.
- Nakayama, K. I., S. Hatakeyama and K. Nakayama (2001). "Regulation of the cell cycle at the G1-S transition by proteolysis of cyclin E and p27Kip1." *Biochem Biophys Res Commun* **282**(4): 853-60.
- Nave, K. A. and J. L. Salzer (2006). "Axonal regulation of myelination by neuregulin 1." *Curr Opin Neurobiol* **16**(5): 492-500.

- Nguyen, L., A. Besson, J. I. Heng, C. Schuurmans, L. Teboul, C. Parras, A. Philpott, J. M. Roberts and F. Guillemot (2007). "[p27Kip1 independently promotes neuronal differentiation and migration in the cerebral cortex]." *Bull Mem Acad R Med Belg* **162**(5-6): 310-4.
- Nguyen, L., B. Malgrange, V. Rocher, G. Hans, G. Moonen, J. M. Rigo and S. Belachew (2003). "Chemical inhibitors of cyclin-dependent kinases control proliferation, apoptosis and differentiation of oligodendroglial cells." *Int J Dev Neurosci* **21**(6): 321-6.
- Nikolopoulos, S. N. and C. E. Turner (2001). "Integrin-linked kinase (ILK) binding to paxillin LD1 motif regulates ILK localization to focal adhesions." *J Biol Chem* **276**(26): 23499-505.
- Norton, J. D., R. W. Deed, G. Craggs and F. Sablitzky (1998). "Id helix-loop-helix proteins in cell growth and differentiation." *Trends Cell Biol* **8**(2): 58-65.
- Norton, W. T. and S. E. Poduslo (1973). "Myelination in rat brain: changes in myelin composition during brain maturation." *J Neurochem* **21**(4): 759-73.
- Ohnuma, S., A. Philpott, K. Wang, C. E. Holt and W. A. Harris (1999). "p27Xic1, a Cdk inhibitor, promotes the determination of glial cells in *Xenopus* retina." *Cell* **99**(5): 499-510.
- Ohtsubo, M., A. M. Theodoras, J. Schumacher, J. M. Roberts and M. Pagano (1995). "Human cyclin E, a nuclear protein essential for the G1-to-S phase transition." *Mol Cell Biol* **15**(5): 2612-24.
- Ophascharoensuk, V., M. L. Fero, J. Hughes, J. M. Roberts and S. J. Shankland (1998). "The cyclin-dependent kinase inhibitor p27Kip1 safeguards against inflammatory injury." *Nat Med* **4**(5): 575-80.
- Orlow, I., A. Iavarone, S. J. Crider-Miller, F. Bonilla, E. Latres, M. H. Lee, W. L. Gerald, J. Massague, B. E. Weissman and C. Cordon-Cardo (1996). "Cyclin-dependent kinase inhibitor p57KIP2 in soft tissue sarcomas and Wilms'tumors." *Cancer Res* **56**(6): 1219-21.
- Paratore, C., D. E. Goerich, U. Suter, M. Wegner and L. Sommer (2001). "Survival and glial fate acquisition of neural crest cells are regulated by an interplay between the transcription factor Sox10 and extrinsic combinatorial signaling." *Development* **128**(20): 3949-61.
- Pardee, A. B. (1989). "G1 events and regulation of cell proliferation." *Science* **246**(4930): 603-8.
- Park, I. H., R. Zhao, J. A. West, A. Yabuuchi, H. Huo, T. A. Ince, P. H. Lerou, M. W. Lensch and G. Q. Daley (2008). "Reprogramming of human somatic cells to pluripotency with defined factors." *Nature* **451**(7175): 141-6.

- Parker, S. B., G. Eichele, P. Zhang, A. Rawls, A. T. Sands, A. Bradley, E. N. Olson, J. W. Harper and S. J. Elledge (1995). "p53-independent expression of p21Cip1 in muscle and other terminally differentiating cells." *Science* **267**(5200): 1024-7.
- Parkinson, D. B., A. Bhaskaran, P. Arthur-Farraj, L. A. Noon, A. Woodhoo, A. C. Lloyd, M. L. Feltri, L. Wrabetz, A. Behrens, R. Mirsky and K. R. Jessen (2008). "c-Jun is a negative regulator of myelination." *J Cell Biol* **181**(4): 625-37.
- Parkinson, D. B., A. Bhaskaran, A. Droggiti, S. Dickinson, M. D'Antonio, R. Mirsky and K. R. Jessen (2004). "Krox-20 inhibits Jun-NH2-terminal kinase/c-Jun to control Schwann cell proliferation and death." *J Cell Biol* **164**(3): 385-94.
- Parkinson, D. B., Z. Dong, H. Bunting, J. Whitfield, C. Meier, H. Marie, R. Mirsky and K. R. Jessen (2001). "Transforming growth factor beta (TGFbeta) mediates Schwann cell death in vitro and in vivo: examination of c-Jun activation, interactions with survival signals, and the relationship of TGFbeta-mediated death to Schwann cell differentiation." *J Neurosci* **21**(21): 8572-85.
- Pechnick, R. N., S. Zonis, K. Wawrowsky, J. Pourmorady and V. Chesnokova (2008). "p21Cip1 restricts neuronal proliferation in the subgranular zone of the dentate gyrus of the hippocampus." *Proc Natl Acad Sci U S A* **105**(4): 1358-63.
- Pedraza, L., J. K. Huang and D. R. Colman (2001). "Organizing principles of the axoglial apparatus." *Neuron* **30**(2): 335-44.
- Pedraza, N., G. Solanes, R. Iglesias, M. Vazquez, M. Giralt and F. Villarroya (2001). "Differential regulation of expression of genes encoding uncoupling proteins 2 and 3 in brown adipose tissue during lactation in mice." *Biochem J* **355**(Pt 1): 105-11.
- Peirano, R. I., D. E. Goerich, D. Riethmacher and M. Wegner (2000). "Protein zero gene expression is regulated by the glial transcription factor Sox10." *Mol Cell Biol* **20**(9): 3198-209.
- Peirano, R. I. and M. Wegner (2000). "The glial transcription factor Sox10 binds to DNA both as monomer and dimer with different functional consequences." *Nucleic Acids Res* **28**(16): 3047-55.
- Perrin-Tricaud, C., U. Rutishauser and N. Tricaud (2007). "P120 catenin is required for thickening of Schwann cell myelin." *Mol Cell Neurosci* **35**(1): 120-9.
- Pingault, V., A. Guiochon-Mantel, N. Bondurand, C. Faure, C. Lacroix, S. Lyonnet, M. Goossens and P. Landrieu (2000). "Peripheral neuropathy with hypomyelination, chronic intestinal pseudo-obstruction and deafness: a developmental "neural crest syndrome" related to a SOX10 mutation." *Ann Neurol* **48**(4): 671-6.
- Podratz, J. L., E. Rodriguez and A. J. Windebank (2001). "Role of the extracellular matrix in myelination of peripheral nerve." *Glia* **35**(1): 35-40.

- Podratz, J. L., E. H. Rodriguez, E. S. DiNonno and A. J. Windebank (1998). "Myelination by Schwann cells in the absence of extracellular matrix assembly." *Glia* **23**(4): 383-8.
- Poliak, S. and E. Peles (2003). "The local differentiation of myelinated axons at nodes of Ranvier." *Nat Rev Neurosci* **4**(12): 968-80.
- Polyak, K., J. Y. Kato, M. J. Solomon, C. J. Sherr, J. Massague, J. M. Roberts and A. Koff (1994). "p27Kip1, a cyclin-Cdk inhibitor, links transforming growth factor-beta and contact inhibition to cell cycle arrest." *Genes Dev* **8**(1): 9-22.
- Polyak, K., M. H. Lee, H. Erdjument-Bromage, A. Koff, J. M. Roberts, P. Tempst and J. Massague (1994). "Cloning of p27Kip1, a cyclin-dependent kinase inhibitor and a potential mediator of extracellular antimitogenic signals." *Cell* **78**(1): 59-66.
- Popko, B. (2003). "Notch signaling: a rheostat regulating oligodendrocyte differentiation?" *Dev Cell* **5**(5): 668-9.
- Potikha, T., S. Kassem, E. P. Haber, I. Ariel and B. Glaser (2005). "p57Kip2 (cdkn1c): sequence, splice variants and unique temporal and spatial expression pattern in the rat pancreas." *Lab Invest* **85**(3): 364-75.
- Previtali, S. C., A. Nodari, C. Taveggia, C. Pardini, G. Dina, A. Villa, L. Wrabetz, A. Quattrini and M. L. Feltri (2003). "Expression of laminin receptors in schwann cell differentiation: evidence for distinct roles." *J Neurosci* **23**(13): 5520-30.
- Privat, A., C. Jacque, J. M. Bourre, P. Dupouey and N. Baumann (1979). "Absence of the major dense line in myelin of the mutant mouse "shiverer"." *Neurosci Lett* **12**(1): 107-12.
- Reid, L. H., S. J. Crider-Miller, A. West, M. H. Lee, J. Massague and B. E. Weissman (1996). "Genomic organization of the human p57KIP2 gene and its analysis in the G401 Wilms' tumor assay." *Cancer Res* **56**(6): 1214-8.
- Ren, S. and B. J. Rollins (2004). "Cyclin C/cdk3 promotes Rb-dependent G0 exit." *Cell* **117**(2): 239-51.
- Reynaud, E. G., M. P. Leibovitch, L. A. Tintignac, K. Pelpel, M. Guillier and S. A. Leibovitch (2000). "Stabilization of MyoD by direct binding to p57(Kip2)." *J Biol Chem* **275**(25): 18767-76.
- Reynisdottir, I., K. Polyak, A. Iavarone and J. Massague (1995). "Kip/Cip and Ink4 Cdk inhibitors cooperate to induce cell cycle arrest in response to TGF-beta." *Genes Dev* **9**(15): 1831-45.
- Robitaille, R. (1998). "Modulation of synaptic efficacy and synaptic depression by glial cells at the frog neuromuscular junction." *Neuron* **21**(4): 847-55.

- Rios, J. C., M. Rubin, M. St Martin, R. T. Downey, S. Einheber, J. Rosenbluth, S. R. Levinson, M. Bhat and J. L. Salzer (2003). "Paranodal interactions regulate expression of sodium channel subtypes and provide a diffusion barrier for the node of Ranvier." *J Neurosci* **23**(18): 7001-11.
- Rosenbluth, J. (1976). "Intramembranous particle distribution at the node of Ranvier and adjacent axolemma in myelinated axons of the frog brain." *J Neurocytol* **5**(6): 731-45.
- Russo, A. A., P. D. Jeffrey, A. K. Patten, J. Massague and N. P. Pavletich (1996). "Crystal structure of the p27Kip1 cyclin-dependent-kinase inhibitor bound to the cyclin A-Cdk2 complex." *Nature* **382**(6589): 325-31.
- Sabri, M. I., A. H. Bone and A. N. Davison (1974). "Turnover of myelin and other structural proteins in the developing rat brain." *Biochem J* **142**(3): 499-507.
- Salzer, J. L. (2003). "Polarized domains of myelinated axons." *Neuron* **40**(2): 297-318.
- Sanger, F., S. Nicklen and A. R. Coulson (1977). "DNA sequencing with chain-terminating inhibitors." *Proc Natl Acad Sci U S A* **74**(12): 5463-7.
- Scherer, S. S. and E. J. Arroyo (2002). "Recent progress on the molecular organization of myelinated axons." *J Peripher Nerv Syst* **7**(1): 1-12.
- Schmetsdorf, S., U. Gartner and T. Arendt (2007). "Constitutive expression of functionally active cyclin-dependent kinases and their binding partners suggests noncanonical functions of cell cycle regulators in differentiated neurons." *Cereb Cortex* **17**(8): 1821-9.
- Shah, N. M., M. A. Marchionni, I. Isaacs, P. Stroobant and D. J. Anderson (1994). "Glial growth factor restricts mammalian neural crest stem cells to a glial fate." *Cell* **77**(3): 349-60.
- Shen, A. G., S. X. Shi, M. L. Chen, J. Qin, S. F. Gao and C. Cheng (2008). "Dynamic changes of p27(kip1) and Skp2 expression in injured rat sciatic nerve." *Cell Mol Neurobiol* **28**(5): 713-25.
- Shen, S., J. Sandoval, V. A. Swiss, J. Li, J. Dupree, R. J. Franklin and P. Casaccia-Bonnel (2008). "Age-dependent epigenetic control of differentiation inhibitors is critical for remyelination efficiency." *Nat Neurosci*.
- Sherman, B. T., W. Huang da, Q. Tan, Y. Guo, S. Bour, D. Liu, R. Stephens, M. W. Baseler, H. C. Lane and R. A. Lempicki (2007). "DAVID Knowledgebase: a gene-centered database integrating heterogeneous gene annotation resources to facilitate high-throughput gene functional analysis." *BMC Bioinformatics* **8**: 426.
- Sherr, C. J. (1994). "Growth factor-regulated G1 cyclins." *Stem Cells* **12 Suppl 1**: 47-55; discussion 55-7.

- Sherr, C. J. (1995). "Mammalian G1 cyclins and cell cycle progression." *Proc Assoc Am Physicians* **107**(2): 181-6.
- Sherr, C. J. and J. M. Roberts (1999). "CDK inhibitors: positive and negative regulators of G1-phase progression." *Genes Dev* **13**(12): 1501-12.
- Shin, J. Y., H. S. Kim, J. Park, J. B. Park and J. Y. Lee (2000). "Mechanism for inactivation of the KIP family cyclin-dependent kinase inhibitor genes in gastric cancer cells." *Cancer Res* **60**(2): 262-5.
- Shivji, M. K., S. J. Grey, U. P. Strausfeld, R. D. Wood and J. J. Blow (1994). "Cip1 inhibits DNA replication but not PCNA-dependent nucleotide excision-repair." *Curr Biol* **4**(12): 1062-8.
- Sledz, C. A., M. Holko, M. J. de Veer, R. H. Silverman and B. R. Williams (2003). "Activation of the interferon system by short-interfering RNAs." *Nat Cell Biol* **5**(9): 834-9.
- Sledz, C. A. and B. R. Williams (2004). "RNA interference and double-stranded-RNA-activated pathways." *Biochem Soc Trans* **32**(Pt 6): 952-6.
- Snipes, G. J., U. Suter, A. A. Welcher and E. M. Shooter (1992). "Characterization of a novel peripheral nervous system myelin protein (PMP-22/SR13)." *J Cell Biol* **117**(1): 225-38.
- Son, Y. J. and W. J. Thompson (1995). "Schwann cell processes guide regeneration of peripheral axons." *Neuron* **14**(1): 125-32.
- Southard-Smith, E. M., L. Kos and W. J. Pavan (1998). "Sox10 mutation disrupts neural crest development in Dom Hirschsprung mouse model." *Nat Genet* **18**(1): 60-4.
- Srinivasan, R., G. M. Mager, R. M. Ward, J. Mayer and J. Svaren (2006). "NAB2 represses transcription by interacting with the CHD4 subunit of the nucleosome remodeling and deacetylase (NuRD) complex." *J Biol Chem* **281**(22): 15129-37.
- Stevaux, O., D. Dimova, M. V. Frolov, B. Taylor-Harding, E. Morris and N. Dyson (2002). "Distinct mechanisms of E2F regulation by Drosophila RBF1 and RBF2." *Embo J* **21**(18): 4927-37.
- Stewart, H. J., L. Morgan, K. R. Jessen and R. Mirsky (1993). "Changes in DNA synthesis rate in the Schwann cell lineage in vivo are correlated with the precursor--Schwann cell transition and myelination." *Eur J Neurosci* **5**(9): 1136-44.
- Stewart, H. J., D. Turner, K. R. Jessen and R. Mirsky (1997). "Expression and regulation of alpha1beta1 integrin in Schwann cells." *J Neurobiol* **33**(7): 914-28.

- Stoffel, W., D. Boison and H. Bussow (1997). "Functional analysis in vivo of the double mutant mouse deficient in both proteolipid protein (PLP) and myelin basic protein (MBP) in the central nervous system." *Cell Tissue Res* **289**(2): 195-206.
- Takahashi, K., K. Nakayama and K. Nakayama (2000). "Mice lacking a CDK inhibitor, p57Kip2, exhibit skeletal abnormalities and growth retardation." *J Biochem* **127**(1): 73-83.
- Takahashi, K. and S. Yamanaka (2006). "Induction of pluripotent stem cells from mouse embryonic and adult fibroblast cultures by defined factors." *Cell* **126**(4): 663-76.
- Tanaka, H., T. Yamashita, M. Asada, S. Mizutani, H. Yoshikawa and M. Tohyama (2002). "Cytoplasmic p21(Cip1/WAF1) regulates neurite remodeling by inhibiting Rho-kinase activity." *J Cell Biol* **158**(2): 321-9.
- Tanaka, H., T. Yamashita, K. Yachi, T. Fujiwara, H. Yoshikawa and M. Tohyama (2004). "Cytoplasmic p21(Cip1/WAF1) enhances axonal regeneration and functional recovery after spinal cord injury in rats." *Neuroscience* **127**(1): 155-64.
- Taveggia, C., G. Zanazzi, A. Petrylak, H. Yano, J. Rosenbluth, S. Einheber, X. Xu, R. M. Esper, J. A. Loeb, P. Shrager, M. V. Chao, D. L. Falls, L. Role and J. L. Salzer (2005). "Neuregulin-1 type III determines the ensheathment fate of axons." *Neuron* **47**(5): 681-94.
- Taylor, C. M., C. B. Marta, R. J. Claycomb, D. K. Han, M. N. Rasband, T. Coetzee and S. E. Pfeiffer (2004). "Proteomic mapping provides powerful insights into functional myelin biology." *Proc Natl Acad Sci U S A* **101**(13): 4643-8.
- Taylor, M. K., K. Yeager and S. J. Morrison (2007). "Physiological Notch signaling promotes gliogenesis in the developing peripheral and central nervous systems." *Development* **134**(13): 2435-47.
- Thatikunta, P., W. Qin, B. A. Christy, G. I. Tennekoon and J. L. Rutkowski (1999). "Reciprocal Id expression and myelin gene regulation in Schwann cells." *Mol Cell Neurosci* **14**(6): 519-28.
- Tikoo, R., P. Casaccia-Bonnel, M. V. Chao and A. Koff (1997). "Changes in cyclin-dependent kinase 2 and p27kip1 accompany glial cell differentiation of central glia-4 cells." *J Biol Chem* **272**(1): 442-7.
- Tikoo, R., D. J. Osterhout, P. Casaccia-Bonnel, P. Seth, A. Koff and M. V. Chao (1998). "Ectopic expression of p27Kip1 in oligodendrocyte progenitor cells results in cell-cycle growth arrest." *J Neurobiol* **36**(3): 431-40.
- Tikoo, R., G. Zanazzi, D. Shiffman, J. Salzer and M. V. Chao (2000). "Cell cycle control of Schwann cell proliferation: role of cyclin-dependent kinase-2." *J Neurosci* **20**(12): 4627-34.

- Tokino, T., T. Urano, T. Furuhata, M. Matsushima, T. Miyatsu, S. Sasaki and Y. Nakamura (1996). "Characterization of the human p57KIP2 gene: alternative splicing, insertion/deletion polymorphisms in VNTR sequences in the coding region, and mutational analysis." *Hum Genet* **97**(5): 625-31.
- Tokumoto, Y. M., J. A. Apperly, F. B. Gao and M. C. Raff (2002). "Posttranscriptional regulation of p18 and p27 Cdk inhibitor proteins and the timing of oligodendrocyte differentiation." *Dev Biol* **245**(1): 224-34.
- Topark-Ngarm, A., O. Golonzhka, V. J. Peterson, B. Barrett, Jr., B. Martinez, K. Crofoot, T. M. Filtz and M. Leid (2006). "CTIP2 associates with the NuRD complex on the promoter of p57KIP2, a newly identified CTIP2 target gene." *J Biol Chem* **281**(43): 32272-83.
- Topilko, P., S. Schneider-Maunoury, G. Levi, A. Baron-Van Evercooren, A. B. Chennoufi, T. Seitanidou, C. Babinet and P. Charnay (1994). "Krox-20 controls myelination in the peripheral nervous system." *Nature* **371**(6500): 796-9.
- Towbin, H., T. Staehelin and J. Gordon (1979). "Electrophoretic transfer of proteins from polyacrylamide gels to nitrocellulose sheets: procedure and some applications." *Proc Natl Acad Sci U S A* **76**(9): 4350-4.
- Toyoshima, H. and T. Hunter (1994). "p27, a novel inhibitor of G1 cyclin-Cdk protein kinase activity, is related to p21." *Cell* **78**(1): 67-74.
- Tumbarello, D. A. and C. E. Turner (2007). "Hic-5 contributes to epithelial-mesenchymal transformation through a RhoA/ROCK-dependent pathway." *J Cell Physiol* **211**(3): 736-47.
- Vabnick, I., J. S. Trimmer, T. L. Schwarz, S. R. Levinson, D. Risal and P. Shrager (1999). "Dynamic potassium channel distributions during axonal development prevent aberrant firing patterns." *J Neurosci* **19**(2): 747-58.
- Waehneltd, T. V. (1990). "Phylogeny of myelin proteins." *Ann N Y Acad Sci* **605**: 15-28.
- Waga, S., G. J. Hannon, D. Beach and B. Stillman (1994). "The p21 inhibitor of cyclin-dependent kinases controls DNA replication by interaction with PCNA." *Nature* **369**(6481): 574-8.
- Wakamatsu, Y., Y. Endo, N. Osumi and J. A. Weston (2004). "Multiple roles of Sox2, an HMG-box transcription factor in avian neural crest development." *Dev Dyn* **229**(1): 74-86.
- Wallquist, W., M. Patarroyo, S. Thams, T. Carlstedt, B. Stark, S. Cullheim and H. Hammarberg (2002). "Laminin chains in rat and human peripheral nerve: distribution and regulation during development and after axonal injury." *J Comp Neurol* **454**(3): 284-93.

- Wang, G., R. Miskimins and W. K. Miskimins (1999). "The cyclin-dependent kinase inhibitor p27Kip1 is localized to the cytosol in Swiss/3T3 cells." *Oncogene* **18**(37): 5204-10.
- Wang, S. and B. A. Barres (2000). "Up a notch: instructing gliogenesis." *Neuron* **27**(2): 197-200.
- Wang, S., A. Sdrulla, J. E. Johnson, Y. Yokota and B. A. Barres (2001). "A role for the helix-loop-helix protein Id2 in the control of oligodendrocyte development." *Neuron* **29**(3): 603-14.
- Wang, S., A. D. Sdrulla, G. diSibio, G. Bush, D. Nofziger, C. Hicks, G. Weinmaster and B. A. Barres (1998). "Notch receptor activation inhibits oligodendrocyte differentiation." *Neuron* **21**(1): 63-75.
- Warner, L. E., P. Mancias, I. J. Butler, C. M. McDonald, L. Keppen, K. G. Koob and J. R. Lupski (1998). "Mutations in the early growth response 2 (EGR2) gene are associated with hereditary myelinopathies." *Nat Genet* **18**(4): 382-4.
- Webster, H. D. (1971). "The geometry of peripheral myelin sheaths during their formation and growth in rat sciatic nerves." *J Cell Biol* **48**(2): 348-67.
- Werner, H. B., K. Kuhlmann, S. Shen, M. Uecker, A. Schardt, K. Dimova, F. Orfaniotou, A. Dhaunchak, B. G. Brinkmann, W. Mobius, L. Guarente, P. Casaccia-Bonnel, O. Jahn and K. A. Nave (2007). "Proteolipid protein is required for transport of sirtuin 2 into CNS myelin." *J Neurosci* **27**(29): 7717-30.
- Winseck, A. K., J. Caldero, D. Ciutat, D. Prevet, S. A. Scott, G. Wang, J. E. Esquerda and R. W. Oppenheim (2002). "In vivo analysis of Schwann cell programmed cell death in the embryonic chick: regulation by axons and glial growth factor." *J Neurosci* **22**(11): 4509-21.
- Woodhoo, A., C. H. Dean, A. Droggiti, R. Mirsky and K. R. Jessen (2004). "The trunk neural crest and its early glial derivatives: a study of survival responses, developmental schedules and autocrine mechanisms." *Mol Cell Neurosci* **25**(1): 30-41.
- Woodhoo, A., V. Sahni, J. Gilson, A. Setzu, R. J. Franklin, W. F. Blakemore, R. Mirsky and K. R. Jessen (2007). "Schwann cell precursors: a favourable cell for myelin repair in the Central Nervous System." *Brain* **130**(Pt 8): 2175-85.
- Xie, Y., J. P. Vessey, A. Konecna, R. Dahm, P. Macchi and M. A. Kiebler (2007). "The GTP-binding protein Septin 7 is critical for dendrite branching and dendritic-spine morphology." *Curr Biol* **17**(20): 1746-51.
- Xiong, Y., G. J. Hannon, H. Zhang, D. Casso, R. Kobayashi and D. Beach (1993). "p21 is a universal inhibitor of cyclin kinases." *Nature* **366**(6456): 701-4.

- Xu, K. and S. Terakawa (1999). "Fenestration nodes and the wide submyelinic space form the basis for the unusually fast impulse conduction of shrimp myelinated axons." *J Exp Biol* **202**(Pt 15): 1979-89.
- Yamauchi, J., J. R. Chan and E. M. Shooter (2003). "Neurotrophin 3 activation of TrkC induces Schwann cell migration through the c-Jun N-terminal kinase pathway." *Proc Natl Acad Sci U S A* **100**(24): 14421-6.
- Yan, Y., J. Frisen, M. H. Lee, J. Massague and M. Barbacid (1997). "Ablation of the CDK inhibitor p57Kip2 results in increased apoptosis and delayed differentiation during mouse development." *Genes Dev* **11**(8): 973-83.
- Yin, X., R. C. Baek, D. A. Kirschner, A. Peterson, Y. Fujii, K. A. Nave, W. B. Macklin and B. D. Trapp (2006). "Evolution of a neuroprotective function of central nervous system myelin." *J Cell Biol* **172**(3): 469-78.
- Yokoo, T., H. Toyoshima, M. Miura, Y. Wang, K. T. Iida, H. Suzuki, H. Sone, H. Shimano, T. Gotoda, S. Nishimori, K. Tanaka and N. Yamada (2003). "p57Kip2 regulates actin dynamics by binding and translocating LIM-kinase 1 to the nucleus." *J Biol Chem* **278**(52): 52919-23.
- Yoshida, M. and D. R. Colman (1996). "Parallel evolution and coexpression of the proteolipid proteins and protein zero in vertebrate myelin." *Neuron* **16**(6): 1115-26.
- Zeller, N. K., M. J. Hunkeler, A. T. Campagnoni, J. Sprague and R. A. Lazzarini (1984). "Characterization of mouse myelin basic protein messenger RNAs with a myelin basic protein cDNA clone." *Proc Natl Acad Sci U S A* **81**(1): 18-22.
- Zhang, P., N. J. Liegeois, C. Wong, M. Finegold, H. Hou, J. C. Thompson, A. Silverman, J. W. Harper, R. A. DePinho and S. J. Elledge (1997). "Altered cell differentiation and proliferation in mice lacking p57KIP2 indicates a role in Beckwith-Wiedemann syndrome." *Nature* **387**(6629): 151-8.

7. ABBREVIATIONS

ATP	adenosine triphosphate
bHLH	basic helix loop helix
BMP	bone morphogenetic protein
BWS	Beckwith Wiedemann syndrome
cAMP	cyclic adenosine monophosphate
CDK	cyclin dependent kinase
CKI	cyclin dependent kinase inhibitor
CMT-1A	Charcot Marie Tooth 1A
CNS	central nervous system
Cx32	connexin 32
Cyp51	sterol 14 alpha demethylase
dpT	day(s) post transfection
DRG	dorsal root ganglia
E	embryonic day
EAE	experimental autoimmune encephalomyelitis
FACS	fluorescence activated cell sorting
FAK	focal adhesion kinase
Fig.	figure
GAPDH	glyceraldehyde-3-phosphate
HDAC	histone deacetylase
HMGCR	3-hydroxy-3-methylglutaryl-coenzyme A reductase
HNPP	hereditary neuropathy with liability to pressure palsies
IFN	interferon
ILK	integrin linked kinase
IPP	ILK-PINCH-parvin complex
MAG	myelin associated glycoprotein
Mal	myelin and lymphocyte protein
Mash2	mammalian achaete scute homolog 2
MBP	myelin basic protein
MOG	myelin oligodendrocyte protein
MS	Multiple Sclerosis
MSC	myelinating Schwann cell
MSE	myelinating Schwann cell element
NMSC	non-myelinating Schwann cell
Nrg	neuregulin
ODC	ornithine decarboxylase
OPC	oligodendrocyte precursor cell
P	postnatal day
P0	myelin protein zero
PCNA	proliferating cell nuclear antigen
PI3-kinase	phosphoinositide-3 kinase
PINCH	particularly interesting new cysteine-histidine-rich protein
PLP	plasmolipin
PMP22	peripheral myelin protein 22
PNS	peripheral nervous system
pRb	retinoblastoma protein
PSC	promyelinating Schwann cell
RNAi	RNA interference
SC	Schwann cell

SCD	stearoyl CoA desaturase
shRNA	small hairpin loop RNA
siRNA	small interference RNA
SREBP	sterol regulatory element-binding protein
TGF	transforming growth factor

8. ACKNOWLEDGEMENTS

First of all I would like to thank PD Dr. Patrick Küry for providing me the opportunity to work on an exciting project, for his excellent supervision, permanent support and for a lot of fun! Thank you, I learned so much!

I also want to thank Prof. Dr. Ulrich Rüter for evaluation of this thesis and the helpful scientific discussions.

I am especially grateful to Peter, Jan, David, Agnes, Kristin and Arne (the p57kip2 gang) for their kind support and inspiration. It was and still is a great pleasure to work with you.

I also would like to thank the further members of the Neurology department, especially Brigida Ziegler, Birgit Blomenkamp and Sabine Hamm, for their support, friendship, wonderful working atmosphere and for the great time with you.

I want to thank all my friends, above all André, Marc and Dominik, for decades of fun, support and great music! You know how much your friendship means to me.

All my love to my family, mom, dad, my sister, her husband and their son Niklas. Thank you for support and encouragement throughout all the years (and those which will follow).

Hiermit erkläre ich, die vorliegende Arbeit selbständig und unter ausschließlicher Verwendung der angegebenen Hilfsmittel und Quellen angefertigt zu haben. Alle Stellen, die aus veröffentlichten und nicht veröffentlichten Schriften entnommen sind, wurden als solche kenntlich gemacht. Diese Arbeit hat in gleicher oder ähnlicher Form noch keiner anderen Prüfungsbehörde vorgelegen.

Düsseldorf, den 24. November 2008